

Alma Mater Studiorum Università di Bologna
Archivio istituzionale della ricerca

Steps towards sustainable solid phase peptide synthesis: use and recovery of N-octyl pyrrolidone

This is the final peer-reviewed author's accepted manuscript (postprint) of the following publication:

Published Version:

Steps towards sustainable solid phase peptide synthesis: use and recovery of N-octyl pyrrolidone / Giulia Martelli; Paolo Cantelmi; Alessandra Tolomelli; Dario Corbisiero; Alexia Mattellone; Antonio Ricci; Tommaso Fantoni; Walter Cabri; Federica Vacondio; Francesca Ferlenghi; Marco Mor; Lucia Ferrazzano. - In: GREEN CHEMISTRY. - ISSN 1463-9270. - ELETTRONICO. - 2021:11(2021), pp. 4095-4106. [10.1039/d1gc00910a]

Availability:

This version is available at: <https://hdl.handle.net/11585/822026> since: 2024-02-01

Published:

DOI: <http://doi.org/10.1039/d1gc00910a>

Terms of use:

Some rights reserved. The terms and conditions for the reuse of this version of the manuscript are specified in the publishing policy. For all terms of use and more information see the publisher's website.

This item was downloaded from IRIS Università di Bologna (<https://cris.unibo.it/>).
When citing, please refer to the published version.

(Article begins on next page)

This is the final peer-reviewed accepted manuscript of:

2021 Green Chem., 2021,23,4095–4106

The final published version is available online at

10.1039/D2GC00963C

Terms of use:

Some rights reserved. The terms and conditions for the reuse of this version of the manuscript are specified in the publishing policy. For all terms of use and more information see the publisher's website.

This item was downloaded from IRIS Università di Bologna (<https://cris.unibo.it/>)

When citing, please refer to the published version.

ARTICLE

Steps towards sustainable Solid Phase Peptide Synthesis: use and recovery of *N*-octyl pyrrolidone.

Received 00th January 20xx,
Accepted 00th January 20xx

DOI: 10.1039/x0xx00000x

Giulia Martelli,^a Paolo Cantelmi,^a Alessandra Tolomelli,^{*a} Dario Corbisiero,^a Alexia Mattellone,^a Antonio Ricci,^b Tommaso Fantoni,^a Walter Cabri,^{*a} Federica Vacondio,^c Francesca Ferlenghi,^c Marco Mor^c and Lucia Ferrazzano.^a

The investigation of new green biogenic pyrrolidinones as alternative solvents to *N,N*-dimethylformamide (DMF) for solid phase peptide synthesis (SPPS) led to the identification of *N*-octyl pyrrolidone (NOP) as the best candidate. NOP gave good performances in terms of swelling, coupling efficiency and low isomerization generating peptides with a very high purity. The mixture of NOP with 20% dimethyl carbonate (DMC) allowed to decrease solvent viscosity making the mixture suitable for the automated solid-phase protocol. Aib-enkephalin and linear Octreotide were successfully used to test the methodologies. It is worth nothing that NOP, DMC and the piperidine used in the deprotection step could be easily recovered by direct distillation from the process waste mixture. The process mass intensity (PMI), being reduced by 63-66%, achieved an outstanding value representing a clear step forward in SPPS greening.

Introduction

The development of the solid-phase peptide synthesis (SPPS) that originates from the seminal work of Bruce Merrifield back in the sixties,¹ gave access to previously unavailable long peptides *via* iterative formation of amide bonds.² Thanks to SPPS availability and its automation, polypeptides became a target for medicinal chemists. This modality is playing a major role in modern therapeutics,³ with more than 70 peptides on the market and about >100 in clinical trial advanced stages.

The different synthetic strategies for peptide synthesis have been clearly described by Albericio in 2009.⁴ Since then, only two novel industrial technologies have been reported, the enzymatic approach by Enzyper⁵ and the hiving technology by Jitsubo.⁶ However, SPPS is still the core technology for peptide synthesis and several research groups are now focusing the attention on the optimization of every single step to increase process greenness.^{7,8,9}

Almost complete conversions are achieved thanks to the use of reagents in excess that can be removed by extensive washing and filtration of the solid support anchored growing peptide. Therefore, in considering process greening, a fundamental role is played by the solvents.^{10,11}

N,N-dimethylformamide (DMF) is technically the perfect solvent for SPPS. However, its toxicological profile¹² is a serious matter of concern in the pharmaceutical industry. In fact, DMF and its most

common substitute, *N*-methylpyrrolidone (NMP)¹³ are reprotoxic and were labeled as hazardous; accordingly, their replacement has been considered "advisable or requested" by the ACS Green Chemistry Institute® Pharmaceutical Round Table (GCIPR)¹⁴ that defined this goal one of the hot topics in the list of the 12 green chemistry key research areas (KRAs). The development of innovative and general methods for sustainable amide bonds formation and peptide synthesis has been also reported in the updated version of the list of priorities.

On the basis of these considerations, selection of greener alternatives needs to keep into consideration the sustainability and the toxicity to natural environment and human health in the whole solvent lifecycle.

Several solvents have been reported to be suitable for a greener SPPS (GSPPS), such as, 2-methyl tetrahydrofuran (2-MeTHF),¹⁵ acetonitrile (ACN) and THF,¹⁶ 2-MeTHF and cyclopentyl methyl ether (CPME),¹⁷ γ -valerolactone (GVL)¹⁸ and *N*-formylmorpholine (NFM),¹⁹ propylene carbonate (PC),²⁰ dimethylisobutyl ether (DMIE),²¹ and *N*-butyl pyrrolidone (NBP).²² Green solvents mixtures affording proper physicochemical properties for all the steps of solid phase processes, Cyrene®/diethyl carbonate (DEC), sulfolane/DEC, anisole/dimethyl carbonate (DMC),²³ dimethyl sulfoxide (DMSO)/ethyl acetate (EtOAc)²⁴ and NFM/1,3-dioxolane (DOL)²⁵ have been also explored. However, some of these solvents like EtOAc, 1,3-dioxolane or 2-MeTHF do not have the optimal characteristics for industrial application because of their low flash point.

In this context, the family of *N*-alkylpyrrolidones may offer new opportunities since, although having a similar structure to NMP, they display a completely different metabolic profile, they are not toxic or reprotoxic and they still retain the main features of the parent dipolar aprotic solvent. NBP has recently been applied by both academia and industrial researchers to SPPS on polystyrene-based resins, affording crude peptides with comparable quality to those synthesized in DMF. In addition, NBP was also employed in mixture with ethyl acetate providing interesting results.²⁶

We have explored herein the characteristics of *N*-alkylpyrrolidones and their use in SPPS, focusing our attention on safest members of

^a Department of Chemistry Giacomo Ciamician
Alma Mater Studiorum, University of Bologna
Via Selmi, 2 40136-BO, Italy

E-mail: alessandra.tolomelli@unibo.it; walter.cabri@unibo.it

^b Fresenius kabi iPsum

via San Leonardo 23, 45010-RO, Italy

^c Department of Food and Drug Sciences
University of Parma

Parco Area delle Scienze 27/a, 43124-Parma, Italy

† Electronic Supplementary Information (ESI) available. See
DOI: 10.1039/x0xx00000x

this class as *N*-octyl-2-pyrrolidone (NOP), *N*-cyclohexyl-2-pyrrolidone (NCP) and *N*-benzyl-2-pyrrolidone (NBnP).

Aiming to the widest application, we have defined protocols for manual or automatic SPPS, decreasing the PMI (product mass intensity) by solvent recycling.

Results and discussion

N-Alkylpyrrolidones chemical-physical parameters, toxicological data and *in vitro* metabolism

In the selection of suitable candidates for DMF or NMP replacement for GSPPS, chemical-physical parameters are the first characteristics to be evaluated (Table 1).

N-alkylpyrrolidones share as a common feature the lack of acid protons, while the elongation of the alkyl chain consistently decreases their polarity moving from NMP to NBnP.

The high boiling point of this family of compounds, together with their high flash point temperatures (always > 100°C, except for NMP), are interesting characteristics for industrial application since there are no safety concerns and solvents can be recovered by distillation.

Table 1. Chemical-physical parameters of *N*-alkylpyrrolidones^a

Solvent	Viscosity at 25°C (mPa·s)	Flash point (°C)	Boiling point °C (pressure mmHg)
DMF	0.8	58	36 (1)
NMP	1.65	91	68 (4)
NBP	4.0	108	80-85 (0.5)
NOP	6.6	142	114-115 (0.8)
NCP	11.5	141	94-97 (0.5)
NBnP	21.4	113	124-125 (0.8)

^a See ref. 22a and 27

Concerning *N*-alkylpyrrolidones' viscosity, the observed values may represent a challenge for large-scale application in automated syntheses, since difficulties in transfer and purging may occur. Anyway, a viscosity close to 4 mPa·s is considered acceptable, if efficiency of all the steps of SPPS (swelling, coupling, protecting group cleavage) is maintained.^{9a} In this context, the simple addition of a low viscosity green cosolvent is a viable solution to overcome this specific issue.

In the perspective of the industrial application of new SPPS protocols, low cost, bulk availability and reliability of the supply chain of the solvent has also to be ensured. Among the other pyrrolidones, NOP is also known as Surfadone™ LP-100²⁸ and is widely used as a low-foaming non-ionic rapid wetting agent and dynamic surface tension modulator in cosmetic industry, pigment industry, cleaning detergent production and polymer manufacturing. For this reason, its price is comparable to that of the most common solvents (about 1-2\$/kg). The industrial preparation of NMP is predominantly derived from the reaction of γ -butyrolactone (GBL) with monomethylamine.²⁹ Similarly, other *N*-alkylpyrrolidones can be prepared using the corresponding amines. Even if GBL is commonly prepared *via* petrochemical route from succinic anhydride or succinic acid, it could be obtained also by fermentation of sugar, and hence be transformed from a fossil-based reagent to a renewable source.³⁰ However, the cost of fermentations and the difficulties in treating complex biomass-deriving matrices are still challenges to be tackled³¹ and, even if the research on biorefineries is advanced, technological implementation is hampered by a low profitability.³² Commercially available pyrrolidones are currently not prepared from

biogenic GBL, but with a perspective of novel economically viable biomass treatment protocols, they might be included in the future in the list of biogenic solvents, displaying a high potential for more sustainable chemical approaches. In this context, since it will become inevitable to move away from a petroleum-based society, scientific and technological efforts to turn these sustainable alternatives into industrially feasible solutions are mandatory.

Table 2. Toxicity parameters of solvents evaluated in this study in comparison with DMF and NMP³³

Solvent	Acute Oral Toxicity (mg/kg bw)	Acute Inhalation Toxicity	Acute Dermal Toxicity (mg/kg bw)	Reproductive Toxicity
DMF	3010	> 5.8 mg/L air	> 3160	Yes
NMP	150	> 5.1 mg/L air	> 5000	Yes
NBP	300	> 5.1 mg/L air	> 2000	No
NOP	> 2200	n.a.	> 4000	No
NCP	370	n.a.	1600	No
NBnP	n.a.	n.a.	n.a.	n.a.

n.a.: not available

Data reported in Table 2 clearly show that NOP, among the *N*-alkyl pyrrolidones, is the safest one, being not reprotoxic and with very high tolerability when administered orally or intradermally.

The metabolism of these products generally shows oxidation at the 5 position of the lactam ring and on the first carbon of the *N*-alkyl side chain. Through this pathway NMP generated consistent quantities of the masked formaldehyde.³⁴

When NOP was incubated in the presence of rat (RLM) and human liver microsomes (HLM), it was rapidly cleared with an average half-life ($t_{1/2}$) of 11.5 (\pm 2.0) min in RLM and 23.8 (\pm 5.6) min in HLM (Fig. 1).

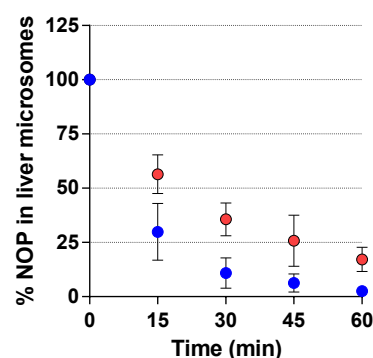


Fig.1 In vitro metabolic stability of *N*-octyl pyrrolidone (NOP). Time course of NOP stability in rat (blue circles) and human (red circles) liver microsomes.

In vitro metabolism of NOP in RLM and HLM were very similar and led to the formation of several metabolites (M1-M11, Fig.2, Fig. S1 and Table S1, Supporting Information). The major one was **M1** (RT = 3.19 min; Fig. 2) having a m/z value of 212.1642, with a mass shift of 14 Da with respect to NOP. As shown in Fig.2 and Table S1, besides **M1**, other minor metabolites were observed. A cluster of metabolites (**M6**, **M7**, **M9-11**) displaying a mass shift $M+16$ with respect to NOP, suggests a hydroxylation reaction (+O) while keto

metabolites (**M1**, **M2**, **M3**, **M4**, **M5**, **M8**) displaying a mass shift M+14 (+O-2H) derive as second-generation metabolites from dehydrogenation of hydroxylated ones. This is compatible with an oxidation reaction of a methylene to keto group involving either the 2-pyrrolidone ring or the N-octyl side chain of NOP. Low and High energy mass spectra related to either keto or mono-hydroxylated metabolites **M1-M11** are reported in the Supporting Information as Fig. S4-S14.

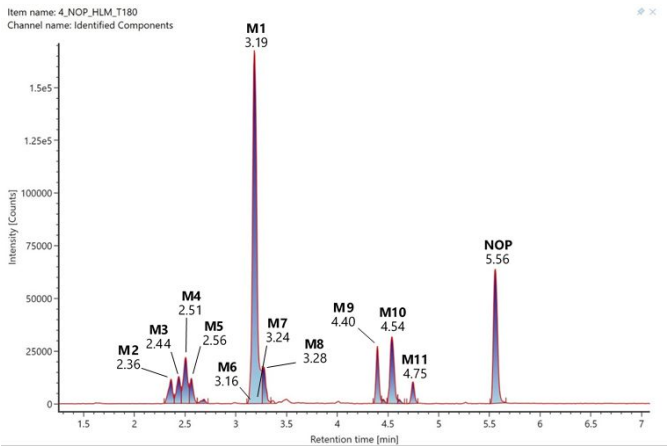


Fig. 2. HPLC-MS/MS trace of a HLM incubation of N-octyl pyrrolidone (NOP) at t=3h. Parent compound NOP and metabolites **M1-M11** are reported together with their RT. The most abundant metabolite (**M1**, with a mass shift of + 14 with respect to NOP) and two minor metabolites (**M6** and **M7**, with a mass shift of + 16 with respect to NOP) co-elute. Co-eluting metabolites are detectable as Extracted Ion Chromatograms in Fig. S3, Supporting information.

Effect of N-Alkylpyrrolidones as solvents in key steps of SPPS

Solvents for SPPS need to fulfill a series of requirements at the same time: good swelling efficacy for different resins, ability to completely solubilize amino acids, coupling reagents and related by-products, promotion of both coupling and deprotection steps. Consequently,

before testing pyrrolidones in SPPS protocols, we firstly evaluated separately their efficiency in all these steps.

Solubility tests

To evaluate the suitability of the selected solvents in SPPS, their ability to solubilize commonly employed protected amino acids and coupling reagents was investigated. Fmoc-Val-OH was initially selected as the reference amino acid, demonstrating a perfect solubilisation in all the tested solvents (NOP, NCP and NBnP) at a standard 0.2 M concentration (Table 3). The same dissolution protocol was applied to the main coupling reagent combinations: OxymaPure®/DIC (**A**), COMU/DIPEA (**B**), PyBOP/DIPEA (**C**), PyOxyma/DIPEA (**D**), HOBt/DIC (**E**), and HBTU (**F**) (Table 4). Optimal results were generally achieved, except for HBTU (**F**), which was scarcely dissolved in all the solvents and was hence excluded from further studies. The solubility screening was then extended to Fmoc-protected natural and non-natural amino acids (Fmoc-Gly-OH, Fmoc-Ala-OH, Fmoc-Aib-OH, Fmoc-Phe-OH, Fmoc-Tyr(tBu)-OH, Fmoc-Lys(Boc)-OH, Fmoc-Cys(Trt)-OH, Fmoc-Pro-OH and Fmoc-Thr(tBu)-OH) that were dissolved at a 0.2 M concentration, both alone and in the presence of the aforementioned additives after a 5 minutes pre-activation (Table 3 and Table S2).

Solubility issues were detected in case of Fmoc-Cys(Trt)-OH, but decreasing the concentration to 0.1 M, a slightly lower value than the standard used in SPPS, good solubility was recovered in NCP, even if not in NBnP (Table 3). When the amino acids were mixed with coupling additives, only in sporadic cases the solubility was incomplete, requiring an extra-dilution to observe clear solutions. Fmoc-Cys(Trt)-OH demonstrated in this case a good solubility when combined with OxymaPure®/DIC (**A**) and COMU/DIPEA (**B**) in NOP and NCP, overcoming the above reported limited solubility of the pure Fmoc-protected amino acid. On the other hand, NBnP was not able to dissolve this amino acid, even in combination with coupling reagents or in more dilute solutions (Table S2).

Overall, OxymaPure®/DIC and COMU/DIPEA showed to be the best coupling systems because of their general good results with all solvents and amino acids (see Figures S16-S18 in Supporting Information).

Table 3. Solubilisation efficacy of Fmoc-AA(PG)-OH amino acids in N-alkylpyrrolidones^a

Solvent	Fmoc-AA(PG)-OH									
	Val	Gly	Ala	Aib	Phe	Pro	Tyr(tBu)	Thr(tBu)	Lys(Boc)	Cys(Trt)
NOP										
NCP										0.1 M
NBnP										0.1 M

^aSolubilisation monitored at 0.2M concentration unless 0.1M is specified. Legend: green=soluble; yellow=moderately soluble; red=insoluble. PG: protecting groups

Table 4. Solubilisation efficacy of coupling reagents A-F and Fmoc-Val-OH with A-E in N-alkylpyrrolidones^a

Solvent	Coupling reagents						Mixture Fmoc-Val-OH + coupling reagents (A-E)				
	OxymaPure®/DIC A	COMU/DIPEA B	PyBop/DIPEA C	PyOxyma/ DIPEA D	HOBt/DIC E	HBTU F	Val+A	Val+B	Val+C	Val+D	Val+E
NOP											
NCP											
NBnP											

^aLegend: green=soluble; yellow=moderately soluble; red=insoluble

ARTICLE

To notice, OxymaPure®/DIC has been reported over the last ten years as a high-efficient coupling agent able to reduce racemization with performances overcoming those displayed by most of the common analogues.³⁵

Swelling tests

The first key step in SPPS is the choice of the resin and its swelling. A suitable solvent should be able to properly swell different commercially available resins, demonstrating the broadest applicability. Polystyrene based resins (PS-resins) cross-linked with 1–2% of divinylbenzene are the most commonly used due to their mechanical and chemical stability as well as for the low cost and bulk availability, but also TentaGel-based resins, made of a polystyrene (PS)/polyethylene glycol (PEG) network are often used for their increased compatibility with polar solvents. PEG-based resins, commonly known as ChemMatrix resins (CM), have recently received great attention for the good performances reported in the synthesis of long peptides. On these basis, cross-linked polystyrene (PS - Merrifield), PEG-PS (TentaGel – TG) and pure PEG-based (ChemMatrix - CM) resins were considered for swelling with *N*-alkylpyrrolidones. Moreover, different acid-sensitive linkers were considered for each matrix: Wang and Trt-Cl linkers for obtaining the final peptide as a C-terminal acid, and Rink Amide linker for a C-terminal amide peptide. Details on bead size, loading and cross-linking of the selected resins are reported in Table S3.

Recently Amadi-Kamalu *et al.*³⁶ developed a model to predict resin swelling in a given solvent, highlighting how the solvent-resin interaction is a complex process especially as the swelling could be related to physical parameters such as bead size and degree of cross-linking. Anyway, experimental evaluation of swelling still represents the most reliable method and reported protocols were applied for all the solvent/resin combinations.^{20,37}

Briefly, a dry resin sample in the desired solvent was allowed to mildly shake in a graduated syringe for 30 minutes; after 5 minutes of re-equilibration, solvent was removed under vacuum and the volume increase of the resin was measured (mL·g⁻¹).

In general, solvents giving resin swellings higher than 4 mL·g⁻¹ are considered good, values between 2 and 4 mL·g⁻¹ correspond to moderately good solvents and swelling lower than 2 mL·g⁻¹ identifies poor candidates.

Table 5. Swelling^a of resins in DMF and pyrrolidones at RT after 30 mins

Resin	DMF (mL·g ⁻¹)	NOP (mL·g ⁻¹)	NCP (mL·g ⁻¹)	NBnP (mL·g ⁻¹)
PS-Wang	5.6	5.5	5.1	2.3
PS-Trt-Cl	3.2	3.4	3.6	1.6
PS-RinkAmide	3.2	1.6	1.6	1.6
TG-Wang	6.0	1.7	2.5	1.3
TG-RinkAmide	6.2	4.3	3.4	4.0
CM-Wang	4.4	1.4	1.6	1.6
CM-RinkAmide	7.8	3.4	6.1	6.7

^aData reported are the average of triplicate measurements, see Table S4 in Supporting Information.

Noteworthy, the degree of swelling should not greatly overcome 4 mL·g⁻¹ since a large volume of solvent would lead to reagents dilution. However, the swelling is considered acceptable if it corresponds to ±30% of the measured volume for DMF.²²

The measured swelling values of pyrrolidones and DMF are reported in Table 5 as a mean value of analyses in triplicate.

NOP and NCP afforded excellent swelling of PS-based resins, commonly employed for industrial purposes and resulted comparable to DMF in swelling the Wang linker. Moreover, better results were observed with Trt-Cl resin. This behaviour suggests that these solvents display a higher affinity to less polar resin matrixes. Concerning 100% PEG-based resins, acceptable results were found for CM-RinkAmide when NCP and NBnP were used, the last one affording a 15% lower swelling in comparison to DMF. Overall, *N*-alkylpyrrolidones cover a satisfying range of applicability since acid terminating peptides can be prepared using PS-Wang or PS Trt-Cl resin with NOP and NCP while amide peptides may be synthesized using CM-RA resin with NCP or NBnP.

Coupling reaction in solution phase

The efficiency of pyrrolidones in promoting the coupling step was first investigated in liquid phase. Accordingly, the synthesis of model dipeptide¹⁷ Z-Phg-Pro-NH₂ was performed in the selected solvents (NOP, NCP, NBnP) and in DMF as benchmark reaction, screening different coupling reagent combinations, and checking both the conversion and the racemization degree (Table 6).

Measuring the racemization ratio is fundamental to predict the efficiency of the solvent in SPPS couplings, and its inhibition is necessary to avoid further purifications and low final yields. Dipeptide Z-Phg-Pro-NH₂ is particularly prone to racemization due to the acidity of the benzylic α-proton in Phg.³⁸ Moreover, proline reacts slower than other amino acids and achieving a complete conversion represent the main hurdle.

All the couplings were performed using (L)-amino acids and the crude was analysed by HPLC-MS injection after 3 h, in order to determine the dipeptide conversion and the racemization degree. The couplings were performed with equimolar amounts of the two amino acids and with a concentration of 0.125 M. The conversions were generally good in all conditions; moreover, DIC/OxymaPure® system provided only about 1% racemization in pyrrolidones (Table 6, entry 6, 11, 16), less than what observed in DMF. PyBOP/HOBT/DIPEA and HOBT/DIC combination afforded high level of racemization in all the solvents tested, including DMF. COMU/DIPEA and PyOxyma/DIPEA showed better values than the latter two combinations, but resulted generally less effective than DIC/OxymaPure®.

Considering these data, together with the solubilisation screening of coupling reagents and activated amino acids, DIC/OxymaPure® was considered the best system for further investigations. This choice was supported also by their very low cost, essential requirement for SPPS use on industrial scale.

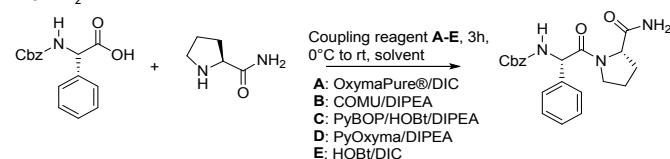
Deprotection kinetic tests

To develop a total DMF-free method, a solvent displaying excellent behaviour in the deprotection step is a fundamental tool. In this

context, the removal of Fmoc group was investigated in liquid-phase to evaluate the effect of the solvent and avoid possible interference of resin swelling or peptide aggregation issues that could occur in solid-phase.³⁹ Piperidine is the base of choice in Fmoc SPPS, due to its role as fast deprotecting agents and dibenzofulvene scavenger. Accordingly, tests were conducted using a 20% piperidine solution to investigate deprotection kinetic, as commonly reported in SPPS protocols.^{9a}

Qualitative kinetic tests on Fmoc-Phe-OH deprotection were carried out according to the method developed by Jad *et al.*⁴⁰ and deprotection rates were monitored by HPLC-MS at fixed time intervals.

Table 6. Conversion (%) and racemization ratio (%) in the synthesis of Z-Phg-Pro-NH₂^a



Entry	Solvent	Coupling Reagent	DL (%) ^b	Conversion (%)
1	DMF	A	1.9	92
2		B	0.9	99
3		C	24.1	98
4		D	1.0	87
5		E	13.2	85
6	NOP	A	0.9	95
7		B	6.6	82
8		C	17.1	94
9		D	2.5	96
10		E	11.7	99
11	NCP	A	1.1	96
12		B	2.2	82
13		C	21.6	92
14		D	2.3	83
15		E	13.2	99
16	NBnP	A	1.4	99
17		B	1.6	99
18		C	32.1	99
19		D	0.7	95
20		E	10.0	99

^aAll the reactions were performed pre-activating (3 min) Z-Phg-OH. Conversion and racemization were calculated by HPLC. ^bDefined as (Z-D-Phg-Pro-NH₂)/(Z-L-Phg-Pro-NH₂) × 100. The DL epimer was identified after synthesis of Z-D-Phg-Pro-NH₂ where Z-D-Phg-OH was used as a starting material.

Fmoc-Phe-OH deprotection was also tested in DMF and NBP as a comparison. Reaction was considered complete at disappearance of the HPLC peak corresponding to Fmoc-Phe-OH; notably, the reactions performed in all investigated pyrrolidones revealed complete Fmoc removal in 2 minutes (see Figures S31-S32 in Supporting information), perfectly in line with DMF performances.

SPPS in environmentally favourable solvents

After investigating the effect of *N*-alkylpyrrolidones as solvents in liquid phase couplings, the study was extended to the SPPS of Aib-enkephalin pentapeptide (H-Tyr-Aib-Aib-Phe-Leu-COOH/COONH₂). Aib residue insertion represents a harsh step because of its steric hindrance that often leads to slow-rate coupling reaction and consequently partial mis-incorporation.¹⁵ The amount of the des-Aib sequences provides a measure of the efficacy of each pyrrolidone in comparison to DMF or standard alternatives.

Aib-enkephalin was manually synthesized on different resin/solvent combinations according to the best swelling results: (i) PS-Wang and PS-Trt-Cl resins with NOP and NCP; (ii) ChemMatrix-RinkAmide (CM-RA) resin with NBnP. Treatment with TFA-based cleavage cocktails afforded the peptide as acid at the C-terminal in case (i) and as amide in case (ii). These conditions also allowed the simultaneous removal of *tert*-butyl group in Tyr side chain. Peptides were assembled on Fmoc-Leu-preloaded resins using 20% piperidine as Fmoc-deprotection agent and DIC/OxymaPure® as coupling reagents. *N*-alkylpyrrolidones were used for all the synthetic steps, including washings. Double Fmoc-Aib-OH couplings were performed in all syntheses, according to common literature procedures.^{15,16,17} HPLC purities of the crudes after cleavage are reported in Table 7.

When the reaction was performed using NOP, excellent purities were observed, providing about 98% of the target pentapeptide and <1% of des-Aib byproduct on Wang resin (entry 1). Less than 3% impurity was generated on TrtCl-resin (entry 2). Interestingly, these results are consistently better than those obtained in the reference solvents DMF and NBP, which provided a des-Aib amount >11% and >8%, respectively (entries 5-6 and 7-8). NCP resulted comparable to DMF in terms of pentapeptide purity, but lower amounts of des-Aib were detected (entries 3-4). NBnP instead demonstrated a very low efficiency since only 4.3% of Aib-enkephalin was detected, while des-Aib tetrapeptide (16%) and other incomplete sequences corresponding to the remaining 80% of the total were identified in the crude (Entry 9).

As a consequence, NCP and NBnP were not further studied while NOP was instead selected as an ideal greener alternative to common solvents.

Table 7. HPLC purities for Aib-Enkephalin pentapeptide assembled on different resins and solvents.

Entry	Solvent	Resin ^a	Pentapeptide ^b %	Des-Aib (%)	Other (%)
1	NOP	PS-Wang	97.7	0.8	1.5
2		PS-Trt-Cl	97.4	2.6	-
3	NCP	PS-Wang	88.5	10.5	1.0
4		PS-Trt-Cl	89.9	10.0	1.1
5	DMF	PS-Wang	85.8	14.2	-
6		PS-Trt-Cl	88.1	11.9	-
7	NBP	PS-Wang	91.1	8.9	-
8		PS-Trt-Cl	91.6	8.4	-
9	NBnP	CM-RA	4.3	16.0	79.7
10 ^c	DMF	CM-RA	53.0	47.0	-

^aPre-loaded Fmoc-Leu-resins were used; ^bDouble Fmoc-Aib-OH couplings; ^cfrom Ref.16

Table 8. HPLC Purity of Linear Octreotide in NOP, NOP/DMC, DMF and NBP.

Compound	RRT	NOP	NOP/DMC 80:20 Manual SPPS	NOP/DMC 80:20 Automated SPPS	DMF	NBP
Cyclized N,O shift	0.83	-	-	-	1.4	-
Cyclized	0.88	0.7	-	-	5.8	2.4
TM-N,O shift 1	0.92	1.0	1.4	-	-	0.7
TM-N,O shift 2	0.95	5.2	2.4	2.0	-	4.2
TM+CO ₂	0.97	-	21.6	-	5.1	4.8
TM	1.00	77.6	65.1	86.0	76.8	77.7
TM+Boc	1.10	-	1.7	-	-	-
TM+tBu	1.14	11.7	5.2	10.0	9.0	7.2
TM+Boc2	1.18	-	0.8	-	-	-
TM+tBu2	1.26	3.8	1.8	2.0	1.9	3.0
Product purity (%) ^a		100	100	100	100	100

^aHPLC purity calculated as sum of all target product adducts; RRT = relative retention time

Consequently, more sustainable conditions for SPPS were applied to the synthesis of linear Octreotide (H-D-Phe¹-Cys²-Phe³-D-Trp⁴-Lys⁵-Thr⁶-Cys⁷-Thr⁸-ol), the final intermediate obtained by solid-phase synthesis in the industrial manufacturing of the API Octreotide.

This peptide was one of the first biologically stable somatostatin analogues to be synthesized and used in oncology.⁴¹ The entire protocol was performed with NOP as solvent and compared with reference syntheses in NBP and DMF. Preloaded Fmoc-Thr(tBu)-ol-Trt-PS resin was used, being highly suitable to the synthesis in NOP. Although Octreotide is a medium-length peptide, frequent misincorporation of Cys⁷ residue occurs and for this reason the coupling step to introduce this residue was repeated twice in all the synthetic sequences. Standard 20% piperidine solution and DIC/OxymaPure[®] reagents were employed for deprotection and coupling steps, respectively. HPLC purities of the crudes after cleavage are reported in Table 8. It is important to mention that all the detected species are related to linear Octreotide and hence precursors of the final cyclic API. Des-Cys⁷ or other truncated sequences were never observed.

The excellent results obtained using NOP both in the synthesis of Aib-enkephalin and linear Octreotide showed that its high viscosity value (6.6 mPa·s for NOP vs 4.0 mPa·s for NBP and 0.8 mPa·s for DMF) does not affect the SPPS efficiency. The issue of viscosity anyway has to be considered when moving from manual synthesis to automatic synthesizers. Heating the reaction system had been previously applied as a solution in SPPS in NBP.³⁴ Instead, in order to decrease NOP viscosity and to perform the reaction at automatic synthesizer without heating, DMC (0.59 mPa·s) was selected as co-solvent. In fact, DMC proved to be a good cosolvent for SPPS.²³ Addition of 20% DMC to NOP allowed to decrease the viscosity down to 3.94 mPa·s (see Table S5), thus allowing the use of automated systems. After having evaluated the swelling degree of NOP/DMC 80:20 in the PS resins (see Table S4), the synthesis of linear Octreotide intermediate was repeated using this sustainable solvents' mixture both with manual and automated protocols (Table 8). In both SPPS protocols the final purity was comparable with the corresponding synthesis carried out in DMF, NBP and NOP alone.

Solvent and base recycling

NOP and NOP/DMC proved to be greener alternatives to DMF, however, in order to achieve a truly sustainable protocol, the Process Mass Intensity (PMI) should be decreased by recovering the main source of waste, namely the solvents (NOP or NOP/DMC) and the piperidine used in the deprotection step. NOP offers several

alternatives for the recovery process, being very lipophilic. The final mixtures can be washed with water and then NOP recovered by distillation or it can be directly distilled in order to recycle all the volatile chemicals. DIC cannot be recycled being unstable and almost completely transformed into 1,3-diisopropylurea during the coupling step.

Coupling streams and deprotection streams should be recovered separately in order to avoid piperidine consumption by the excess of Fmoc-amino acids used in the coupling steps. When the mixture NOP/DMC is used, due to the small difference between piperidine and DMC boiling points (106 °C vs 90 °C at 760 mmHg), these two components are recovered in the same fraction and reused for deprotection steps in further SPPS processes, after rebalancing the required relative ratio.

The results obtained by applying these protocols to the SPPS of linear octreotide in comparison with the DMF standard process are reported in Table 9.

Table 9. Process Mass Intensity (PMI) and recovery in GSPPS

Entry	Solvent ^a	PMI	Waste Stream	Recovery (yield %)	PMI after recovery
1	NOP	722	Depr	NOP (85)	268
			Coupling	Pip ^b (95)	
				NOP (85)	
2	NOP/DMC	748	Depr	NOP (85)	256
			Coupling	DMC/Pip ^b (95)	
				DMC (95)	
3	DMF	735	-	-	-

^aThe wastes coming from coupling steps and from deprotection steps were distilled separately. ^bPiperidine (Pip) involved in the formation of DBF-piperidine adduct was subtracted from the total piperidine volume.

The percentage of waste related to the solvents involved in swelling, coupling, deprotection and washing steps is very similar in all different protocols (NOP 67.8%, NOP/DMC 69.0%, DMF 68.4%, see Table S7 and Table S8). Concerning the synthesis performed in NOP (entry 1), piperidine was easily recovered in 95% yield, considering the maximum amount that could be collected. NOP was recovered in the second fraction of condensed liquid in 85% amount. Under these conditions, PMI value for the global process was more than halved (268 with solvent/base recovery vs 722 without).

When the green mixture NOP/DMC was used for the same synthesis (entry 2), distillation of the deprotection streams under vacuum allowed to distil, at 25 mmHg, DMC and piperidine together (95% each) in a 1:0.86 ratio (V/V), as confirmed by ^1H NMR (see Supporting Information). Further, vacuum increase to 0.25 mmHg allowed to recover NOP in 85% yield. Finally, the distillation under vacuum of the coupling wastes allowed to recover in high yield both DMC (95%) and NOP (85%), decreasing the total PMI from 748 (without recovery) to 256. The final waste related to solvent is limited to 10% for the process with NOP and to 8.7% when DMC/NOP were used. OxymaPure[®] could be isolated from the solid residue following the protocol reported by Rasmussen.²⁴ However, this additional recovery procedure increased the PMI and allowed to isolate OxymaPure[®] in 38% yield; therefore, in our protocol we did not consider coupling agent recovery.

A full evaluation of NOP compared to other solvents commonly used in SPPS should comprise a complete lifecycle perspective of the solvent impact. A quantitative comparison concerning the carbon footprint between SPPS protocols in DMF and NOP cannot be performed due to lack of literature data on NOP. Anyway, for a qualitative estimation, since all the reactants and procedures in the two SPPS protocols are the same, the attention can be exclusively focused on the solvent carbon intensity (contribution to CO_2 emission), considering the primary production and the disposal by incineration or recycling. The production technologies of NMP and NOP are very similar. Thus, the carbon footprint can be calculated from the NMP's one (4.22 kg CO_2/Kg)⁴² by considering a 20-30% increase in carbon content per kg due to the octyl chain and to the higher boiling point. Therefore, the estimated range could be between 5.06-5.49 kg CO_2/kg . The carbon footprint related to DMF production has been reported to be lower than NMP (3.57 kg CO_2/Kg).⁴³ However, NMP recovery by double distillation decreases the carbon footprint by 40%.⁴² On the other hand, NOP can be recovered by single distillation and contribution of this process to carbon footprint is consistently lower than the advantage arising from the reduced amount of virgin solvent required. We can expect to have an impact on NOP recycling on the carbon footprint similar to the one of NMP (>40%).

These considerations allow to rebalance the apparent disadvantages of NOP in comparison with DMF. The comparable carbon footprint combined with the health, environmental and safety data and the future perspective of a sustainable production of NOP from biomasses make this potential solvent a credible sustainable alternative.

Conclusions

The evaluation of alternative green and safe pyrrolidones allowed to identify NOP and NOP/DMC as the best solvents in term of yield and selectivity for SPPS. To test the solvent performances Aib-enkephalin and linear Octreotide were synthesized by SPPS producing the final products in excellent purities using both manual and automated procedures. The solvents and the piperidine could be easily recovered decreasing the process PMI by 63% for NOP protocol and 66% for NOP/DMC one. Selecting green alternatives to dipolar solvents for SPPS is an extensively investigated issue, but the development of a methodology including solvents and reagents recovery and recycle represents a step forward in the achievement of a really green SPPS.

Experimental procedures

General Methods

Unless otherwise stated, all materials, solvents and reagents were obtained from commercial suppliers, of the best grade, and used without further purification. The solvents used were of high-performance liquid chromatography (HPLC) reagent grade. Specifically, Fmoc amino acids and resins were supplied by Iris Biotech, Merck or Fluorochem. Coupling reagents were purchased from Merck or Novabiochem. Piperidine was supplied by Merck. DMF, other organic solvents, and HPLC-quality acetonitrile (CH_3CN) were purchased from Merck. Milli-Q water was used for RP-HPLC analyses. NOP was purchased Merck.

Solid-phase synthesis of the peptides was carried out manually or using CSBio-CS136X peptide synthesizer (automated syntheses).

HPLC-MS analyses were performed on Agilent 1260 Infinity II system coupled to an electrospray ionization mass spectrometer (positive-ion mode, m/z = 100–3000 amu, fragmentor 30 V), using columns Agilent Zorbax-SB-C18 5 μm , 250 x 4.6 mm or Phenomenex Luna C18 5 μm , 250 x 4.6 mm; temperature: 25 $^\circ\text{C}$; injection volume: 10 μL , UV: 220 nm, elution phases: H_2O +0.08%TFA (mobile phase A) and CH_3CN +0.08%TFA (mobile phase B), flow: 0.5 mL/min or 1.0 mL/min. Chemstation software was used for data processing.

^1H NMR spectra were recorded with an INOVA 400 MHz instrument with a 5 mm probe. All chemical shifts were quoted relative to deuterated solvent signals.

Distillations were performed with an Edwards RV3 vacuum pump.

The viscosity was measured on CS10 Bohlin (Malvern) rheometer in a titanium cylinder/steal cup (Bob-Cup C25) configuration at temperature of 25 $^\circ\text{C}$ controlled by Julabo MP thermostat. The calibration of the instrument was previously verified with an appropriate standard, namely 2,2,4-Trimethyl-1,3-pentanediol monoisobutyrate (tabulated viscosity at 30 $^\circ\text{C}$ = 9.96 mPa s).

In vitro metabolism of NOP in rat and human liver microsomes

A NADPH-generating solution (10 mM glucose-6-phosphate, 2 mM NADP⁺, 5 mM MgCl_2 and 0.4 U/mL glucose-6-phosphate-dehydrogenase) was prepared in 100 mM phosphate buffered saline (PBS) pH 7.4. 15 μL of RLM or HLM preparation (final protein concentration = 1 mg/mL) were added to 60 μL of co-factors mix and 222 μL of PBS buffer. Samples were pre-incubated under continuous stirring at 37 $^\circ\text{C}$ for 5 min, then 3 μL of stock solution of NOP were added to start the reaction. The compound was incubated at the final concentration of 10 or 100 μM . Aliquots of RLM and HLM incubations were collected at the beginning of the experiment ($t=0$ min) and at $t=3$ h, enzymatic reaction was quenched by addition of a double volume of CH_3CN , samples were centrifuged (16,000 x g, 10 min, 4 $^\circ\text{C}$) and the supernatant directly injected into the HPLC-HRMS system for metabolite identification.

UPLC-HRMS conditions for *in vitro* NOP metabolite profiling

A Waters Acquity UPLC I-Class (Waters, USA) coupled to a Waters V-Ion IMS qToF was employed for ion mobility-enabled acquisitions in metabolite ID workflow. The V-Ion IMS qToF was daily calibrated employing Waters Major Mix (Waters, USA) and system performance were daily checked for accurate mass and

Collisional Cross Section (CCS) accuracy and precision by injecting system suitability test (SST) mixture composed of nine QC standards. For UPLC separation, mobile phases A and B were CH₃CN and ultra-pure water both with 0.1% v/v formic acid and column was an Acquity UPLC CSH C18 (2.1 x 100 mm, 1.7 μ m; Waters, USA). The linear gradient was: 0 min: 5%A; 0-15 min: 5-95%A; 15-16 min: 95%A; 16-17 min: 95-5%A; 17-20 min: 5%A. Total run time: 20 min. Flow rate: 0.5 mL/min; injection volume: 2 μ L; column temperature: 50 °C. Acquisition range: *m/z* = 50-300 amu. Instrumental parameters were set as follows: source temperature: 120 °C; desolvation temperature: 500 °C; source gas flow: 20 L/h; desolvation gas flow: 800 L/h; capillary voltage: 0.8 kV (ESI+); cone voltage: 20 V; collision energy: low energy: 4 eV; high energy: 10-45 eV; reference mass: leucine enkephalin [M+H]⁺ *m/z* = 556.27658. The software UNIFI v.1.8.2 (Waters, USA) was employed for data acquisition and processing.

Solubility Tests

1 mL of the desired pyrrolidone was added to 0.2 mmol of either the protected amino acid/coupling reagent (pair of reagents) or both protected amino acid and coupling reagent(s), and stirred at room temperature until a clear solution was observed. In case of not complete dissolution (see red boxes in Tables 3,4 and S2), an extra addition of solvent was added to reach a concentration of 0.1 M and to achieve total solubilisation, unless otherwise specified.

Resin Swelling

Weighted resin (0.1 g) was introduced into a 5 mL syringe fitted with a polypropylene fritted disc (the void volume of the tip and the syringe was estimated to be 0.2 mL). The desired solvent or mixture of solvents (2 mL) was added to the resin, which was shaken for 30 minutes at room temperature. The swollen resin was allowed to stand for further 5 minutes, then the solvent was removed under vacuum. The volume of the dry resin was then read and the swelling value was calculated from the following formula:

Degree of swelling (mL/g) = $100 \times (\text{volume of the swelled resin} - 0.2 \text{ mL}) / 0.1 \text{ g}$.

All the measurements were performed in triplicate, data were reported as medium value. Triplicate measurements with the related standard deviation values are reported in Table S4.

Fmoc cleavage kinetics in solution phase

Fmoc-Phe-OH (0.1 mmol) was dissolved in the desired pyrrolidone. Piperidine was added to the suspension in order to achieve the desired concentration (20% base solution) in the final 1 mL deprotection mixture total volume. The reaction mixture was stirred at room temperature and samples of the solution (20 μ L) were taken at *t*=0 (before base addition) and after 2, 4, 6, 8, 10, 15 minutes. The samples were diluted with 1.5 mL of CH₃CN/TFA (1% v/v) and injected in HPLC-UV. Reaction was considered complete at disappearance of the HPLC peak corresponding to Fmoc-Phe-OH. All kinetics resulted complete after 2 minutes from the reaction beginning, independently from the employed solvent. Selected chromatograms are reported in the Supporting Information. For HPLC separation, mobile phases A and B were H₂O+0.08%TFA and CH₃CN+0.08%TFA and column was an Agilent Zorbax-SB-C18 5 μ m, 250 x 4.6 mm. The linear gradient was: 0 min: 95%A; 0-15 min: 95-5%A; 15-20 min: 5-95%A; 20-22 min: 95%A. Total run time: 22 min. Flow rate: 1 mL/min.

Coupling in solution phase: synthesis of Z-Phg-Pro-NH₂

Z-Phg-OH (0.2 mmol) was dissolved in a glass vial with 2.5 mL of DMF or the selected pyrrolidone (NCP, NOP or NBnP). The desired coupling reagents combination (0.3 mmol) was then added (reagents A-E in Table 6: OxymaPure/DIC, COMU/DIPEA, PyBOP/HOBt/DIPEA, PyOxyma/DIPEA, HOBt/DIC). After 5 minutes of preactivation, H-Pro-NH₂ (0.2 mmol) was added. The solution was stirred at 0 °C for 1 h, then at room temperature. After 3 h from the beginning of the reaction, an aliquot (80 μ L) of the solution was diluted with 0.5 mL of a 1:2 CH₃CN/H₂O mixture and injected in HPLC-MS, in order to monitor the conversion and the racemization ratio. Selected chromatograms are reported in the Supporting Information. For HPLC separation, mobile phases A and B were H₂O+0.08%TFA and CH₃CN+0.08%TFA and column was an Agilent Zorbax-SB-C18 5 μ m, 250 x 4.6 mm. The linear gradient was: 0 min: 80%A; 0-15 min: 80-60%A; 15-20 min: 60%A; 20-30 min: 60-80%A. Total run time: 30 min. Flow rate: 1 mL/min.

Solid phase synthesis of H-Tyr-Aib-Aib-Phe-Leu-OH/ H-Tyr-Aib-Aib-Phe-Leu-NH₂ (Aib Enkephalin)

Aib-Enkephalin manual syntheses were carried out at room temperature in glass syringes fitted with a polyethylene porous disc, connected to a vacuum source to remove excess of reagents and solvents, by using 0.2 g of preloaded Fmoc-Leu-resins. Specifically, preloaded PS-Wang and PS-Trt-Cl resins (loading 1.1 mmol/g) were used for synthesis with NBP, NOP and NCP, preloaded ChemMatrix-RinkAmide resin (loading 0.5 mmol/g) was used with NBnP. After swelling of the resin in 2 mL of the selected solvent (DMF, NBP, NCP, NOP or NBnP), Fmoc protective group was removed by 20% piperidine in the selected solvent (2 times \times 2 mL, 15 min each), then the resin was washed with the selected solvent (3 times \times 1.5 mL, 1 min each). Fmoc-Phe-OH, Fmoc-Aib-OH, Fmoc-Aib-OH, Fmoc-Tyr(tBu)-OH (three-fold excess with respect to the loading of the resin) were pre-activated by OxymaPure® and DIC (three-fold excess of the reagents with respect to the loading of the resin) for 3 minutes and coupled to the resin for 60 minutes. In case of both Aib residues in the sequence, the coupling of Fmoc-Aib-OH was repeated a second time. After each coupling step the Fmoc protective group was removed by treating the peptide resin with 20% piperidine in the selected solvent (2 times \times 2 mL, 15 min each), and the resin was washed with the selected solvent (3 times \times 1.5 mL, 1 min each). After Fmoc cleavage of the *N*-terminal amino group, the peptide resin was further washed with DCM (3 times \times 2 mL, 1 min each) and dried under vacuum for 12 hours. Dry peptide resin was suspended in 5 mL of the mixture TFA/TIS/H₂O (95/2.5/2.5 v/v/v) and stirred for 2 h. The resin was filtered off, washed with TFA (1 time \times 1mL, 1 min) and diisopropylether (25 mL) cooled to 4 °C was added to the solution dropwise. The peptide was filtered and dried *in vacuo* to obtain crude Aib-Enkephalin that was directly analysed by HPLC-MS (Table 7). Related chromatograms and MS spectra are reported in the Supporting Information. For HPLC separation, mobile phases A and B were H₂O+0.08%TFA and CH₃CN+0.08%TFA and column was a Phenomenex Luna C18 5 μ m, 250 x 4.6 mm. The linear gradient was: 0 min: 80%A; 0-15 min: 80-60%A; 15-20 min: 60%A; 20-30 min: 60-80%A. Total run time: 30 min. Flow rate: 0.5 mL/min.

Solid phase synthesis of H-D-Phe-Cys-Phe-D-Trp-Lys-Thr-Cys-Thr-ol (Linear Octreotide)

Linear Octreotide manual syntheses were carried out at room temperature by using Fmoc-Thr(tBu)-ol-Trt-PS resin (0.2 g, loading 1.1 mmol/g) in glass syringes fitted with a polyethylene porous disc, connected to a vacuum source to remove excess of reagents and solvents. After swelling of the resin in 2 mL of the selected solvent (DMF, NBP, NOP or NOP/DMC), Fmoc protective group was removed by 20% piperidine in the selected solvent (2 times $\times 2$ mL, 15 min each), then the resin was washed (3 times $\times 1.5$ mL, 1 min each). Fmoc-Cys(Trt)-OH, Fmoc-Thr(tBu)-OH, Fmoc-Lys(Boc)-OH, Fmoc-D-Trp(Boc)-OH, Fmoc-Phe-OH, Fmoc-Cys(Trt)-OH, Fmoc-D-Phe-OH (three-fold excess with respect to the loading of the resin) were pre-activated by OxymaPure® and DIC (three-fold excess of the reagents with respect to the loading of the resin) for 3 minutes and coupled to the resin for 60 minutes. In case of the first inserted Fmoc-Cys(Trt)-OH (Cys⁷ in the final sequence) the coupling was repeated a second time. After each coupling step the Fmoc protective group was removed by treating the peptide resin with 20% piperidine in the selected solvent (2 times $\times 2$ mL, 15 min each), and the resin was washed (3 times $\times 1.5$ mL, 1 min each). After Fmoc cleavage of the *N*-terminal amino group the peptide resin was further washed with DCM (3 times $\times 2$ mL, 1 min each) and dried under vacuum for 12 hours. Dry peptide resin was suspended in 5 mL of the mixture TFA/TIS/1-dodecanethiol (90/5/5 v/v/v) and stirred for 4 h. The resin was filtered off, washed with TFA (1 time $\times 1$ mL, 1 min) and diisopropylether (25 mL) cooled to 4 °C was added to the solution dropwise. The peptide was filtered and dried *in vacuo* to obtain crude linear octreotide. HPLC purities calculated as sum of all target molecule adducts are reported in Table 8.

Automated syntheses of linear Octreotide was performed at room temperature with CSBio-CS136X peptide synthesizer using the same conditions reported for manual protocol with the only exception that the mixture NOP/DMC 80:20 was used as solvent through all the steps (Fmoc cleavage, coupling, washings).

Final global deprotection/cleavage on dry resin was carried out analogously to the manual synthesis. Related chromatograms and MS spectra are reported in the Supporting Information.

For HPLC separation, mobile phases A and B were H₂O+0.08%TFA and CH₃CN+0.08%TFA and column was a Phenomenex Luna C18 5 μ m, 250 \times 4.6 mm. The linear gradient was: 0 min: 80%A; 0-15 min: 80-60%A; 15-20 min: 60%A; 20-30 min: 60-80%A. Total run time: 30 min. Flow rate: 0.5 mL/min.

Solvent/base recycling

Deprotection stream waste (including washings) and coupling stream waste (including swelling and washings) were collected separately and directly distilled under vacuum. When SPPS of linear Octreotide was performed in NOP alone, the recovery of the deprotection waste was obtained by initially setting vacuum to 25 mmHg and temperature at 40 °C to recover piperidine (95% yield), then increased to 0.25 mmHg (temperature 130 °C) to collect NOP (85% yield). Coupling waste was directly distilled under high vacuum since only NOP was recovered (85%).

When SPPS of linear Octreotide was performed in NOP/DMC 80:20, the recovery of the deprotection waste was obtained by initially setting vacuum to 25 mmHg and temperature at 40 °C to recover piperidine (95% yield) and DMC (95% yield) together, then increased to 0.25 mmHg (temperature 130°C) to collect

NOP (85% yield). In the same way, coupling waste was distilled in two steps allowing the recovery of DMC first (95%), then of NOP (85%) under higher vacuum.

Author contributions

G.M. and P.C. equally contributed to the research. A.T., W.C., A.R. and M.M. designed research; G.M., P.C., A.M., L.F., D.C., T.F. and F.F. performed experiments; A.T., W.C. and F.V. analyzed data and all authors contributed to writing the manuscript.

Conflicts of interest

There are no conflicts to declare.

Acknowledgements

We kindly acknowledge Alma Mater Studiorum University of Bologna, University of Parma and Fresenius kabi for financial support. We thank METCO srl (Monteveglia, Bologna, Italy) for kind support.

Notes and references

1. B. R. Merrifield, *J. Am. Chem. Soc.*, 1963, **85**, 2149.
2. B. L. Bray, *Nat. Rev. Drug Discovery* 2003, **2**, 587.
3. B. G. de la Torre, F. Albericio, *Molecules* 2020, **25**, 2293.
4. A. A. Zompra, A. S. Galanis, O. Werbitzky, F. Albericio, *Futur. Med. Chem.* 2009, **1**, 361.
5. a) T. Nuijens, A. Toplak, M. Schmidt, A. Ricci, W. Cabri, *Frontiers Chem.* 2019, **7**, 829. b) A. M. Weeks, J. A. Wells *Chem. Rev.* 2020, **120**, 3127.
6. S. Kitada, S. Fujita, Y. Okada, S. Kim, K. Chiba *Biorg. Chem. Med. Lett.* 2011, **21**, 4476.
7. J. H. Rasmussen, *Bioorg. Med. Chem.* 2018, **26**, 2914.
8. A. Isidro-Llobet, M. N. Kenworthy, S. Mukherjee, M. E. Kopach, K. Wegner, F. Gallou, A. G. Smith and F. Roschangar, *J. Org. Chem.*, 2019, **84**, 4615.
9. a) P. H. Martin, G. Egelund, H. Johansson, S. Thordal LeQuement, F. Wojcik and D. Sejer Pedersen, *RSC Adv.*, 2020, **10**, 42457. b) G. Martelli, L. Ferrazzano, A. Tolomelli, A. Ricci, W. Cabri, *Chemistry Today* 2020, **38**, 14. c) C. De Luca, S. Felletti, G. Lievore, A. Buratti, S. Vogg, M. Morbidelli, A. Cavazzini, M. Catani, M. Macis, A. Ricci, W. Cabri, *Journal of Chromatography A* 2020, **1625**, 461304. d) I. Guryanov, A. Orlandin, A. Viola, B. Biondi, F. Formaggio, A. Ricci, W. Cabri, *Org. Process Res. Dev.* 2020, **2**, 274.
10. K. Wegner, D. Barnes, K. Manzor, A. Jardine, D. Moran, *Green Chem. Lett. and Rev.* 2021, **14**, 152;
11. a) D. Prat, A. Wells, J. Hayler, H. Sneddon, C. Robert McElroy, S. Abou-Shehadad, P. J. Dunne *Green Chem.*, 2016, **18**, 288; b) R. K. Henderson, C. Jimenez-Gonzalez, D. J. C. Constable, S. R. Alston, G. G. A. Inglis, G. Fisher, J. Sherwood, S. P. Binks, A. D. Curzons *Green Chem.*, 2011, **13**, 854 c) C. J. Clarke, W.-C. Tu, O. Levers, A. Bröhl and J. P. Hallett, *Chem. Rev.*, 2018, **118**, 747 d) S. L. Giudicessi, S. L. Saavedra, A. B. Cardillo, S. A. Camperi, O. Cascone, F. Albericio, M. C. Martínez Ceron. in *Green Sustainable Process for Chemical and Environmental Engineering and Science - Solvents for the Pharmaceutical*

- Industry*; Chapter 5 : Green solvents in the biotechnology-based pharmaceutical industry, 2021, 87.
12. ECHA reference for DMF: <https://echa.europa.eu/it/registration-dossier/-/registered-dossier/13179>. The registration that is only referred to European countries is supporting use, storage and transportation of $\geq 10\,000$ to $< 100\,000$ tonnes per annum.
 13. ECHA reference for NMP see: a) <https://echa.europa.eu/it/registration-dossier/-/registered-dossier/15493/1>. The registration that is only referred to European countries is supporting use, storage and transportation of $\geq 10\,000$ to $< 100\,000$ tonnes per annum.
 14. M. C. Bryan, P. J. Dunn, D. Entwistle, F. Gallou, S. G. Koenig, J. D. Hayler, M. R. Hickey, S. Hughes, M. E. Kopach, G. Moine, P. Richardson, F. Roschangar, A. Steven, F. J. Weiberth *Green Chem.*, 2018, **20**, 5082
 15. Y. E. Jad, G. A. Acosta, T. Govender, H. G. Kruger, A. El Faham, B. G. de la Torre, F. Albericio, *ACS Sus. Chem. Eng.* 2016, **4** (12), 6809.
 16. Y. E. Jad, G. A. Acosta, S. N. Khattab, B. G. de la Torre, T. Govender, H. G. Kruger, A. El Faham, F. Albericio, *Org. Biomol. Chem.* 2015, **13**, 2393.
 17. Y. E. Jad, G. A. Acosta, S. N. Khattab, B. G. de la Torre, T. Govender, H. G. Kruger, A. El Faham, F. Albericio, *Amino Acids*, 2016, **48**, 419.
 18. A. Kumar, Y. E. Jad, J. M. Collins, F. Albericio, B. G. de la Torre, *ACS Sus. Chem. Eng.* 2018, **6**, 8034.
 19. A. Kumar, Y. E. Jad, A. El-Faham, B. G. de la Torre, F. Albericio, *Tetrahedron Lett.* 2017, **58** (30), 2986.
 20. S. B. Lawrenson, R. Arav and M. North, *Green Chem.*, 2017, **19**, 1685.
 21. S. Lawrenson, M. North, F. Peigneguy, A. Routledge *Green Chem.*, 2017, **19**, 952.
 22. a) J. Lopez, S. Pletscher,, A. Aemissegger, C. Bucher and F. Gallou, *Org. Process Res. Dev.*, 2018, **22**, 494. b) A. Kumar, M. Alhassan, J. Lopez, F. Albericio, B. G. de la Torre, *ChemSusChem*, 2020, 5288.
 23. L. Ferrazzano, D. Corbisiero, G. Martelli, A. Tolomelli, A. Viola, A. Ricci and W. Cabri, *ACS Sus. Chem. Eng.*, 2019, **7**, 12867.
 24. J. Pawlas, J. H. Rasmussen *Green Chem.* 2019, **21**, 5990.
 25. F. Dettner (Bachem Americas), Tides – Oligonucleotide and peptide therapeutics, September 15-18, 2020, oral communication.
 26. J. Pawlas, B. Antonic, M. Lundqvist, T. Svensson, J. Finnman and J. H. Rasmussen, *Green Chem.*, 2019, **21**, 2594.
 27. B. A. Pethica, L. Senak, Z. Zhu, A. Lou, *Colloids Surf. A: Physiochem. Eng. Asp.* 2001, **186**, 113
 28. Surfadone™ LP100 is a registered trademark by Ashland: <https://www.ashland.com/industries/energy/oil-and-gas/surfadone-wetting-agent>.
 29. F. Zhou, B. Zhang, H. Liu, Z. Wen, K. Wang, G. Chen, *Org. Proc. Res. Dev.* 2018, **22**, 504–511.
 30. R. Mariscal, P. Maireles-Torres, M. Ojeda, I. Sádaba, M. López Granados, *Energy Environ. Sci.*, 2016, **9**, 1144,
 31. J. F. White, J. E. Holladay, A. A. Zacher, J. G. Frye Jr., T. A. Werpy, *Top Catal.*, 2014, **57**, 1325.
 32. M. Ventura, · A. Marinas, · M. E. Domine, *Top. Catal.*, 2020, **63**, 846.
 33. a) DMF: ECHA, <https://echa.europa.eu/it/registration-dossier/-/registered-dossier/15093/7/3/1>; b) NMP: ECHA, <https://echa.europa.eu/it/registration-dossier/-/registered-dossier/15493/7/3/1>; NBP: ECHA, <https://echa.europa.eu/it/registration-dossier/-/registered-dossier/10579/7/3/1>; NOP: <https://echa.europa.eu/it/registration-dossier/-/registered-dossier/16946/7/3/1>.
 34. B. K. Schindler, S. Koslitz, S. Meier, V. N. Belov, H. M. Koch, T. Weiss, T. Brüning and H. U. Käßlerlein, *Anal. Chem.* 2012, **84** (8), 3787.
 35. F. Albericio, A. El-Faham. *Org. Process Res. Dev.*, 2018, **22**, 760.
 36. C. Amadi-Kamalu, H. Clarke, M. McRobie, J. Mortimer, M. North, Y. Ran, A. Routledge, D. Sibbald, M. Tickias, K. Tse, H. Willway, *Chemistry Open*, 2020, **9**, 431.
 37. Y. Ran, F. Byrne, I. D. V. Ingram and M. North, *Chem.Eur. J.*, 2019, **25**, 4951.
 38. C. Liang, M. A. Behnam, T. R. Sundermann and C. D. Klein, *Tetrahedron Lett.*, 2017, **58**, 2325.
 39. M. Paradis-Bas, J. Tulla-Puche, F. Albericio. *Chem. Soc. Rev.* 2016, **45** (3), 631.
 40. Y. E. Jad, T. Govender, H. G. Kruger, A. El-Faham, B. G. de la Torre and F. Albericio, *Org. Process Res. Dev.*, 2017, **21**, 365.
 41. S. W. J. Lamberts and L. J. Hofland, *Eur. J. Endocrin.* 2019, **181**, R173
 42. B.M. Pastore, M. J. Savelski, C. S. Slater, F. A. Richetti , *Clean Techn Environ Policy*, 2016, **18**, 2635.
 43. J. Pawlas, T. Nuijens, J. Persson, T. Svensson, M. Schmidt, A. Toplak, M. Nilsson, Rasmussen *Green Chem.*, 2019, **21**, 6451.

ARTICLE

Steps towards sustainable Solid Phase Peptide Synthesis: use and recovery of *N*-octyl pyrrolidone.

Received 00th January 20xx,
Accepted 00th January 20xx

DOI: 10.1039/x0xx00000x

Giulia Martelli,^a Paolo Cantelmi,^a Alessandra Tolomelli,^{*a} Dario Corbisiero,^a Alexia Mattellone,^a Antonio Ricci,^b Tommaso Fantoni,^a Walter Cabri,^{*a} Federica Vacondio,^c Francesca Ferlenghi,^c Marco Mor^c and Lucia Ferrazzano.^a

The investigation of new green biogenic pyrrolidinones as alternative solvents to *N,N*-dimethylformamide (DMF) for solid phase peptide synthesis (SPPS) led to the identification of *N*-octyl pyrrolidone (NOP) as the best candidate. NOP gave good performances in terms of swelling, coupling efficiency and low isomerization generating peptides with a very high purity. The mixture of NOP with 20% dimethyl carbonate (DMC) allowed to decrease solvent viscosity making the mixture suitable for the automated solid-phase protocol. Aib-enkephalin and linear Octreotide were successfully used to test the methodologies. It is worth noting that NOP, DMC and the piperidine used in the deprotection step could be easily recovered by direct distillation from the process waste mixture. The process mass intensity (PMI), being reduced by 63–66%, achieved an outstanding value representing a clear step forward in SPPS greening.

Introduction

The development of the solid-phase peptide synthesis (SPPS) that originates from the seminal work of Bruce Merrifield back in the sixties,¹ gave access to previously unavailable long peptides via iterative formation of amide bonds.² Thanks to SPPS availability and its automation, polypeptides became a target for medicinal chemists. This modality is playing a major role in modern therapeutics,³ with more than 70 peptides on the market and about >100 in clinical trial advanced stages.

The different synthetic strategies for peptide synthesis have been clearly described by Albericio in 2009.⁴ Since then, only two novel industrial technologies have been reported, the enzymatic approach by Enzyper⁵ and the hiving technology by Jitsubo.⁶ However, SPPS is still the core technology for peptide synthesis and several research groups are now focusing the attention on the optimization of every single step to increase process greenness.^{7,8,9}

Almost complete conversions are achieved thanks to the use of reagents in excess that can be removed by extensive washing and filtration of the solid support anchored growing peptide. Therefore, in considering process greening, a fundamental role is played by the solvents.^{10,11}

N,N-dimethylformamide (DMF) is technically the perfect solvent for SPPS. However, its toxicological profile¹² is a serious matter of concern in the pharmaceutical industry. In fact, DMF and its most

common substitute, *N*-methylpyrrolidone (NMP)¹³ are reprotoxic and were labeled as hazardous; accordingly, their replacement has been considered “advisable or requested” by the ACS Green Chemistry Institute® Pharmaceutical Round Table (GCIPR)¹⁴ that defined this goal one of the hot topics in the list of the 12 green chemistry key research areas (KRAs). The development of innovative and general methods for sustainable amide bonds formation and peptide synthesis has been also reported in the updated version of the list of priorities.

On the basis of these considerations, selection of greener alternatives needs to keep into consideration the sustainability and the toxicity to natural environment and human health in the whole solvent lifecycle.

Several solvents have been reported to be suitable for a greener SPPS (GSPPS), such as, 2-methyl tetrahydrofuran (2-MeTHF),¹⁵ acetonitrile (ACN) and THF,¹⁶ 2-MeTHF and cyclopentyl methyl ether (CPME),¹⁷ γ -valerolactone (GVL)¹⁸ and *N*-formylmorpholine (NFM),¹⁹ propylene carbonate (PC),²⁰ dimethylisobutyl ether (DMIE),²¹ and *N*-butyl pyrrolidone (NBP).²² Green solvents mixtures affording proper physicochemical properties for all the steps of solid phase processes, Cyrene®/diethyl carbonate (DEC), sulfolane/DEC, anisole/dimethyl carbonate (DMC),²³ dimethyl sulfoxide (DMSO)/ethyl acetate (EtOAc)²⁴ and NFM/1,3-dioxolane (DOL)²⁵ have been also explored. However, some of these solvents like EtOAc, 1,3-dioxolane or 2-MeTHF do not have the optimal characteristics for industrial application because of their low flash point.

In this context, the family of *N*-alkylpyrrolidones may offer new opportunities since, although having a similar structure to NMP, they display a completely different metabolic profile, they are not toxic or reprotoxic and they still retain the main features of the parent dipolar aprotic solvent. NBP has recently been applied by both academia and industrial researchers to SPPS on polystyrene-based resins, affording crude peptides with comparable quality to those synthesized in DMF. In addition, NBP was also employed in mixture with ethyl acetate providing interesting results.²⁶

We have explored herein the characteristics of *N*-alkylpyrrolidones and their use in SPPS, focusing our attention on safest members of

^a Department of Chemistry Giacomo Ciamician
Alma Mater Studiorum, University of Bologna
Via Selmi, 2 40136-BO, Italy

E-mail: alessandra.tolomelli@unibo.it; walter.cabri@unibo.it

^b Fresenius kabi iPsum

via San Leonardo 23, 45010-RO, Italy

^c Department of Food and Drug Sciences
University of Parma

Parco Area delle Scienze 27/a, 43124-Parma, Italy

† Electronic Supplementary Information (ESI) available. See
DOI: 10.1039/x0xx00000x

this class as *N*-octyl-2-pyrrolidone (NOP), *N*-cyclohexyl-2-pyrrolidone (NCP) and *N*-benzyl-2-pyrrolidone (NBnP).

Aiming to the widest application, we have defined protocols for manual or automatic SPPS, decreasing the PMI (product mass intensity) by solvent recycling.

Results and discussion

N-Alkylpyrrolidones chemical-physical parameters, toxicological data and *in vitro* metabolism

In the selection of suitable candidates for DMF or NMP replacement for GSPPS, chemical-physical parameters are the first characteristics to be evaluated (Table 1).

N-alkylpyrrolidones share as a common feature the lack of acid protons, while the elongation of the alkyl chain consistently decreases their polarity moving from NMP to NBnP.

The high boiling point of this family of compounds, together with their high flash point temperatures (always > 100°C, except for NMP), are interesting characteristics for industrial application since there are no safety concerns and solvents **can be recovered by distillation**.

Table 1. Chemical-physical parameters of *N*-alkylpyrrolidones^a

Solvent	Viscosity at 25°C (mPa·s)	Flash point (°C)	Boiling point °C (pressure mmHg)
DMF	0.8	58	36 (1)
NMP	1.65	91	68 (4)
NBP	4.0	108	80-85 (0.5)
NOP	6.6	142	114-115 (0.8)
NCP	11.5	141	94-97 (0.5)
NBnP	21.4	113	124-125 (0.8)

^a See ref. 22a and 27

Concerning *N*-alkylpyrrolidones' viscosity, the observed values may represent a challenge for large-scale application in automated syntheses, since difficulties in transfer and purging may occur. Anyway, a viscosity close to 4 mPa·s is considered acceptable, if efficiency of all the steps of SPPS (swelling, coupling, protecting group cleavage) is maintained.^{9a} In this context, the simple addition of a low viscosity green cosolvent is a viable solution to overcome this specific issue.

In the perspective of the industrial application of new SPPS protocols, low cost, bulk availability and reliability of the supply chain of the solvent has also to be ensured. Among the other pyrrolidones, NOP is also known as Surfadone™ LP-100²⁸ and is widely used as a low-foaming non-ionic rapid wetting agent and dynamic surface tension modulator in cosmetic industry, pigment industry, cleaning detergent production and polymer manufacturing. For this reason, its price is comparable to that of the most common solvents (about 1-2\$/kg). The industrial preparation of NMP is predominantly derived from the reaction of γ -butyrolactone (GBL) with monomethylamine.²⁹ Similarly, other *N*-alkylpyrrolidones can be prepared using the corresponding amines. Even if GBL is commonly prepared *via* petrochemical route from succinic anhydride or succinic acid, it could be obtained also by fermentation of sugar, and hence be transformed from a fossil-based reagent to a renewable source.³⁰ **However, the cost of fermentations and the difficulties in treating complex biomass-deriving matrices are still challenges to be tackled³¹ and, even if the research on biorefineries is advanced, technological implementation is hampered by a low profitability.³² Commercially available pyrrolidones are currently not prepared from**

biogenic GBL, but with a perspective of novel economically viable biomass treatment protocols, they might be included in the future in the list of biogenic solvents, displaying a high potential for more sustainable chemical approaches. In this context, since it will become inevitable to move away from a petroleum-based society, scientific and technological efforts to turn these sustainable alternatives into industrially feasible solutions are mandatory.

Considering this aspect, pyrrolidones may be included in the list of biogenic solvents and show a high potential in a more sustainable chemical approach.

Table 2. Toxicity parameters of solvents evaluated in this study in comparison with DMF and NMP³³

Solvent	Acute Oral Toxicity (mg/kg bw)	Acute Inhalation Toxicity	Acute Dermal Toxicity (mg/kg bw)	Reproductive Toxicity
DMF	3010	> 5.8 mg/L air	> 3160	Yes
NMP	150	> 5.1 mg/L air	> 5000	Yes
NBP	300	> 5.1 mg/L air	> 2000	No
NOP	> 2200	n.a.	> 4000	No
NCP	370	n.a.	1600	No
NBnP	n.a.	n.a.	n.a.	n.a.

n.a.: not available

Data reported in Table 2 clearly show that NOP, among the *N*-alkyl pyrrolidones, is the safest one, being not reprotoxic and with very high tolerability when administered orally or intradermally.

The metabolism of these products generally shows oxidation at the 5 position of the lactam ring and on the first carbon of the *N*-alkyl side chain. Through this pathway NMP generated consistent quantities of the masked formaldehyde.³⁴

When NOP was incubated in the presence of rat (RLM) and human liver microsomes (HLM), it was rapidly cleared with an average half-life ($t_{1/2}$) of 11.5 (\pm 2.0) min in RLM and 23.8 (\pm 5.6) min in HLM (Fig. 1).

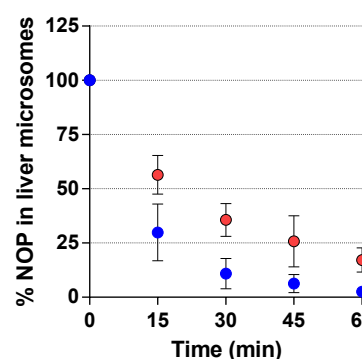


Fig.1 In vitro metabolic stability of *N*-octyl pyrrolidone (NOP). Time course of NOP stability in rat (blue circles) and human (red circles) liver microsomes.

In vitro metabolism of NOP in RLM and HLM were very similar and led to the formation of several metabolites (M1-M11, Fig.2, Fig. S1 and Table S1, Supporting Information). The major one was **M1** (RT = 3.19 min; Fig. 2) having a m/z value of 212.1642, with a mass shift of

14 Da with respect to NOP. As shown in Fig.2 and Table S1, besides **M1**, other minor metabolites were observed. A cluster of metabolites (**M6**, **M7**, **M9-11**) displaying a mass shift M+16 with respect to NOP, suggests a hydroxylation reaction (+O) while keto metabolites (**M1**, **M2**, **M3**, **M4**, **M5**, **M8**) displaying a mass shift M+14 (+O-2H) derive as second-generation metabolites from dehydrogenation of hydroxylated ones. This is compatible with an oxidation reaction of a methylene to keto group involving either the 2-pyrrolidone ring or the N-octyl side chain of NOP. Low and High energy mass spectra related to either keto or mono-hydroxylated metabolites **M1-M11** are reported in the Supporting Information as Fig. S4-S14.

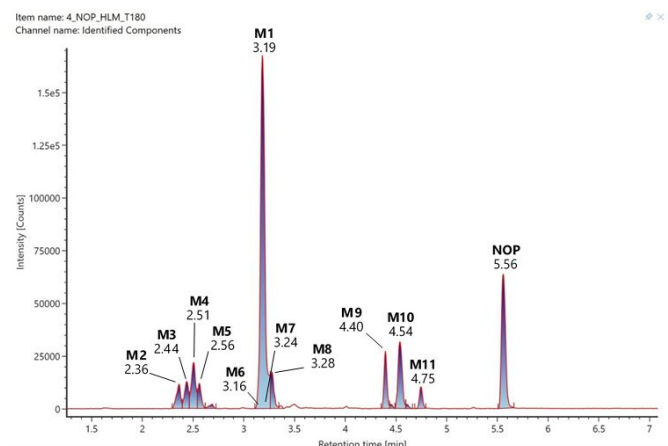


Fig. 2. HPLC-MS/MS trace of a HLM incubation of N-octyl pyrrolidone (NOP) at $t=3h$. Parent compound NOP and metabolites **M1-M11** are reported together with their RT. The most abundant metabolite (**M1**, with a mass shift of + 14 with respect to NOP) and two minor metabolites (**M6** and **M7**, with a mass shift of + 16 with respect to NOP) co-elute. Co-eluting metabolites are detectable as Extracted Ion Chromatograms in Fig. S3, Supporting information.

Effect of N-Alkylpyrrolidones as solvents in key steps of SPPS

Solvents for SPPS need to fulfill a series of requirements at the same time: good swelling efficacy for different resins, ability to completely

solubilize amino acids, coupling reagents and related by-products, promotion of both coupling and deprotection steps. Consequently, before testing pyrrolidones in SPPS protocols, we firstly evaluated separately their efficiency in all these steps.

Solubility tests

To evaluate the suitability of the selected solvents in SPPS, their ability to solubilize commonly employed protected amino acids and coupling reagents was investigated. Fmoc-Val-OH was initially selected as the reference amino acid, demonstrating a perfect solubilisation in all the tested solvents (NOP, NCP and NBnP) at a standard 0.2 M concentration (Table 3). The same dissolution protocol was applied to the main coupling reagent combinations: OxymaPure®/DIC (**A**), COMU/DIPEA (**B**), PyBOP/DIPEA (**C**), PyOxyma/DIPEA (**D**), HOBt/DIC (**E**), and HBTU (**F**) (Table 4). Optimal results were generally achieved, except for HBTU (**F**), which was scarcely dissolved in all the solvents and was hence excluded from further studies. The solubility screening was then extended to Fmoc-protected natural and non-natural amino acids (Fmoc-Gly-OH, Fmoc-Ala-OH, Fmoc-Aib-OH, Fmoc-Phe-OH, Fmoc-Tyr(tBu)-OH, Fmoc-Lys(Boc)-OH, Fmoc-Cys(Trt)-OH, Fmoc-Pro-OH and Fmoc-Thr(tBu)-OH) that were dissolved at a 0.2 M concentration, both alone and in the presence of the aforementioned additives after a 5 minutes pre-activation (Table 3 and Table S2).

Solubility issues were detected in case of Fmoc-Cys(Trt)-OH, but decreasing the concentration to 0.1 M, a slightly lower value than the standard used in SPPS, good solubility was recovered in NCP, even if not in NBnP (Table 3). When the amino acids were mixed with coupling additives, only in sporadic cases the solubility was incomplete, requiring an extra-dilution to observe clear solutions. Fmoc-Cys(Trt)-OH demonstrated in this case a good solubility when combined with OxymaPure®/DIC (**A**) and COMU/DIPEA (**B**) in NOP and NCP, overcoming the above reported limited solubility of the pure Fmoc-protected amino acid. On the other hand, NBnP was not able to dissolve this amino acid, even in combination with coupling reagents or in more dilute solutions (Table S2).

Overall, OxymaPure®/DIC and COMU/DIPEA showed to be the best coupling systems because of their general good results with all solvents and amino acids (see Figures S16-S18 in Supporting Information).

Table 3. Solubilisation efficacy of Fmoc-AA(PG)-OH amino acids in N-alkylpyrrolidones^a

Fmoc-AA(PG)-OH										
Solvent	Val	Gly	Ala	Aib	Phe	Pro	Tyr(tBu)	Thr(tBu)	Lys(Boc)	Cys(Trt)
NOP										
NCP										0.1 M
NBnP										0.1 M

^aSolubilisation monitored at 0.2M concentration unless 0.1M is specified. Legend: green=soluble; yellow=moderately soluble; red=insoluble. PG: protecting groups

Table 4. Solubilisation efficacy of coupling reagents A-F and Fmoc-Val-OH with A-E in N-alkylpyrrolidones^a

Solvent	Coupling reagents						Mixture Fmoc-Val-OH + coupling reagents (A-E)				
	OxymaPure®/DIC A	COMU/DIPEA B	PyBop/DIPEA C	PyOxyma/ DIPEA D	HOBt/DIC E	HBTU F	Val+A	Val+B	Val+C	Val+D	Val+E
NOP											
NCP											
NBnP											

^aLegend: green=soluble; yellow=moderately soluble; red=insoluble

ARTICLE

To notice, OxymaPure®/DIC has been reported over the last ten years as a high-efficient coupling agent able to reduce racemization with performances overcoming those displayed by most of the common analogues.³⁵

Swelling tests

The first key step in SPPS is the choice of the resin and its swelling. A suitable solvent should be able to properly swell different commercially available resins, demonstrating the broadest applicability. Polystyrene based resins (PS-resins) cross-linked with 1–2% of divinylbenzene are the most commonly used due to their mechanical and chemical stability as well as for the low cost and bulk availability, but also TentaGel-based resins, made of a polystyrene (PS)/polyethylene glycol (PEG) network are often used for their increased compatibility with polar solvents. PEG-based resins, commonly known as ChemMatrix resins (CM), have recently received great attention for the good performances reported in the synthesis of long peptides. On these basis, cross-linked polystyrene (PS - Merrifield), PEG-PS (TentaGel – TG) and pure PEG-based (ChemMatrix - CM) resins were considered for swelling with *N*-alkylpyrrolidones. Moreover, different acid-sensitive linkers were considered for each matrix: Wang and Trt-Cl linkers for obtaining the final peptide as a C-terminal acid, and Rink Amide linker for a C-terminal amide peptide. Details on bead size, loading and cross-linking of the selected resins are reported in Table S3.

Recently Amadi-Kamalu *et al.*³⁶ developed a model to predict resin swelling in a given solvent, highlighting how the solvent-resin interaction is a complex process especially as the swelling could be related to physical parameters such as bead size and degree of cross-linking. Anyway, experimental evaluation of swelling still represents the most reliable method and reported protocols were applied for all the solvent/resin combinations.^{20,37}

Briefly, a dry resin sample in the desired solvent was allowed to mildly shake in a graduated syringe for 30 minutes; after 5 minutes of re-equilibration, solvent was removed under vacuum and the volume increase of the resin was measured (mL·g⁻¹).

In general, solvents giving resin swellings higher than 4 mL·g⁻¹ are considered good, values between 2 and 4 mL·g⁻¹ correspond to moderately good solvents and swelling lower than 2 mL·g⁻¹ identifies poor candidates.

Table 5. Swelling^a of resins in DMF and pyrrolidones at RT after 30 mins

Resin	DMF (mL·g ⁻¹)	NOP (mL·g ⁻¹)	NCP (mL·g ⁻¹)	NBnP (mL·g ⁻¹)
PS-Wang	5.6	5.5	5.1	2.3
PS-Trt-Cl	3.2	3.4	3.6	1.6
PS-RinkAmide	3.2	1.6	1.6	1.6
TG-Wang	6.0	1.7	2.5	1.3
TG-RinkAmide	6.2	4.3	3.4	4.0
CM-Wang	4.4	1.4	1.6	1.6
CM-RinkAmide	7.8	3.4	6.1	6.7

^aData reported are the average of triplicate measurements, see Table S4 in Supporting Information.

Noteworthy, the degree of swelling should not greatly overcome 4 mL·g⁻¹ since a large volume of solvent would lead to reagents dilution. However, the swelling is considered acceptable if it corresponds to ±30% of the measured volume for DMF.²²

The measured swelling values of pyrrolidones and DMF are reported in Table 5 as a mean value of analyses in triplicate.

NOP and NCP afforded excellent swelling of PS-based resins, commonly employed for industrial purposes and resulted comparable to DMF in swelling the Wang linker. Moreover, better results were observed with Trt-Cl resin. This behaviour suggests that these solvents display a higher affinity to less polar resin matrixes. Concerning 100% PEG-based resins, acceptable results were found for CM-RinkAmide when NCP and NBnP were used, the last one affording a 15% lower swelling in comparison to DMF. Overall, *N*-alkylpyrrolidones cover a satisfying range of applicability since acid terminating peptides can be prepared using PS-Wang or PS Trt-Cl resin with NOP and NCP while amide peptides may be synthesized using CM-RA resin with NCP or NBnP.

Coupling reaction in solution phase

The efficiency of pyrrolidones in promoting the coupling step was first investigated in liquid phase. Accordingly, the synthesis of model dipeptide¹⁷ Z-Phg-Pro-NH₂ was performed in the selected solvents (NOP, NCP, NBnP) and in DMF as benchmark reaction, screening different coupling reagent combinations, and checking both the conversion and the racemization degree (Table 6).

Measuring the racemization ratio is fundamental to predict the efficiency of the solvent in SPPS couplings, and its inhibition is necessary to avoid further purifications and low final yields. Dipeptide Z-Phg-Pro-NH₂ is particularly prone to racemization due to the acidity of the benzylic α-proton in Phg.³⁸ Moreover, proline reacts slower than other amino acids and achieving a complete conversion represent the main hurdle.

All the couplings were performed using (L)-amino acids and the crude was analysed by HPLC-MS injection after 3 h, in order to determine the dipeptide conversion and the racemization degree. The couplings were performed with equimolar amounts of the two amino acids and with a concentration of 0.125 M. The conversions were generally good in all conditions; moreover, DIC/OxymaPure® system provided only about 1% racemization in pyrrolidones (Table 6, entry 6, 11, 16), less than what observed in DMF. PyBOP/HOBT/DIPEA and HOBT/DIC combination afforded high level of racemization in all the solvents tested, including DMF. COMU/DIPEA and PyOxyma/DIPEA showed better values than the latter two combinations, but resulted generally less effective than DIC/OxymaPure®.

Considering these data, together with the solubilisation screening of coupling reagents and activated amino acids, DIC/OxymaPure® was considered the best system for further investigations. This choice was supported also by their very low cost, essential requirement for SPPS use on industrial scale.

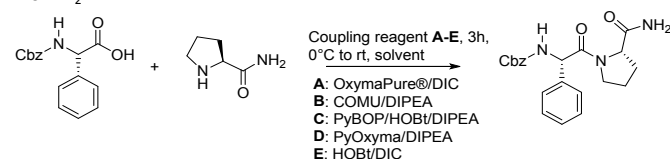
Deprotection kinetic tests

To develop a total DMF-free method, a solvent displaying excellent behaviour in the deprotection step is a fundamental tool. In this

context, the removal of Fmoc group was investigated in liquid-phase to evaluate the effect of the solvent and avoid possible interference of resin swelling or peptide aggregation issues that could occur in solid-phase.³⁹ Piperidine is the base of choice in Fmoc SPPS, due to its role as fast deprotecting agents and dibenzofulvene scavenger. Accordingly, tests were conducted using a 20% piperidine solution to investigate deprotection kinetic, as commonly reported in SPPS protocols.^{9a}

Qualitative kinetic tests on Fmoc-Phe-OH deprotection were carried out according to the method developed by Jad *et al.*⁴⁰ and deprotection rates were monitored by HPLC-MS at fixed time intervals.

Table 6. Conversion (%) and racemization ratio (%) in the synthesis of Z-Phg-Pro-NH₂^a



Entry	Solvent	Coupling Reagent	DL (%) ^b	Conversion (%)
1	DMF	A	1.9	92
2		B	0.9	99
3		C	24.1	98
4		D	1.0	87
5		E	13.2	85
6	NOP	A	0.9	95
7		B	6.6	82
8		C	17.1	94
9		D	2.5	96
10		E	11.7	99
11	NCP	A	1.1	96
12		B	2.2	82
13		C	21.6	92
14		D	2.3	83
15		E	13.2	99
16	NBnP	A	1.4	99
17		B	1.6	99
18		C	32.1	99
19		D	0.7	95
20		E	10.0	99

^aAll the reactions were performed pre-activating (3 min) Z-Phg-OH. Conversion and racemization were calculated by HPLC. ^bDefined as (Z-D-Phg-Pro-NH₂)/(Z-L-Phg-Pro-NH₂) × 100. The DL epimer was identified after synthesis of Z-D-Phg-Pro-NH₂ where Z-D-Phg-OH was used as a starting material.

Fmoc-Phe-OH deprotection was also tested in DMF and NBP as a comparison. Reaction was considered complete at disappearance of the HPLC peak corresponding to Fmoc-Phe-OH; notably, the reactions performed in all investigated pyrrolidones revealed complete Fmoc removal in 2 minutes (see Figures S31-S32 in Supporting information), perfectly in line with DMF performances.

SPPS in environmentally favourable solvents

After investigating the effect of *N*-alkylpyrrolidones as solvents in liquid phase couplings, the study was extended to the SPPS of Aib-enkephalin pentapeptide (H-Tyr-Aib-Aib-Phe-Leu-COOH/COONH₂). Aib residue insertion represents a harsh step because of its steric hindrance that often leads to slow-rate coupling reaction and consequently partial mis-incorporation.¹⁵ The amount of the des-Aib sequences provides a measure of the efficacy of each pyrrolidone in comparison to DMF or standard alternatives.

Aib-enkephalin was manually synthesized on different resin/solvent combinations according to the best swelling results: (i) PS-Wang and PS-Trt-Cl resins with NOP and NCP; (ii) ChemMatrix-RinkAmide (CM-RA) resin with NBnP. Treatment with TFA-based cleavage cocktails afforded the peptide as acid at the C-terminal in case (i) and as amide in case (ii). These conditions also allowed the simultaneous removal of *tert*-butyl group in Tyr side chain. Peptides were assembled on Fmoc-Leu-preloaded resins using 20% piperidine as Fmoc-deprotection agent and DIC/OxymaPure® as coupling reagents. *N*-alkylpyrrolidones were used for all the synthetic steps, including washings. Double Fmoc-Aib-OH couplings were performed in all syntheses, according to common literature procedures.^{15,16,17} HPLC purities of the crudes after cleavage are reported in Table 7.

When the reaction was performed using NOP, excellent purities were observed, providing about 98% of the target pentapeptide and <1% of des-Aib byproduct on Wang resin (entry 1). Less than 3% impurity was generated on TrtCl-resin (entry 2). Interestingly, these results are consistently better than those obtained in the reference solvents DMF and NBP, which provided a des-Aib amount >11% and >8%, respectively (entries 5-6 and 7-8). NCP resulted comparable to DMF in terms of pentapeptide purity, but lower amounts of des-Aib were detected (entries 3-4). NBnP instead demonstrated a very low efficiency since only 4.3% of Aib-enkephalin was detected, while des-Aib tetrapeptide (16%) and other incomplete sequences corresponding to the remaining 80% of the total were identified in the crude (Entry 9).

As a consequence, NCP and NBnP were not further studied while NOP was instead selected as an **ideal greener** alternative to common solvents.

Table 7. HPLC purities for Aib-Enkephalin pentapeptide assembled on different resins and solvents.

Entry	Solvent	Resin ^a	Pentapeptide ^b %	Des-Aib (%)	Other (%)
1	NOP	PS-Wang	97.7	0.8	1.5
2		PS-Trt-Cl	97.4	2.6	-
3	NCP	PS-Wang	88.5	10.5	1.0
4		PS-Trt-Cl	89.9	10.0	1.1
5	DMF	PS-Wang	85.8	14.2	-
6		PS-Trt-Cl	88.1	11.9	-
7	NBP	PS-Wang	91.1	8.9	-
8		PS-Trt-Cl	91.6	8.4	-
9	NBnP	CM-RA	4.3	16.0	79.7
10 ^c	DMF	CM-RA	53.0	47.0	-

^aPre-loaded Fmoc-Leu-resins were used; ^bDouble Fmoc-Aib-OH couplings; ^cfrom Ref.16

Table 8. HPLC Purity of Linear Octreotide in NOP, NOP/DMC, DMF and NBP.

Compound	RRT	NOP	NOP/DMC 80:20 Manual SPPS	NOP/DMC 80:20 Automated SPPS	DMF	NBP
Cyclized N,O shift	0.83	-	-	-	1.4	-
Cyclized	0.88	0.7	-	-	5.8	2.4
TM-N,O shift 1	0.92	1.0	1.4	-	-	0.7
TM-N,O shift 2	0.95	5.2	2.4	2.0	-	4.2
TM+CO ₂	0.97	-	21.6	-	5.1	4.8
TM	1.00	77.6	65.1	86.0	76.8	77.7
TM+Boc	1.10	-	1.7	-	-	-
TM+tBu	1.14	11.7	5.2	10.0	9.0	7.2
TM+Boc2	1.18	-	0.8	-	-	-
TM+tBu2	1.26	3.8	1.8	2.0	1.9	3.0
Product purity (%) ^a		100	100	100	100	100

^aHPLC purity calculated as sum of all target product adducts; RRT = relative retention time

Consequently, more sustainable conditions for SPPS were applied to the synthesis of linear Octreotide (H-D-Phe¹-Cys²-Phe³-D-Trp⁴-Lys⁵-Thr⁶-Cys⁷-Thr⁸-ol), the final intermediate obtained by solid-phase synthesis in the industrial manufacturing of the API Octreotide.

This peptide was one of the first biologically stable somatostatin analogues to be synthesized and used in oncology.⁴¹ The entire protocol was performed with NOP as solvent and compared with reference syntheses in NBP and DMF. Preloaded Fmoc-Thr(tBu)-ol-Trt-PS resin was used, being highly suitable to the synthesis in NOP. Although Octreotide is a medium-length peptide, frequent misincorporation of Cys⁷ residue occurs and for this reason the coupling step to introduce this residue was repeated twice in all the synthetic sequences. Standard 20% piperidine solution and DIC/OxymaPure[®] reagents were employed for deprotection and coupling steps, respectively. HPLC purities of the crudes after cleavage are reported in Table 8. It is important to mention that all the detected species are related to linear Octreotide and hence precursors of the final cyclic API. Des-Cys⁷ or other truncated sequences were never observed.

The excellent results obtained using NOP both in the synthesis of Aib-enkephalin and linear Octreotide showed that its high viscosity value (6.6 mPa·s for NOP vs 4.0 mPa·s for NBP and 0.8 mPa·s for DMF) does not affect the SPPS efficiency. The issue of viscosity anyway has to be considered when moving from manual synthesis to automatic synthesizers. Heating the reaction system had been previously applied as a solution in SPPS in NBP.³⁴ Instead, in order to decrease NOP viscosity and to perform the reaction at automatic synthesizer without heating, DMC (0.59 mPa·s) was selected as co-solvent. In fact, DMC proved to be a good cosolvent for SPPS.²³ Addition of 20% DMC to NOP allowed to decrease the viscosity down to 3.94 mPa·s (see Table S5), thus allowing the use of automated systems. After having evaluated the swelling degree of NOP/DMC 80:20 in the PS resins (see Table S4), the synthesis of linear Octreotide intermediate was repeated using this sustainable solvents' mixture both with manual and automated protocols (Table 8). In both SPPS protocols the final purity was comparable with the corresponding synthesis carried out in DMF, NBP and NOP alone.

Solvent and base recycling

NOP and NOP/DMC proved to be greener alternatives to DMF, however, in order to achieve a truly sustainable protocol, the Process Mass Intensity (PMI) should be decreased by recovering the main source of waste, namely the solvents (NOP or NOP/DMC) and the piperidine used in the deprotection step. NOP offers several

alternatives for the recovery process, being very lipophilic. The final mixtures can be washed with water and then NOP recovered by distillation or it can be directly distilled in order to recycle all the volatile chemicals. DIC cannot be recycled being unstable and almost completely transformed into 1,3-diisopropylurea during the coupling step.

Coupling streams and deprotection streams should be recovered separately in order to avoid piperidine consumption by the excess of Fmoc-amino acids used in the coupling steps. When the green mixture NOP/DMC is used, due to the small difference between piperidine and DMC boiling points (106 °C vs 90 °C at 760 mmHg), these two components are recovered in the same fraction and reused for deprotection steps in further SPPS processes, after rebalancing the required relative ratio.

The results obtained by applying these protocols to the SPPS of linear octreotide in comparison with the DMF standard process are reported in Table 9.

Table 9. Process Mass Intensity (PMI) and recovery in GSPPS

Entry	Solvent ^a	PMI	Waste Stream	Recovery (yield %)	PMI after recovery
1	NOP	722	Depr	NOP (85)	268
			Coupling	Pip ^b (95)	
				NOP (85)	
2	NOP/DMC	748	Depr	NOP (85)	256
			Coupling	DMC/Pip ^b (95)	
				DMC (95)	
3	DMF	735		NOP (85)	

^aThe wastes coming from coupling steps and from deprotection steps were distilled separately. ^bPiperidine (Pip) involved in the formation of DBF-piperidine adduct was subtracted from the total piperidine volume.

The percentage of waste related to the solvents involved in swelling, coupling, deprotection and washing steps is very similar in all different protocols (NOP 67.8%, NOP/DMC 69.0%, DMF 68.4%, see Table S7 and Table S8). Concerning the synthesis performed in NOP (entry 1), piperidine was easily recovered in 95% yield, considering the maximum amount that could be collected. NOP was recovered in the second fraction of condensed liquid in 85% amount. Under these conditions, PMI value for the global process was more than halved (268 with solvent/base recovery vs 722 without).

When the green mixture NOP/DMC was used for the same synthesis (entry 2), distillation of the deprotection streams under vacuum allowed to distil, at 25 mmHg, DMC and piperidine together (95% each) in a 1:0.86 ratio (V/V), as confirmed by ^1H NMR (see Supporting Information). Further, vacuum increase to 0.25 mmHg allowed to recover NOP in 85% yield. Finally, the distillation under vacuum of the coupling wastes allowed to recover in high yield both DMC (95%) and NOP (85%), decreasing the total PMI from 748 (without recovery) to 256. The final waste related to solvent is limited to 10% for the process with NOP and to 8.7% when DMC/NOP were used.

OxymaPure[®] could be isolated from the solid residue following the protocol reported by Rasmussen.²⁴ However, this additional recovery procedure increased the PMI and allowed to isolate OxymaPure[®] in 38% yield; therefore, in our protocol we did not consider coupling agent recovery.

A full evaluation of NOP compared to other solvents commonly used in SPPS should comprise a complete lifecycle perspective of the solvent impact. A quantitative comparison concerning the carbon footprint between SPPS protocols in DMF and NOP cannot be performed due to lack of literature data on NOP. Anyway, for a qualitative estimation, since all the reactants and procedures in the two SPPS protocols are the same, the attention can be exclusively focused on the solvent carbon intensity (contribution to CO_2 emission), considering the primary production and the disposal by incineration or recycling. The production technologies of NMP and NOP are very similar. Thus, the carbon footprint can be calculated from the NMP's one (4.22 kg CO_2/Kg)⁴² by considering a 20-30% increase in carbon content per kg due to the octyl chain and to the higher boiling point. Therefore, the estimated range could be between 5.06-5.49 kg CO_2/kg . The carbon footprint related to DMF production has been reported to be lower than NMP (3.57 kg CO_2/Kg).⁴³ However, NMP recovery by double distillation decreases the carbon footprint by 40%.⁴² On the other hand, NOP can be recovered by single distillation and contribution of this process to carbon footprint is consistently lower than the advantage arising from the reduced amount of virgin solvent required. We can expect to have an impact on NOP recycling on the carbon footprint similar to the one of NMP (>40%).

These considerations allow to rebalance the apparent disadvantages of NOP in comparison with DMF. The comparable carbon footprint combined with the health, environmental and safety data and the future perspective of a sustainable production of NOP from biomasses make this potential solvent a credible sustainable alternative.

Conclusions

The evaluation of alternative green and safe pyrrolidones allowed to identify NOP and NOP/DMC as the best solvents in term of yield and selectivity for SPPS. To test the solvent performances Aib-enkephalin and linear Octreotide were synthesized by SPPS producing the final products in excellent purities using both manual and automated procedures. The solvents and the piperidine could be easily recovered decreasing the process PMI by 63% for NOP protocol and 66% for NOP/DMC one. Selecting green alternatives to dipolar solvents for SPPS is an extensively investigated issue, but the development of a methodology including solvents and reagents recovery and recycle represents a step forward in the achievement of a really green SPPS.

Experimental procedures

General Methods

Unless otherwise stated, all materials, solvents and reagents were obtained from commercial suppliers, of the best grade, and used without further purification. The solvents used were of high-performance liquid chromatography (HPLC) reagent grade. Specifically, Fmoc amino acids and resins were supplied by Iris Biotech, Merck or Fluorochem. Coupling reagents were purchased from Merck or Novabiochem. Piperidine was supplied by Merck. DMF, other organic solvents, and HPLC-quality acetonitrile (CH_3CN) were purchased from Merck. Milli-Q water was used for RP-HPLC analyses. NOP was purchased Merck.

Solid-phase synthesis of the peptides was carried out manually or using CSBio-CS136X peptide synthesizer (automated syntheses).

HPLC-MS analyses were performed on Agilent 1260 Infinity II system coupled to an electrospray ionization mass spectrometer (positive-ion mode, m/z = 100–3000 amu, fragmentor 30 V), using columns Agilent Zorbax-SB-C18 5 μm , 250 x 4.6 mm or Phenomenex Luna C18 5 μm , 250 x 4.6 mm; temperature: 25 $^\circ\text{C}$; injection volume: 10 μL , UV: 220 nm, elution phases: $\text{H}_2\text{O}+0.08\%\text{TFA}$ (mobile phase A) and $\text{CH}_3\text{CN}+0.08\%\text{TFA}$ (mobile phase B), flow: 0.5 mL/min or 1.0 mL/min. Chemstation software was used for data processing.

^1H NMR spectra were recorded with an INOVA 400 MHz instrument with a 5 mm probe. All chemical shifts were quoted relative to deuterated solvent signals.

Distillations were performed with an Edwards RV3 vacuum pump.

The viscosity was measured on CS10 Bohlin (Malvern) rheometer in a titanium cylinder/steal cup (Bob-Cup C25) configuration at temperature of 25 $^\circ\text{C}$ controlled by Julabo MP thermostat. The calibration of the instrument was previously verified with an appropriate standard, namely 2,2,4-Trimethyl-1,3-pentanediol monoisobutyrate (tabulated viscosity at 30 $^\circ\text{C}$ = 9,96 mPa s).

In vitro metabolism of NOP in rat and human liver microsomes

A NADPH-generating solution (10 mM glucose-6-phosphate, 2 mM NADP⁺, 5 mM MgCl_2 and 0.4 U/mL glucose-6-phosphate-dehydrogenase) was prepared in 100 mM phosphate buffered saline (PBS) pH 7.4. 15 μL of RLM or HLM preparation (final protein concentration = 1 mg/mL) were added to 60 μL of co-factors mix and 222 μL of PBS buffer. Samples were pre-incubated under continuous stirring at 37 $^\circ\text{C}$ for 5 min, then 3 μL of stock solution of NOP were added to start the reaction. The compound was incubated at the final concentration of 10 or 100 μM . Aliquots of RLM and HLM incubations were collected at the beginning of the experiment ($t=0$ min) and at $t=3$ h, enzymatic reaction was quenched by addition of a double volume of CH_3CN , samples were centrifuged (16,000 x g, 10 min, 4 $^\circ\text{C}$) and the supernatant directly injected into the HPLC-HRMS system for metabolite identification.

UPLC-HRMS conditions for *in vitro* NOP metabolite profiling

A Waters Acquity UPLC I-Class (Waters, USA) coupled to a Waters V-Ion IMS qToF was employed for ion mobility-enabled acquisitions in metabolite ID workflow. The V-Ion IMS qToF was daily calibrated employing Waters Major Mix (Waters, USA) and system performance were daily checked for accurate mass and

Collisional Cross Section (CCS) accuracy and precision by injecting system suitability test (SST) mixture composed of nine QC standards. For UPLC separation, mobile phases A and B were CH₃CN and ultra-pure water both with 0.1% v/v formic acid and column was an Acquity UPLC CSH C18 (2.1 x 100 mm, 1.7 μ m; Waters, USA). The linear gradient was: 0 min: 5%A; 0-15 min: 5-95%A; 15-16 min: 95%A; 16-17 min: 95-5%A; 17-20 min: 5%A. Total run time: 20 min. Flow rate: 0.5 mL/min; injection volume: 2 μ L; column temperature: 50 °C. Acquisition range: *m/z* = 50-300 amu. Instrumental parameters were set as follows: source temperature: 120 °C; desolvation temperature: 500 °C; source gas flow: 20 L/h; desolvation gas flow: 800 L/h; capillary voltage: 0.8 kV (ESI+); cone voltage: 20 V; collision energy: low energy: 4 eV; high energy: 10-45 eV; reference mass: leucine enkephalin [M+H]⁺ *m/z* = 556.27658. The software UNIFI v.1.8.2 (Waters, USA) was employed for data acquisition and processing.

Solubility Tests

1 mL of the desired pyrrolidone was added to 0.2 mmol of either the protected amino acid/coupling reagent (pair of reagents) or both protected amino acid and coupling reagent(s), and stirred at room temperature until a clear solution was observed. In case of not complete dissolution (see red boxes in Tables 3,4 and S2), an extra addition of solvent was added to reach a concentration of 0.1 M and to achieve total solubilisation, unless otherwise specified.

Resin Swelling

Weighted resin (0.1 g) was introduced into a 5 mL syringe fitted with a polypropylene fritted disc (the void volume of the tip and the syringe was estimated to be 0.2 mL). The desired solvent or mixture of solvents (2 mL) was added to the resin, which was shaken for 30 minutes at room temperature. The swollen resin was allowed to stand for further 5 minutes, then the solvent was removed under vacuum. The volume of the dry resin was then read and the swelling value was calculated from the following formula:

Degree of swelling (mL/g) = $100 \times (\text{volume of the swelled resin} - 0.2 \text{ mL}) / 0.1 \text{ g}$.

All the measurements were performed in triplicate, data were reported as medium value. Triplicate measurements with the related standard deviation values are reported in Table S4.

Fmoc cleavage kinetics in solution phase

Fmoc-Phe-OH (0.1 mmol) was dissolved in the desired pyrrolidone. Piperidine was added to the suspension in order to achieve the desired concentration (20% base solution) in the final 1 mL deprotection mixture total volume. The reaction mixture was stirred at room temperature and samples of the solution (20 μ L) were taken at *t*=0 (before base addition) and after 2, 4, 6, 8, 10, 15 minutes. The samples were diluted with 1.5 mL of CH₃CN/TFA (1% v/v) and injected in HPLC-UV. Reaction was considered complete at disappearance of the HPLC peak corresponding to Fmoc-Phe-OH. All kinetics resulted complete after 2 minutes from the reaction beginning, independently from the employed solvent. Selected chromatograms are reported in the Supporting Information. For HPLC separation, mobile phases A and B were H₂O+0.08%TFA and CH₃CN+0.08%TFA and column was an Agilent Zorbax-SB-C18 5 μ m, 250 x 4.6 mm. The linear gradient was: 0 min: 95%A; 0-15 min: 95-5%A; 15-20 min: 5-95%A; 20-22 min: 95%A. Total run time: 22 min. Flow rate: 1 mL/min.

Coupling in solution phase: synthesis of Z-Phg-Pro-NH₂

Z-Phg-OH (0.2 mmol) was dissolved in a glass vial with 2.5 mL of DMF or the selected pyrrolidone (NCP, NOP or NBnP). The desired coupling reagents combination (0.3 mmol) was then added (reagents A-E in Table 6: OxymaPure/DIC, COMU/DIPEA, PyBOP/HOBt/DIPEA, PyOxyma/DIPEA, HOBt/DIC). After 5 minutes of preactivation, H-Pro-NH₂ (0.2 mmol) was added. The solution was stirred at 0 °C for 1 h, then at room temperature. After 3 h from the beginning of the reaction, an aliquot (80 μ L) of the solution was diluted with 0.5 mL of a 1:2 CH₃CN/H₂O mixture and injected in HPLC-MS, in order to monitor the conversion and the racemization ratio. Selected chromatograms are reported in the Supporting Information. For HPLC separation, mobile phases A and B were H₂O+0.08%TFA and CH₃CN+0.08%TFA and column was an Agilent Zorbax-SB-C18 5 μ m, 250 x 4.6 mm. The linear gradient was: 0 min: 80%A; 0-15 min: 80-60%A; 15-20 min: 60%A; 20-30 min: 60-80%A. Total run time: 30 min. Flow rate: 1 mL/min.

Solid phase synthesis of H-Tyr-Aib-Aib-Phe-Leu-OH/ H-Tyr-Aib-Aib-Phe-Leu-NH₂ (Aib Enkephalin)

Aib-Enkephalin manual syntheses were carried out at room temperature in glass syringes fitted with a polyethylene porous disc, connected to a vacuum source to remove excess of reagents and solvents, by using 0.2 g of preloaded Fmoc-Leu-resins. Specifically, preloaded PS-Wang and PS-Trt-Cl resins (loading 1.1 mmol/g) were used for synthesis with NBP, NOP and NCP, preloaded ChemMatrix-RinkAmide resin (loading 0.5 mmol/g) was used with NBnP. After swelling of the resin in 2 mL of the selected solvent (DMF, NBP, NCP, NOP or NBnP), Fmoc protective group was removed by 20% piperidine in the selected solvent (2 times x2 mL, 15 min each), then the resin was washed with the selected solvent (3 times x1.5 mL, 1 min each). Fmoc-Phe-OH, Fmoc-Aib-OH, Fmoc-Aib-OH, Fmoc-Tyr(tBu)-OH (three-fold excess with respect to the loading of the resin) were pre-activated by OxymaPure® and DIC (three-fold excess of the reagents with respect to the loading of the resin) for 3 minutes and coupled to the resin for 60 minutes. In case of both Aib residues in the sequence, the coupling of Fmoc-Aib-OH was repeated a second time. After each coupling step the Fmoc protective group was removed by treating the peptide resin with 20% piperidine in the selected solvent (2 times x2 mL, 15 min each), and the resin was washed with the selected solvent (3 times x1.5 mL, 1 min each). After Fmoc cleavage of the *N*-terminal amino group, the peptide resin was further washed with DCM (3 times x2 mL, 1 min each) and dried under vacuum for 12 hours. Dry peptide resin was suspended in 5 mL of the mixture TFA/TIS/H₂O (95/2.5/2.5 v/v/v) and stirred for 2 h. The resin was filtered off, washed with TFA (1 time x 1mL, 1 min) and diisopropylether (25 mL) cooled to 4 °C was added to the solution dropwise. The peptide was filtered and dried *in vacuo* to obtain crude Aib-Enkephalin that was directly analysed by HPLC-MS (Table 7). Related chromatograms and MS spectra are reported in the Supporting Information. For HPLC separation, mobile phases A and B were H₂O+0.08%TFA and CH₃CN+0.08%TFA and column was a Phenomenex Luna C18 5 μ m, 250 x 4.6 mm. The linear gradient was: 0 min: 80%A; 0-15 min: 80-60%A; 15-20 min: 60%A; 20-30 min: 60-80%A. Total run time: 30 min. Flow rate: 0.5 mL/min.

Solid phase synthesis of H-D-Phe-Cys-Phe-D-Trp-Lys-Thr-Cys-Thr-ol (Linear Octreotide)

Linear Octreotide manual syntheses were carried out at room temperature by using Fmoc-Thr(tBu)-ol-Trt-PS resin (0.2 g, loading 1.1 mmol/g) in glass syringes fitted with a polyethylene porous disc, connected to a vacuum source to remove excess of reagents and solvents. After swelling of the resin in 2 mL of the selected solvent (DMF, NBP, NOP or NOP/DMC), Fmoc protective group was removed by 20% piperidine in the selected solvent (2 times $\times 2$ mL, 15 min each), then the resin was washed (3 times $\times 1.5$ mL, 1 min each). Fmoc-Cys(Trt)-OH, Fmoc-Thr(tBu)-OH, Fmoc-Lys(Boc)-OH, Fmoc-D-Trp(Boc)-OH, Fmoc-Phe-OH, Fmoc-Cys(Trt)-OH, Fmoc-D-Phe-OH (three-fold excess with respect to the loading of the resin) were pre-activated by OxymaPure® and DIC (three-fold excess of the reagents with respect to the loading of the resin) for 3 minutes and coupled to the resin for 60 minutes. In case of the first inserted Fmoc-Cys(Trt)-OH (Cys⁷ in the final sequence) the coupling was repeated a second time. After each coupling step the Fmoc protective group was removed by treating the peptide resin with 20% piperidine in the selected solvent (2 times $\times 2$ mL, 15 min each), and the resin was washed (3 times $\times 1.5$ mL, 1 min each). After Fmoc cleavage of the *N*-terminal amino group the peptide resin was further washed with DCM (3 times $\times 2$ mL, 1 min each) and dried under vacuum for 12 hours. Dry peptide resin was suspended in 5 mL of the mixture TFA/TIS/1-dodecanethiol (90/5/5 v/v/v) and stirred for 4 h. The resin was filtered off, washed with TFA (1 time $\times 1$ mL, 1 min) and diisopropylether (25 mL) cooled to 4 °C was added to the solution dropwise. The peptide was filtered and dried *in vacuo* to obtain crude linear octreotide. HPLC purities calculated as sum of all target molecule adducts are reported in Table 8.

Automated syntheses of linear Octreotide was performed at room temperature with CSBio-CS136X peptide synthesizer using the same conditions reported for manual protocol with the only exception that the mixture NOP/DMC 80:20 was used as solvent through all the steps (Fmoc cleavage, coupling, washings).

Final global deprotection/cleavage on dry resin was carried out analogously to the manual synthesis. Related chromatograms and MS spectra are reported in the Supporting Information.

For HPLC separation, mobile phases A and B were H₂O+0.08%TFA and CH₃CN+0.08%TFA and column was a Phenomenex Luna C18 5 μ m, 250 \times 4.6 mm. The linear gradient was: 0 min: 80%A; 0-15 min: 80-60%A; 15-20 min: 60%A; 20-30 min: 60-80%A. Total run time: 30 min. Flow rate: 0.5 mL/min.

Solvent/base recycling

Deprotection stream waste (including washings) and coupling stream waste (including swelling and washings) were collected separately and directly distilled under vacuum. When SPPS of linear Octreotide was performed in NOP alone, the recovery of the deprotection waste was obtained by initially setting vacuum to 25 mmHg and temperature at 40 °C to recover piperidine (95% yield), then increased to 0.25 mmHg (temperature 130 °C) to collect NOP (85% yield). Coupling waste was directly distilled under high vacuum since only NOP was recovered (85%).

When SPPS of linear Octreotide was performed in NOP/DMC 80:20, the recovery of the deprotection waste was obtained by initially setting vacuum to 25 mmHg and temperature at 40 °C to recover piperidine (95% yield) and DMC (95% yield) together, then increased to 0.25 mmHg (temperature 130°C) to collect

NOP (85% yield). In the same way, coupling waste was distilled in two steps allowing the recovery of DMC first (95%), then of NOP (85%) under higher vacuum.

Author contributions

G.M. and P.C. equally contributed to the research. A.T., W.C., A.R. and M.M. designed research; G.M., P.C., A.M., L.F., D.C., T.F. and F.F. performed experiments; A.T., W.C. and F.V. analyzed data and all authors contributed to writing the manuscript.

Conflicts of interest

There are no conflicts to declare.

Acknowledgements

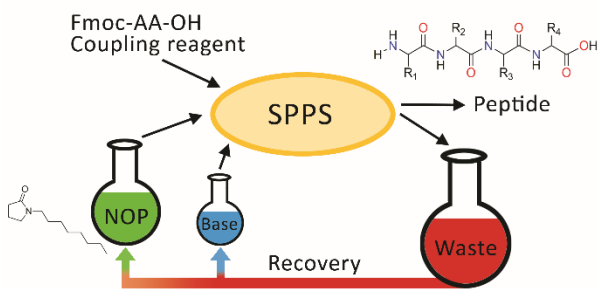
We kindly acknowledge Alma Mater Studiorum University of Bologna, University of Parma and Fresenius kabi for financial support. We thank METCO srl (Monteveglia, Bologna, Italy) for kind support.

Notes and references

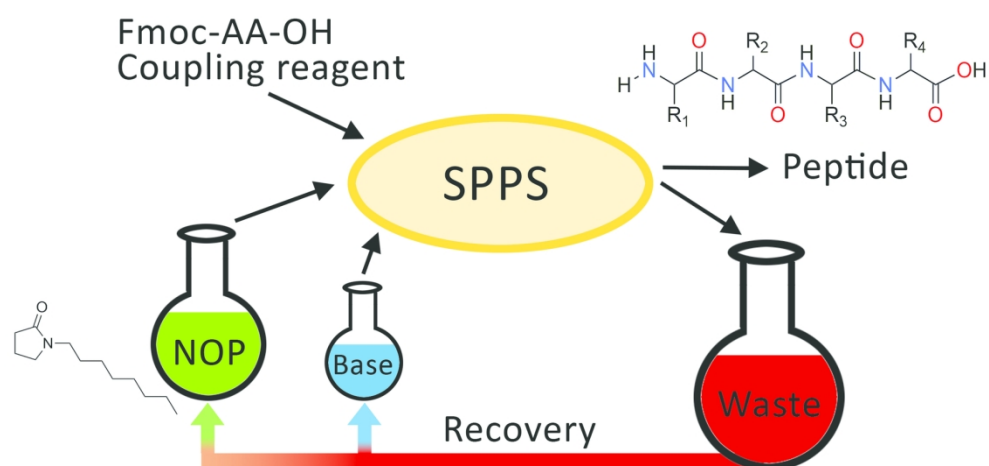
1. B. R. Merrified, *J. Am. Chem. Soc.*, 1963, **85**, 2149.
2. B. L. Bray, *Nat. Rev. Drug Discovery* 2003, **2**, 587.
3. B. G. de la Torre, F. Albericio, *Molecules* 2020, **25**, 2293.
4. A. A. Zompra, A. S. Galanis, O. Werbitzky, F. Albericio, *Futur. Med. Chem.* 2009, **1**, 361.
5. a) T. Nuijens, A. Toplak, M. Schmidt, A. Ricci, W. Cabri, *Frontiers Chem.* 2019, **7**, 829. b) A. M. Weeks, J. A. Wells *Chem. Rev.* 2020, **120**, 3127.
6. S. Kitada, S. Fujita, Y. Okada, S. Kim, K. Chiba *Biorg. Chem. Med. Lett.* 2011, **21**, 4476.
7. J. H. Rasmussen, *Bioorg. Med. Chem.* 2018, **26**, 2914.
8. A. Isidro-Llobet, M. N. Kenworthy, S. Mukherjee, M. E. Kopach, K. Wegner, F. Gallou, A. G. Smith and F. Roschangar, *J. Org. Chem.*, 2019, **84**, 4615.
9. a) P. H. Martin, G. Egelund, H. Johansson, S. Thordal LeQuement, F. Wojcik and D. Sejer Pedersen, *RSC Adv.*, 2020, **10**, 42457. b) G. Martelli, L. Ferrazzano, A. Tolomelli, A. Ricci, W. Cabri, *Chemistry Today* 2020, **38**, 14. c) C. De Luca, S. Felletti, G. Lievore, A. Buratti, S. Vogg, M. Morbidelli, A. Cavazzini, M. Catani, M. Macis, A. Ricci, W. Cabri, *Journal of Chromatography A* 2020, **1625**, 461304. d) I. Guryanov, A. Orlandin, A. Viola, B. Biondi, F. Formaggio, A. Ricci, W. Cabri, *Org. Process Res. Dev.* 2020, **2**, 274.
10. K. Wegner, D. Barnes, K. Manzor, A. Jardine, D. Moran, *Green Chem. Lett. and Rev.* 2021, **14**, 152;
11. a) D. Prat, A. Wells, J. Hayler, H. Sneddon, C. Robert McElroy, S. Abou-Shehadad, P. J. Dunne *Green Chem.*, 2016, **18**, 288; b) R. K. Henderson, C. Jimenez-Gonzalez, D. J. C. Constable, S. R. Alston, G. G. A. Inglis, G. Fisher, J. Sherwood, S. P. Binksa, A. D. Curzons *Green Chem.*, 2011, **13**, 854 c) C. J. Clarke, W.-C. Tu, O. Levers, A. Bröhl and J. P. Hallett, *Chem. Rev.*, 2018, **118**, 747 d) S. L. Giudicessi, S. L. Saavedra, A. B. Cardillo, S. A. Camperi, O. Cascone, F. Albericio, M. C. Martínez Ceron. in *Green Sustainable Process for Chemical and Environmental Engineering and Science - Solvents for the Pharmaceutical*

- Industry*; Chapter 5 : Green solvents in the biotechnology-based pharmaceutical industry, 2021, 87.
12. ECHA reference for DMF: <https://echa.europa.eu/it/registration-dossier/-/registered-dossier/13179>. The registration that is only referred to European countries is supporting use, storage and transportation of $\geq 10\,000$ to $< 100\,000$ tonnes per annum.
 13. ECHA reference for NMP see: a) <https://echa.europa.eu/it/registration-dossier/-/registered-dossier/15493/1>. The registration that is only referred to European countries is supporting use, storage and transportation of $\geq 10\,000$ to $< 100\,000$ tonnes per annum.
 14. M. C. Bryan, P. J. Dunn, D. Entwistle, F. Gallou, S. G. Koenig, J. D. Hayler, M. R. Hickey, S. Hughes, M. E. Kopach, G. Moine, P. Richardson, F. Roschangar, A. Steven, F. J. Weiberth *Green Chem.*, 2018, **20**, 5082
 15. Y. E. Jad, G. A. Acosta, T. Govender, H. G. Kruger, A. El Faham, B. G. de la Torre, F. Albericio, *ACS Sus. Chem. Eng.* 2016, **4** (12), 6809.
 16. Y. E. Jad, G. A. Acosta, S. N. Khattab, B. G. de la Torre, T. Govender, H. G. Kruger, A. El Faham, F. Albericio, *Org. Biomol. Chem.* 2015, **13**, 2393.
 17. Y. E. Jad, G. A. Acosta, S. N. Khattab, B. G. de la Torre, T. Govender, H. G. Kruger, A. El Faham, F. Albericio, *Amino Acids*, 2016, **48**, 419.
 18. A. Kumar, Y. E. Jad, J. M. Collins, F. Albericio, B. G. de la Torre, *ACS Sus. Chem. Eng.* 2018, **6**, 8034.
 19. A. Kumar, Y. E. Jad, A. El-Faham, B. G. de la Torre, F. Albericio, *Tetrahedron Lett.* 2017, **58** (30), 2986.
 20. S. B. Lawrenson, R. Arav and M. North, *Green Chem.*, 2017, **19**, 1685.
 21. S. Lawrenson, M. North, F. Peigneguy, A. Routledge *Green Chem.*, 2017, **19**, 952.
 22. a) J. Lopez, S. Pletscher,, A. Aemissegger, C. Bucher and F. Gallou, *Org. Process Res. Dev.*, 2018, **22**, 494. b) A. Kumar, M. Alhassan, J. Lopez, F. Albericio, B. G. de la Torre, *ChemSusChem*, 2020, 5288.
 23. L. Ferrazzano, D. Corbisiero, G. Martelli, A. Tolomelli, A. Viola, A. Ricci and W. Cabri, *ACS Sus. Chem. Eng.*, 2019, **7**, 12867.
 24. J. Pawlas, J. H. Rasmussen *Green Chem.* 2019, **21**, 5990.
 25. F. Dettner (Bachem Americas), Tides – Oligonucleotide and peptide therapeutics, September 15-18, 2020, oral communication.
 26. J. Pawlas, B. Antonic, M. Lundqvist, T. Svensson, J. Finnman and J. H. Rasmussen, *Green Chem.*, 2019, **21**, 2594.
 27. B. A. Pethica, L. Senak, Z. Zhu, A. Lou, *Colloids Surf. A: Physiochem. Eng. Asp.* 2001, **186**, 113
 28. Surfadone™ LP100 is a registered trademark by Ashland: <https://www.ashland.com/industries/blue/gas/surfadone-wetting-agent>.
 29. F. Zhou, B. Zhang, H. Liu, Z. Wen, K. Wang, G. Chen, *Org. Proc. Res. Dev.* 2018, **22**, 504–511.
 30. R. Mariscal, P. Maireles-Torres, M. Ojeda, I. Sádaba, M. López Granados, *Energy Environ. Sci.*, 2016, **9**, 1144,
 31. J. F. White, J. E. Holladay, A. A. Zacher, J. G. Frye Jr., T. A. Werpy, *Top Catal.*, 2014, **57**, 1325.
 32. M. Ventura, A. Marinas, M. E. Domine, *Top. Catal.*, 2020, **63**, 846.
 33. a) DMF: ECHA, <https://echa.europa.eu/it/registration-dossier/-/registered-dossier/15093/7/3/1>; b) NMP: ECHA, <https://echa.europa.eu/it/registration-dossier/-/registered-dossier/15493/7/3/1>; NBP: ECHA, <https://echa.europa.eu/it/registration-dossier/-/registered-dossier/10579/7/3/1>; NOP: <https://echa.europa.eu/it/registration-dossier/-/registered-dossier/16946/7/3/1>.
 34. B. K. Schindler, S. Koslitz, S. Meier, V. N. Belov, H. M. Koch, T. Weiss, T. Brüning and H. U. Käßlerlein, *Anal. Chem.* 2012, **84** (8), 3787.
 35. F. Albericio, A. El-Faham. *Org. Process Res. Dev.*, 2018, **22**, 760.
 36. C. Amadi-Kamalu, H. Clarke, M. McRobie, J. Mortimer, M. North, Y. Ran, A. Routledge, D. Sibbald, M. Tickias, K. Tse, H. Willway, *Chemistry Open*, 2020, **9**, 431.
 37. Y. Ran, F. Byrne, I. D. V. Ingram and M. North, *Chem.Eur. J.*, 2019, **25**, 4951.
 38. C. Liang, M. A. Behnam, T. R. Sundermann and C. D. Klein, *Tetrahedron Lett.*, 2017, **58**, 2325.
 39. M. Paradis-Bas, J. Tulla-Puche, F. Albericio. *Chem. Soc. Rev.* 2016, **45** (3), 631.
 40. Y. E. Jad, T. Govender, H. G. Kruger, A. El-Faham, B. G. de la Torre and F. Albericio, *Org. Process Res. Dev.*, 2017, **21**, 365.
 41. S. W. J. Lamberts and L. J. Hofland, *Eur. J. Endocrin.* 2019, **181**, R173
 42. B.M. Pastore, M. J. Savelski, C. S. Slater, F. A. Richetti, *Clean Techn Environ Policy*, 2016, **18**, 2635.
 43. J. Pawlas, T. Nuijens, J. Persson, T. Svensson, M. Schmidt, A. Toplak, M. Nilsson, Rasmussen *Green Chem.*, 2019, **21**, 6451.

Table of content:



A green protocol for SPPS allows to recover and recycle solvent and base from the process waste mixture



A green protocol for SPPS allows to recover and recycle solvent and base from the process waste mixture

80x39mm (600 x 600 DPI)

Electronic Supplementary Information

Steps towards sustainable solid phase peptide synthesis: use and recovery of *N*-octyl pyrrolidone.

Giulia Martelli,^a Paolo Cantelmi,^a Alessandra Tolomelli,^{a*} Dario Corbisiero,^a Alexia Mattellone,^a Antonio Ricci,^b Tommaso Fantoni,^a Walter Cabri,^{a*} Federica Vacondio,^c Francesca Ferlenghi,^c Marco Mor^c and Lucia Ferrazzano^a

^a Department of Chemistry Giacomo Ciamician Alma Mater Studiorum, University of Bologna Via Selmi,2 40136-BO, Italy

^b Fresenius kabi iPsum via San Leonardo 23, 45010-RO, Italy

^c Department of Food and Drug Sciences University of Parma Parco Area delle Scienze 27/a, 43124-Parma, Italy

*Corresponding authors. E-mail: alessandra.tolomelli@unibo.it; walter.cabri@unibo.it

Table of Contents

In vitro metabolism of NOP	S2
Solubility tests.....	S17
Swelling tests	S19
Coupling reactions in solution phase	S21
Deprotection kinetic tests	S28
SPPS of Aib-Enkephalin in Green Solvents.....	S29
SPPS of linear Octreotide in Green Solvents.....	S37
Green solvent mixtures.....	S44
Recycling of linear Octreotide SPPS waste stream	S44

In vitro metabolism of NOP

Table S1. NOP metabolites identified in rat and human liver microsomes by HPLC-HRMS

Compound ID	Formula	RT (min)	Ion	Observed mass (m/z)	Mass error (ppm)	Metabolic Reaction	% of Parent response	Found in
NOP	C ₁₂ H ₂₃ NO	5.56	[M+H] ⁺	198.1849	-1.8	--	100	HLM/RLM
M1	C ₁₂ H ₂₁ NO ₂	3.19	[M+H] ⁺	212.1642	-1.6	+O – H2	83.5	HLM/RLM
M2	C ₁₂ H ₂₁ NO ₂	2.36	[M+H] ⁺	212.1645	-0.2	+O – H2	6.0	HLM/RLM
M3	C ₁₂ H ₂₁ NO ₂	2.44	[M+H] ⁺	212.1642	-1.5	+O – H2	3.4	HLM/RLM
M4	C ₁₂ H ₂₁ NO ₂	2.51	[M+H] ⁺	212.1641	-2.0	+O – H2	7.7	HLM/RLM
M5	C ₁₂ H ₂₁ NO ₂	2.56	[M+H] ⁺	212.1641	-2.3	+O – H2	5.0	HLM
M6	C ₁₂ H ₂₃ NO ₂	3.16	[M+Na] ⁺	236.1615	-2.5	+O	8.1	HLM/RLM
M7	C ₁₂ H ₂₃ NO ₂	3.24	[M+Na] ⁺	236.1616	-1.9	+O	17.1	HLM/RLM
M8	C ₁₂ H ₂₃ NO ₂	3.28	[M+H] ⁺	212.1640	-2.7	+O – H2	6.3	HLM/RLM
M9	C ₁₂ H ₂₃ NO ₂	4.40	[M+H] ⁺	214.1795	-3.0	+O	18.3	HLM/RLM
M10	C ₁₂ H ₂₃ NO ₂	4.54	[M+H] ⁺	214.1796	-2.5	+O	28.9	HLM/RLM
M11	C ₁₂ H ₂₃ NO ₂	4.75	[M+H] ⁺	214.1796	-2.7	+O	6.7	HLM

Figure S1. HPLC-HRMS trace of a RLM incubation of N-octyl pyrrolidone (NOP) at t=3h. Parent compound NOP and metabolites are reported together with their RT. At RT = 3.18 min, the most abundant metabolite (**M1**, with a mass shift of + 14 with respect to NOP) and two minor metabolites (**M6** and **M7**, with a mass shift of + 16 with respect to NOP) co-elute. Extracted Ion Chromatograms (XIC) of co-eluting metabolites **M1**, **M6** and **M7** are reported in Figure S2.

Item name: 5_NOP_RLM_T180

Channel name: Identified Components

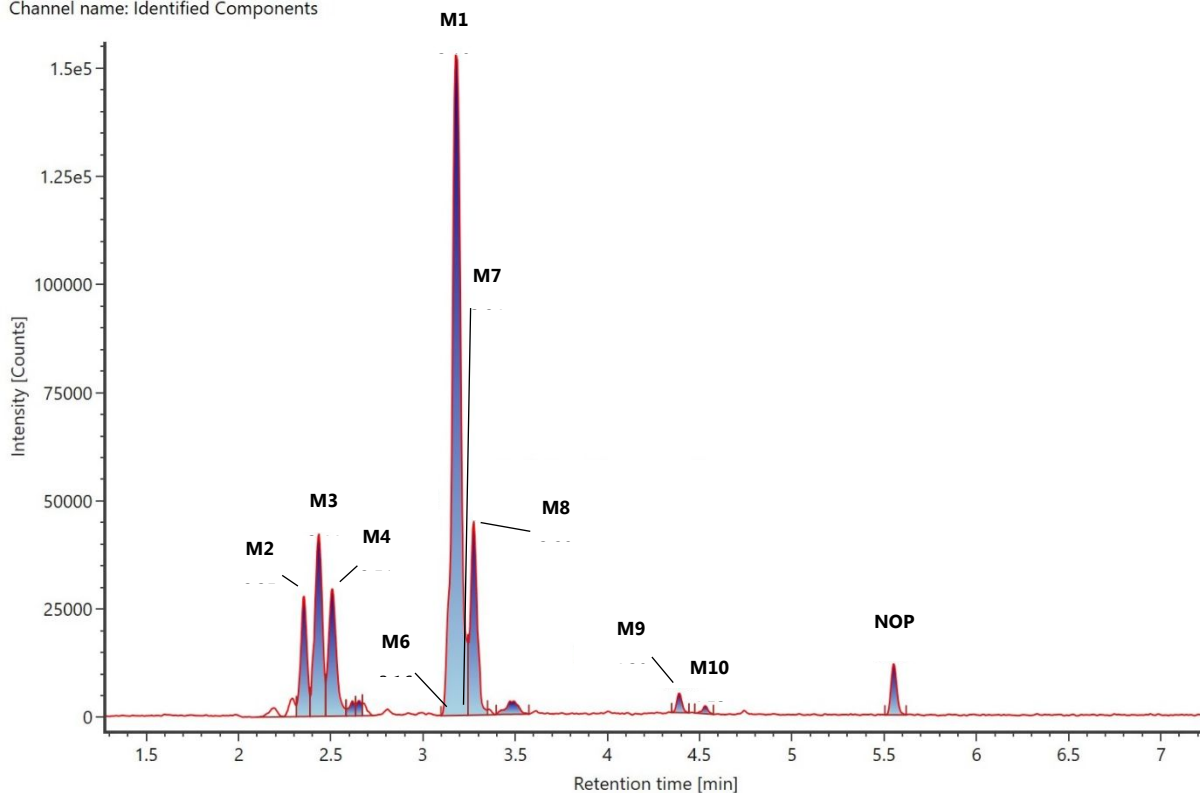


Figure S2. Extracted Ion Chromatogram (XIC) of co-eluting metabolites **M1**, **M6** and **M7** in RLM at t=3h

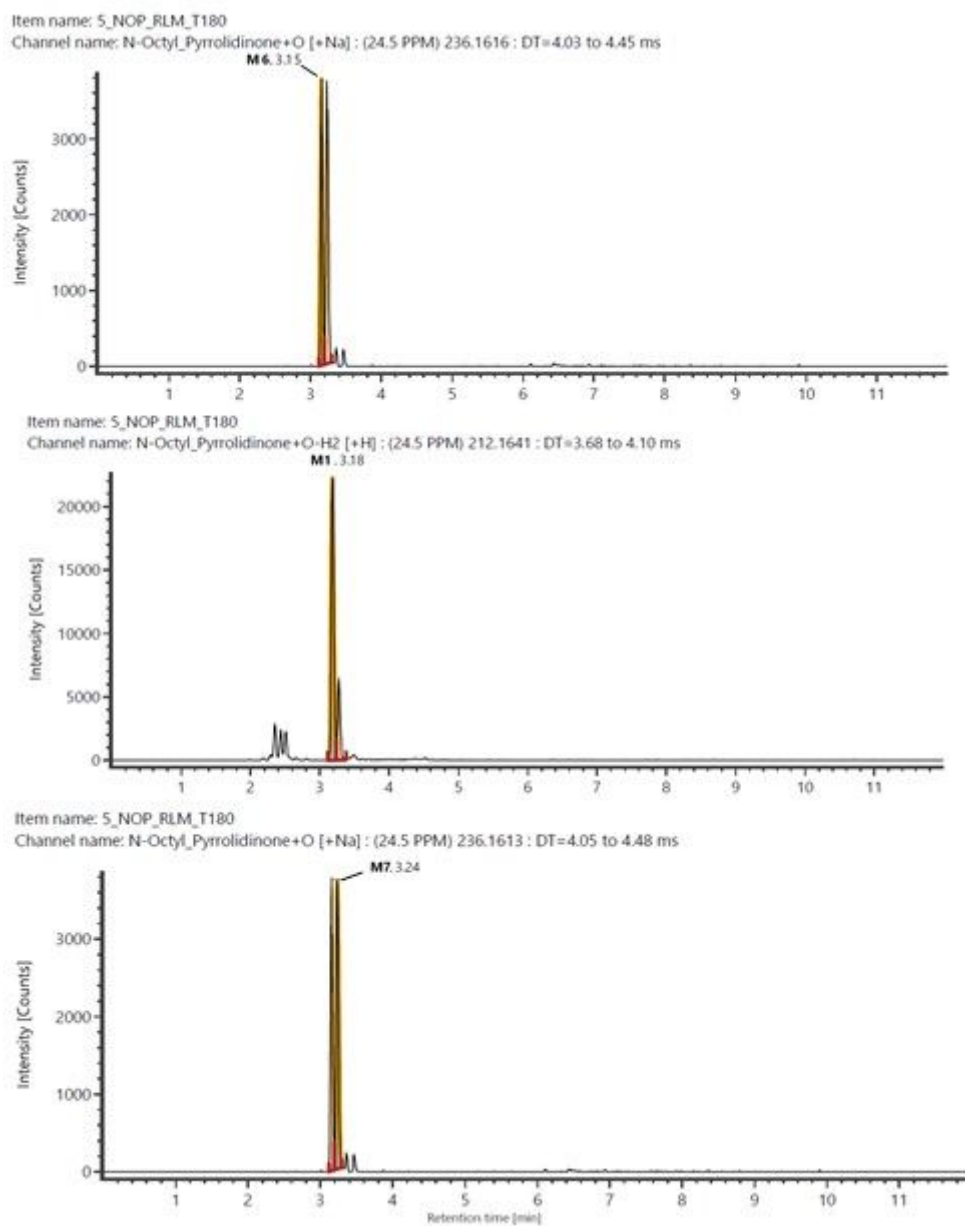


Figure S3. Extracted Ion Chromatogram (XIC) of co-eluting metabolites **M1**, **M6** and **M7** in HLM at t=3h

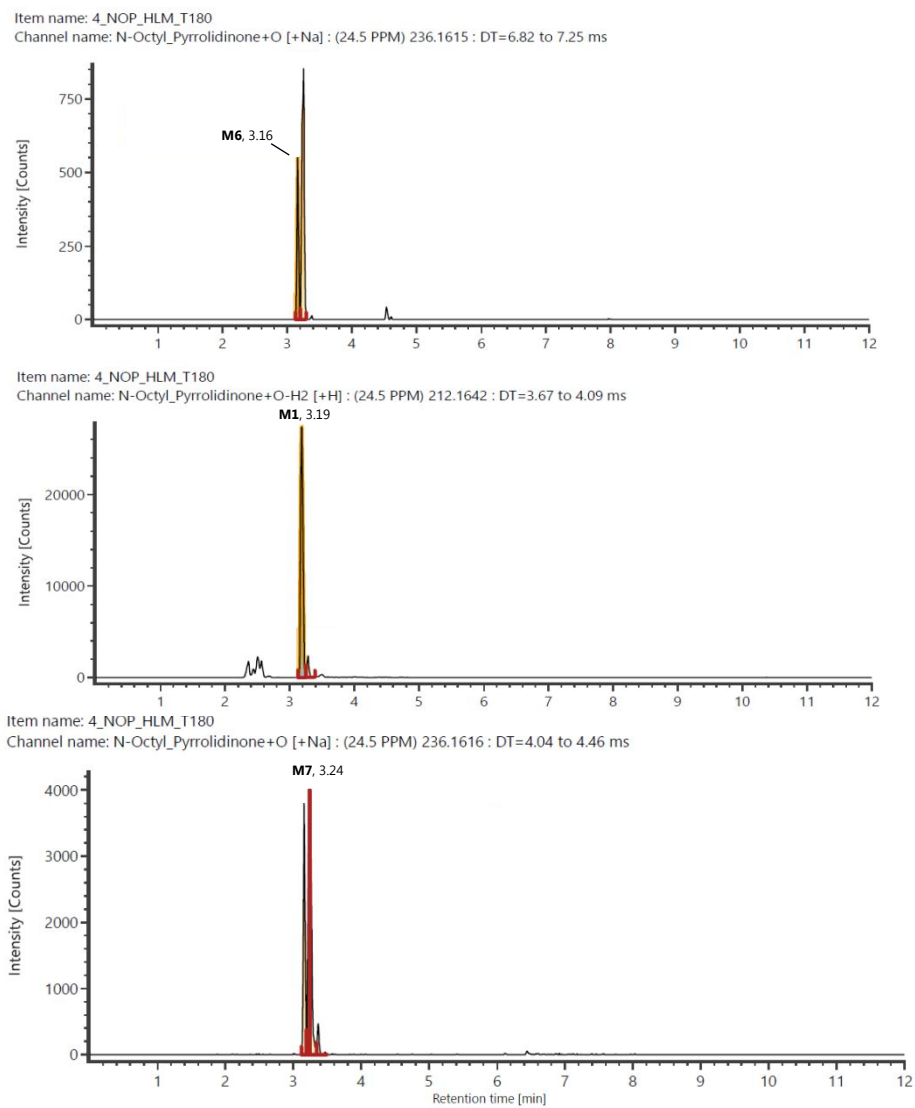


Figure S4. a. Low (upper) and high (lower) energy (HDMS^E) mass spectra for metabolite **M1** (RT = 3.18 min) in RLM (incubation time: t=3h)

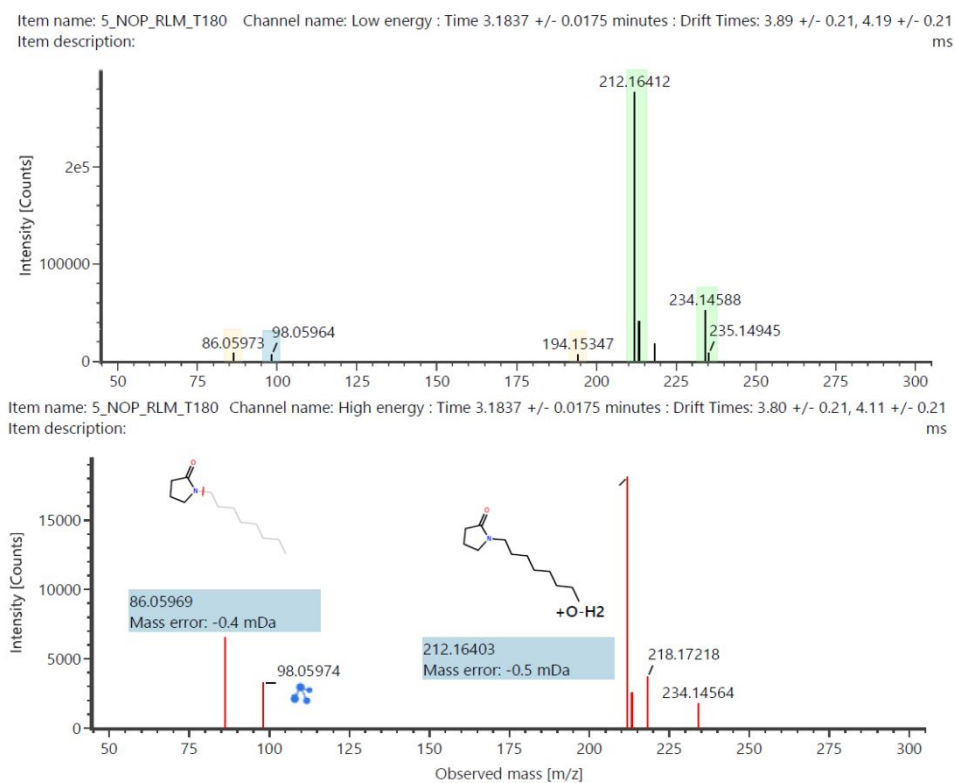


Figure S4. b. Low (upper) and high (lower) energy (HDMS^E) mass spectra for metabolite **M1** (RT = 3.19 min) in HLM (incubation time: t=3h)

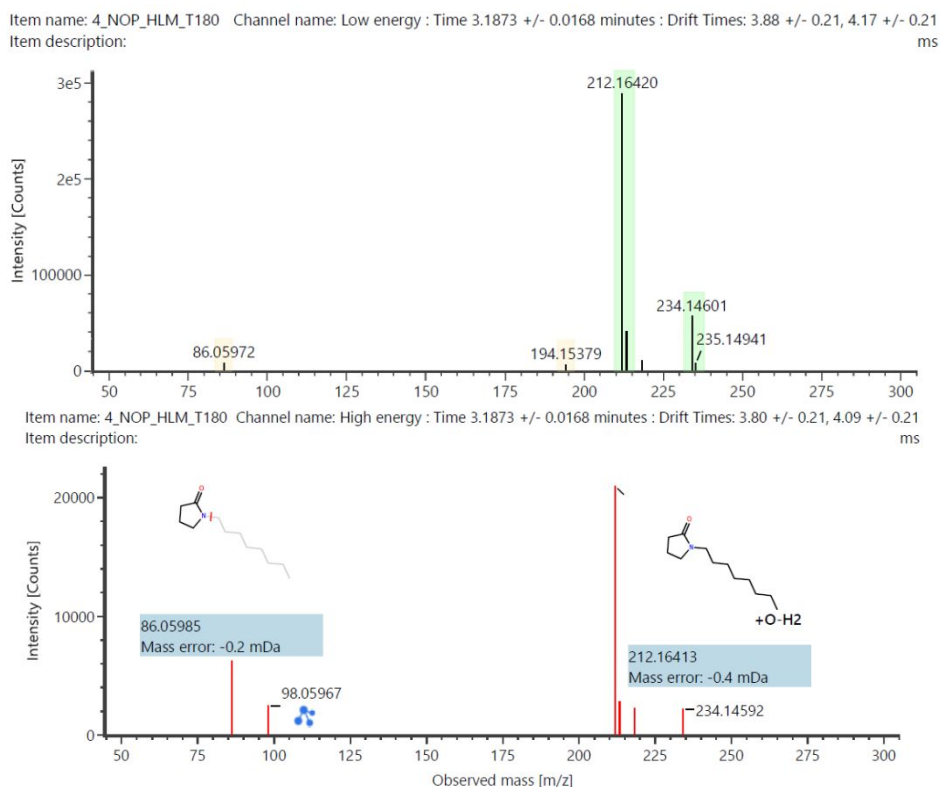


Figure S5. a. Low (upper) and high (lower) energy (HDMS^E) mass spectra for metabolite **M2** (RT = 2.35 min) in RLM (incubation time: t=3h)

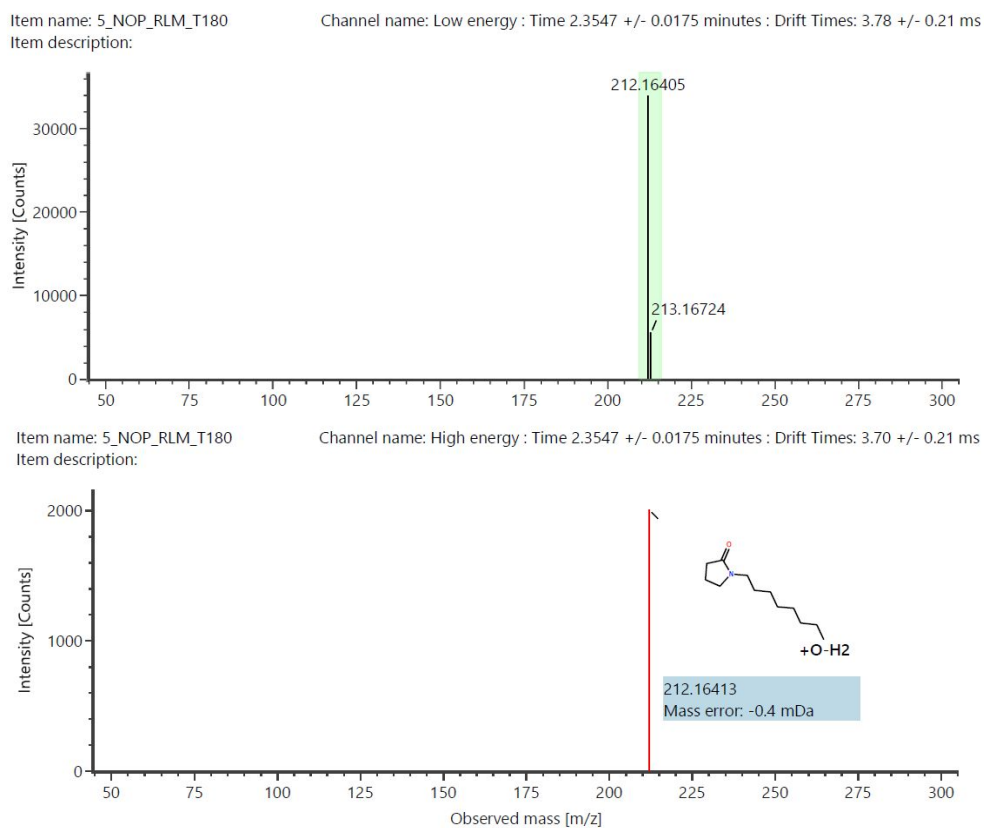


Figure S5. b. Low (upper) and high (lower) energy (HDMS^E) mass spectra for metabolite **M2** (RT = 2.36 min) in HLM (incubation time: t=3h)

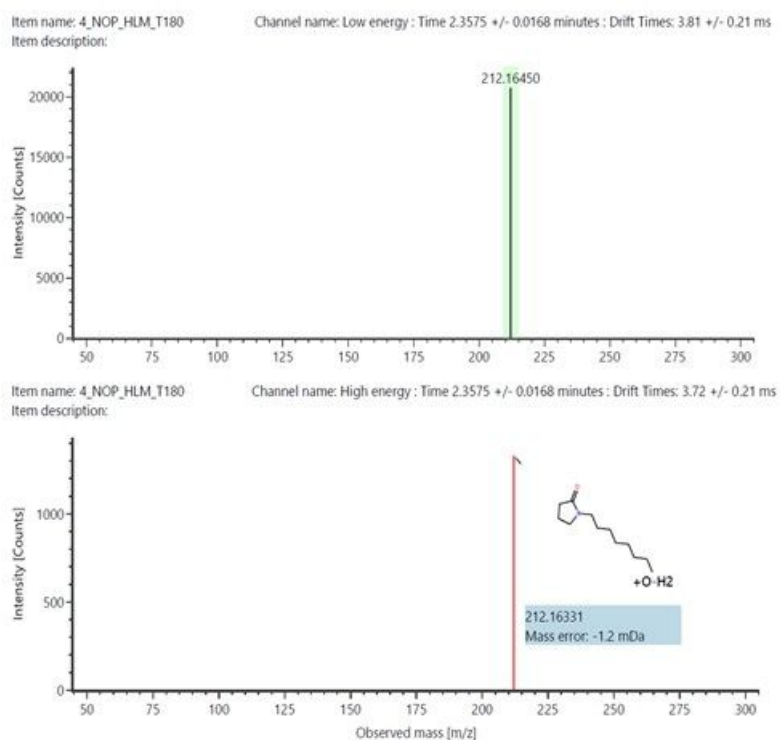


Figure S6. a. Low (upper) and high (lower) energy (HDMS^E) mass spectra for metabolite **M3** (RT = 2.44 min) in RLM (incubation time: t=3h)

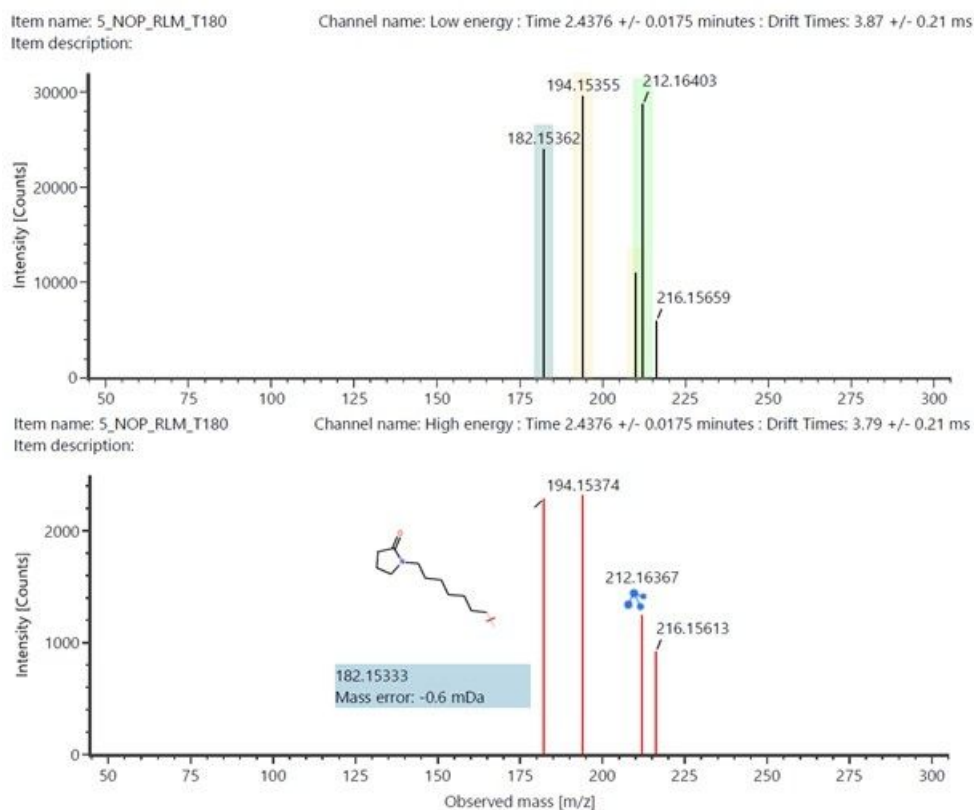


Figure S6. b. Low energy mass spectrum for metabolite **M3** (RT = 2.44 min) in HLM (incubation time: t=3h). Due to the low intensity of parent ion no high energy fragmentation was collected

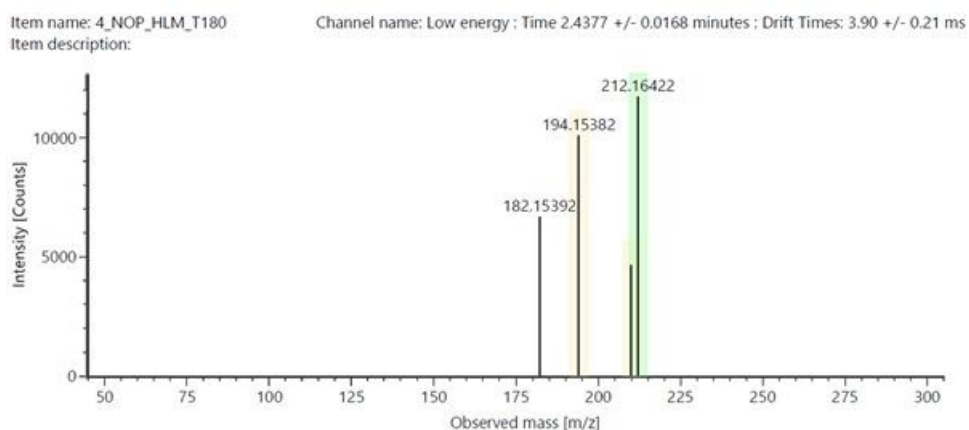


Figure S7. a. Low (upper) and high (lower) energy (HDMS^E) mass spectra for metabolite **M4** (RT = 2.51 min) in RLM (incubation time: t=3h)

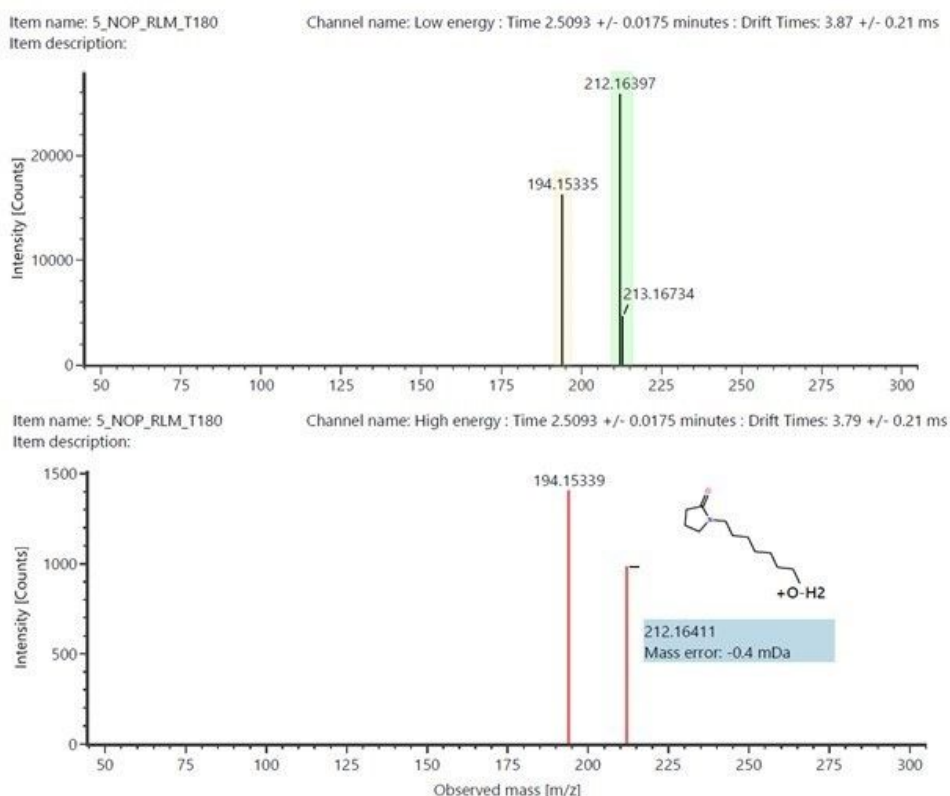


Figure S7. b. Low (upper) and high (lower) energy (HDMS^E) mass spectra for metabolite **M4** (RT = 2.51 min) in HLM (incubation time: t=3h)

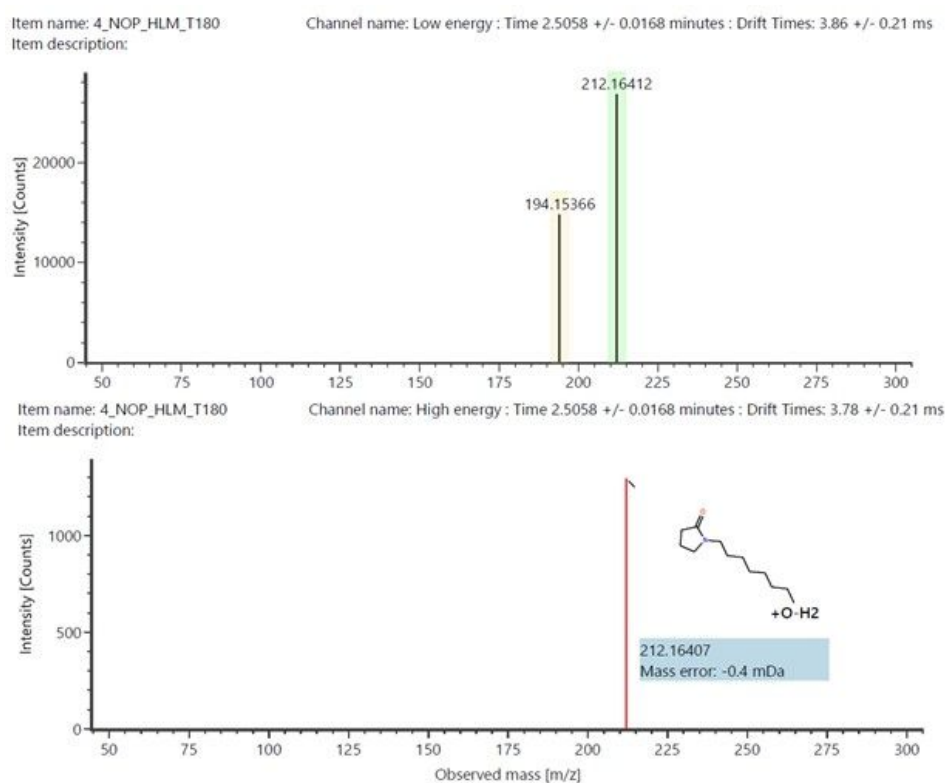


Figure S8. Low energy mass spectrum for metabolite **M5** (RT = 2.56 min) in HLM (incubation time: t=3h). Due to the low intensity of parent ion, no high energy fragmentation was collected

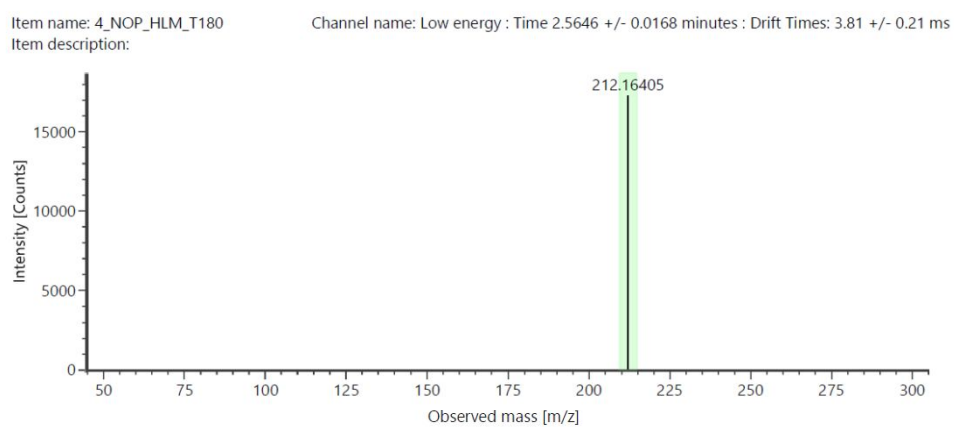


Figure S9. a. Low (upper) and high (lower) energy (HDMS^E) mass spectra for metabolite **M6** (RT = 3.16 min) in RLM (incubation time: t=3h)

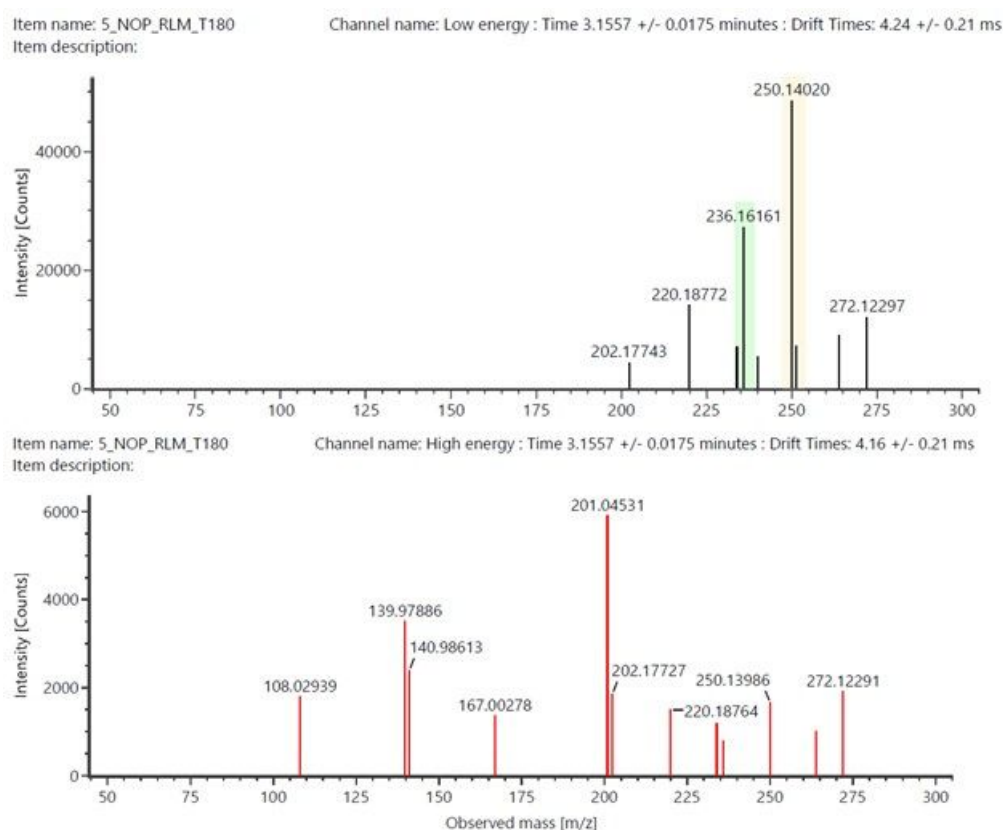


Figure S9. b. Low (upper) and high (lower) energy (HDMS^E) mass spectra for metabolite **M6** (RT = 3.16 min) in HLM (incubation time: t=3h). Due to the low intensity of parent ion, no high energy fragmentation was collected

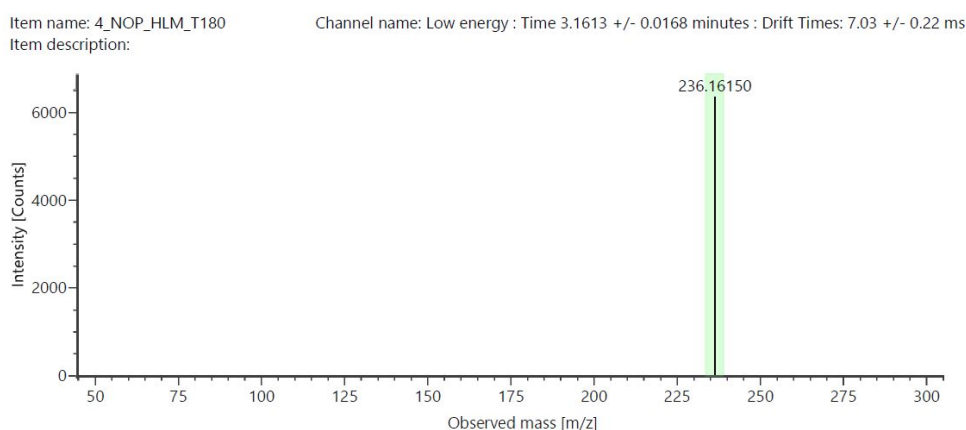


Figure S10. a. Low (upper) and high (lower) energy (HDMSE^E) mass spectra for metabolite **M7** (RT = 3.24 min) in RLM (incubation time: t=3h)

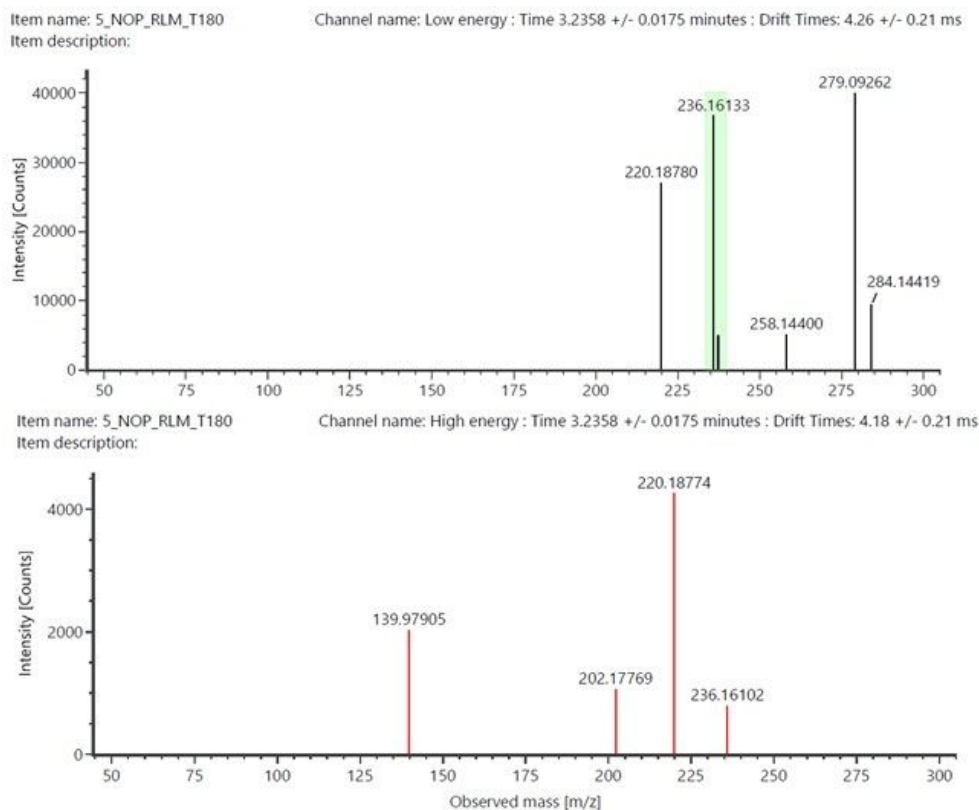


Figure S10. b. Low (upper) and high (lower) energy (HDMSE^E) mass spectra for metabolite **M7** (RT = 3.24 min) in HLM (incubation time: t=3h)

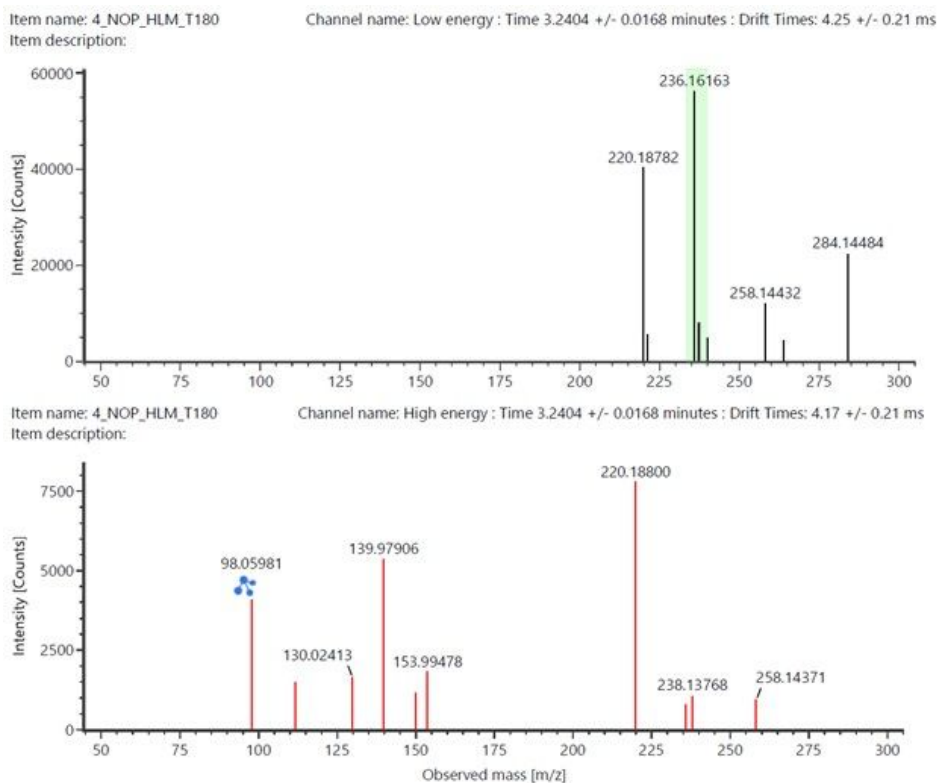


Figure S11. a. Low (upper) and high (lower) energy (HDMSE) mass spectra for metabolite **M8** (RT = 3.28 min) in RLM (incubation time: t=3h)

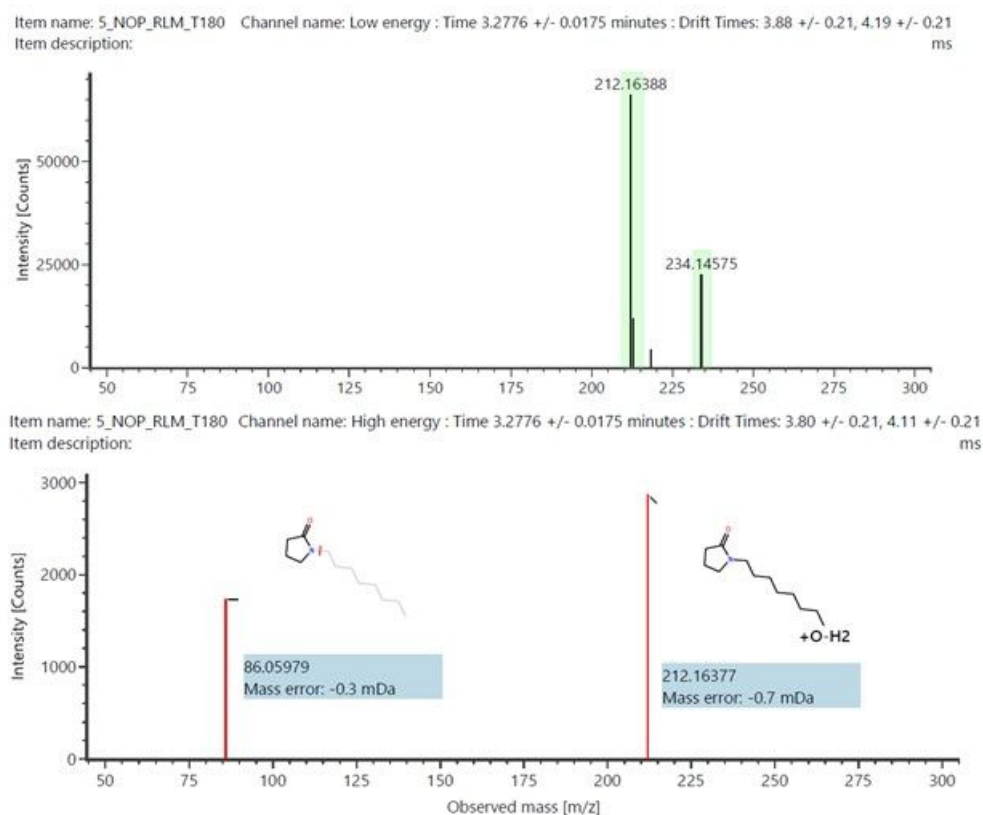


Figure S11. b. Low (upper) and high (lower) energy (HDMSE) mass spectra for metabolite **M8** (RT = 3.28 min) in HLM (incubation time: t=3h). Due to the low intensity of parent ion, no high energy fragmentation was collected

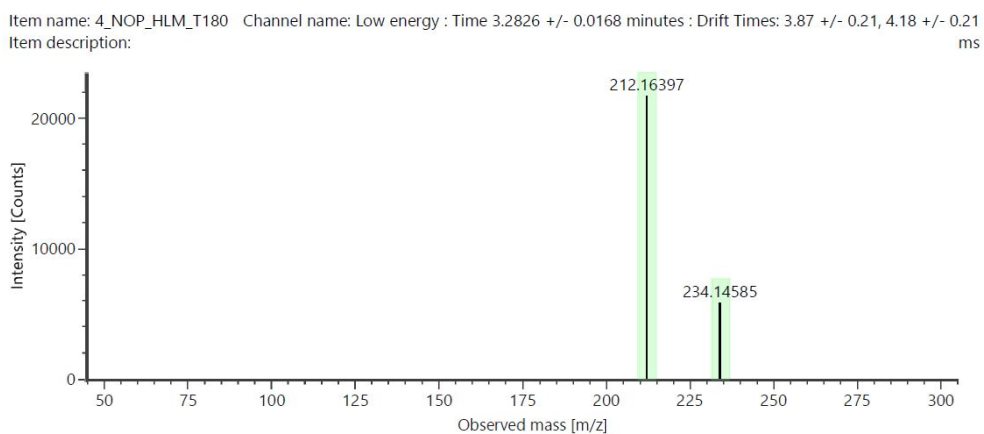


Figure S12. a. Low (upper) and high (lower) energy (HDMSE) mass spectra for metabolite **M9** (RT = 4.40 min) in RLM (incubation time: t=3h)

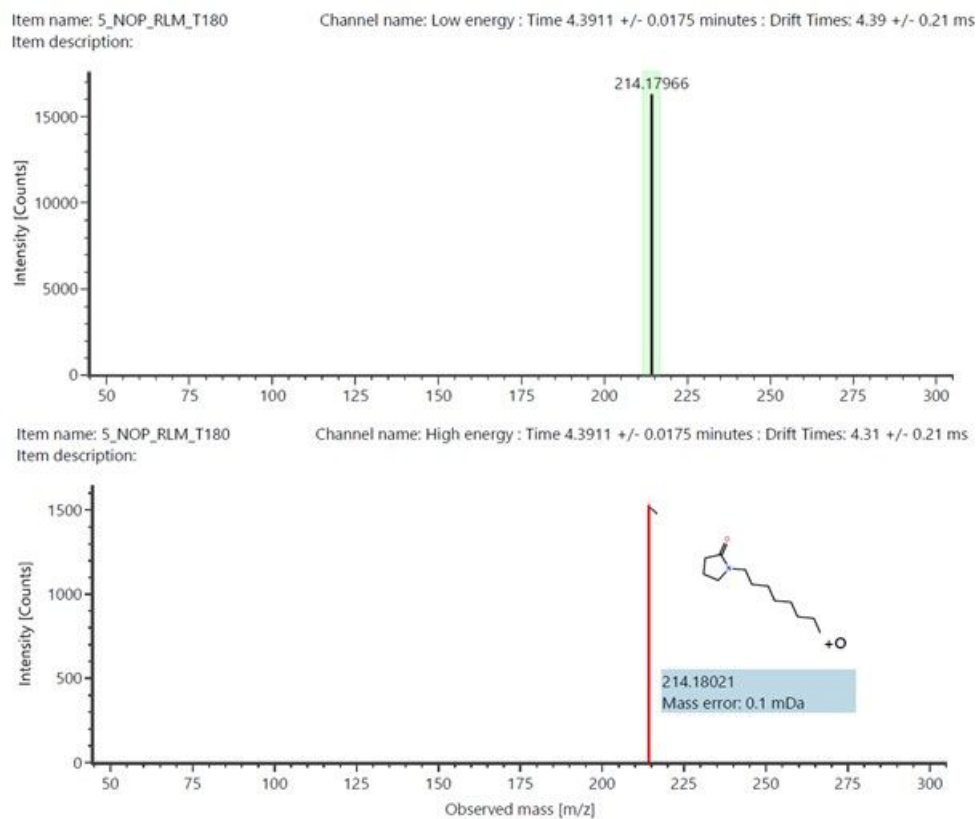


Figure S12. b. Low (upper) and high (lower) energy (HDMSE) mass spectra for metabolite **M9** (RT = 4.40 min) in HLM (incubation time: t=3h)

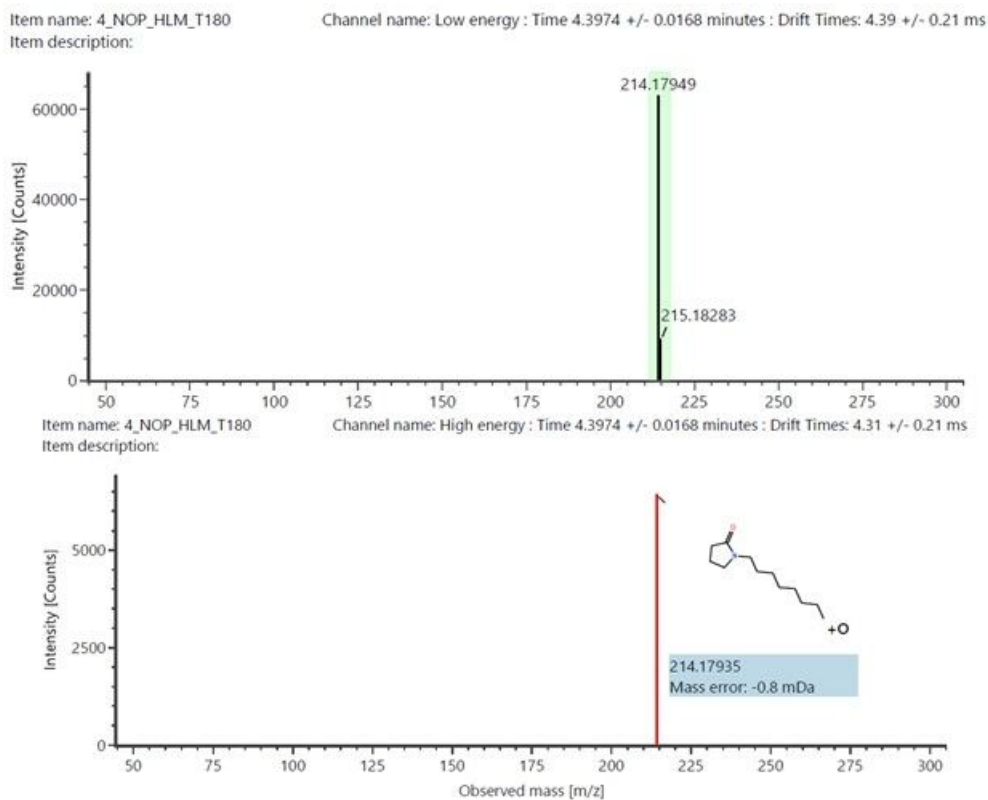


Figure S13. a. Low energy mass spectrum for metabolite **M10** (RT = 4.53 min) in RLM (incubation time: t=3h). Due to the low intensity of parent ion, no high energy fragmentation was collected

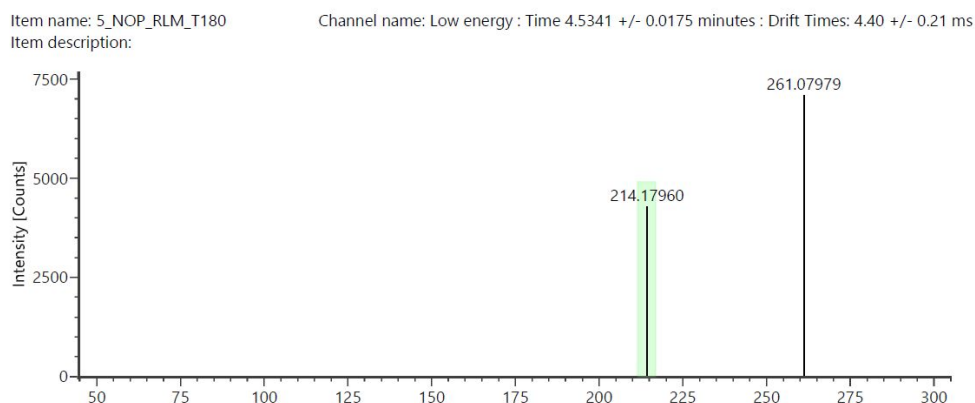


Figure S13. b. Low (upper) and high (lower) energy (HDMS^E) mass spectra for metabolite **M10** (RT = 4.54 min) in HLM (incubation time: t=3h)

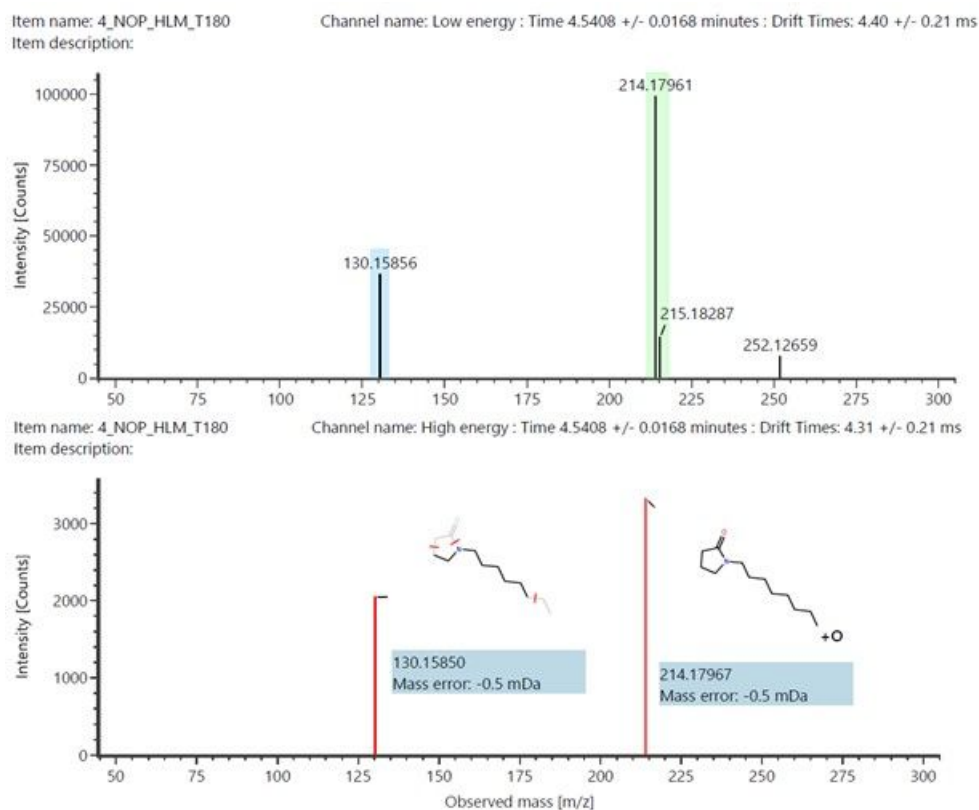


Figure S14. Low (upper) and high (lower) energy (HDMS^E) mass spectra for metabolite **M11** (RT = 4.75 min) in HLM (incubation time: t=3h). Due to the low intensity of parent ion, no high energy fragmentation was collected

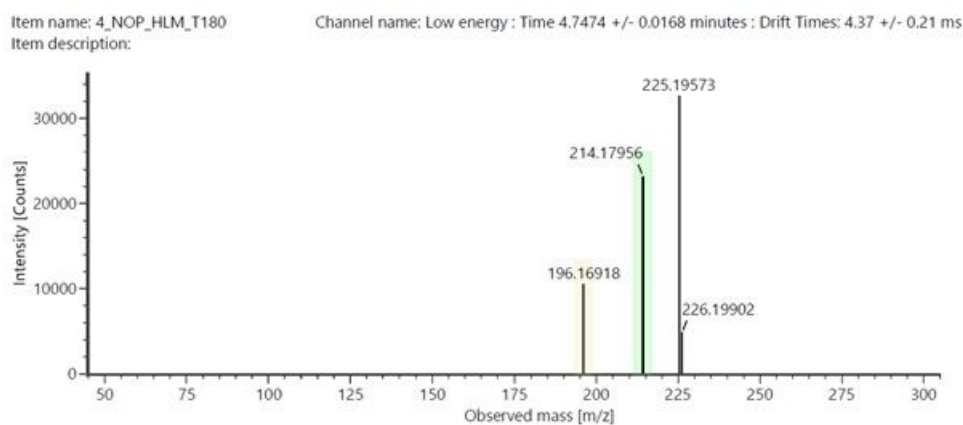
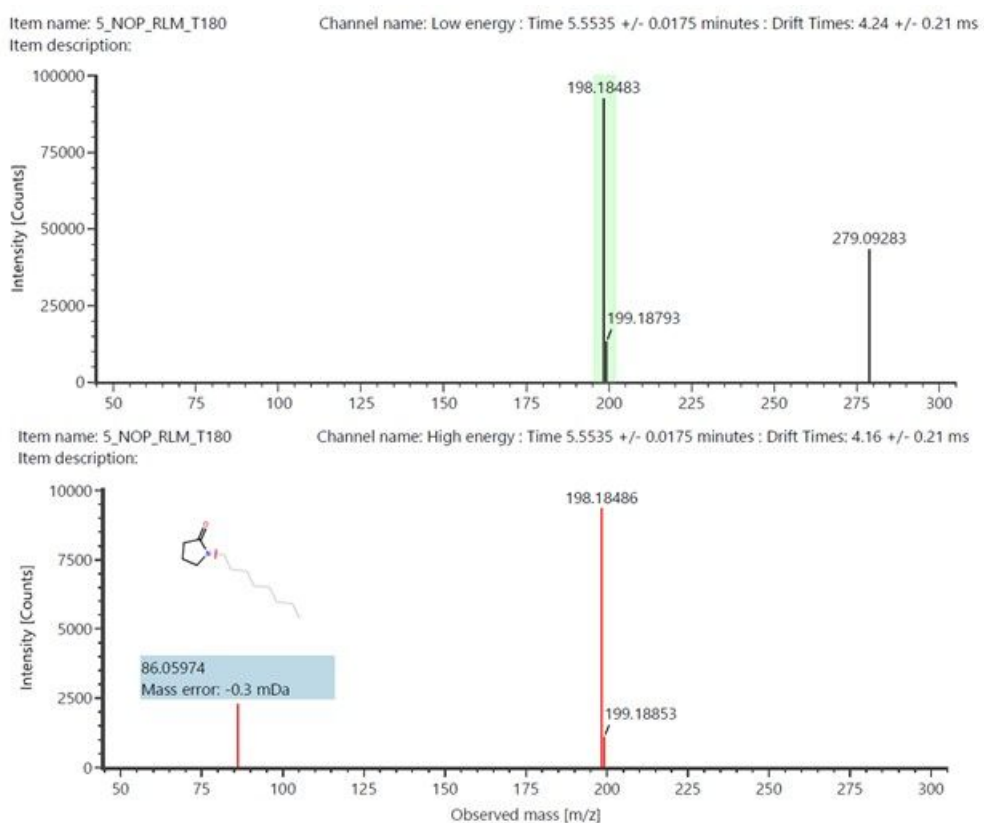


Figure S15. Low (upper) and high (lower) energy (HDMS^E) mass spectra for metabolite parent compound NOP (RT = 5.55 min) in RLM (incubation time: t=3h)



Solubility tests

Table S2. Solubilization efficacy of Fmoc-AA(PG)-OH amino acids and coupling reagents mixtures in green solvents^a

Mixture Fmoc-AA(PG)-OH + coupling reagents (A-E)															
Solvent	Gly +A	Gly +B	Gly +C	Gly +D	Gly +E	Ala +A	Ala +B	Ala +C	Ala +D	Ala +E	Aib +A	Aib +B	Aib +C	Aib +D	Aib +E
NOP															
NCP															
NBnP															

Mixture Fmoc-AA(PG)-OH + coupling reagents (A-E)															
Solvent	Phe +A	Phe +B	Phe +C	Phe +D	Phe +E	Pro +A	Pro +B	Pro +C	Pro +D	Pro +E	Tyr (tBu) +A	Tyr (tBu) +B	Tyr (tBu) +C	Tyr (tBu) +D	Tyr (tBu) +E
NOP															
NCP															
NBnP															

Mixture Fmoc-AA(PG)-OH + coupling reagents (A-E)															
Solvent	Thr (tBu) +A	Thr (tBu) +B	Thr (tBu) +C	Thr (tBu) +D	Thr (tBu) +E	Lys (Boc) +A	Lys (Boc) +B	Lys (Boc) +C	Lys (Boc) +D	Lys (Boc) +E	Cys (Trt) +A	Cys (Trt) +B	Cys (Trt) +C	Cys (Trt) +D	Cys (Trt) +E
NOP															
NCP															0.1 M
NBnP													0.1 M	0.1 M	0.1 M

Legend: OxymaPure®/DIC (A), COMU/DIPEA (B), PyBOP/DIPEA (C), PyOxyma/DIPEA (D), HOBt/DIC (E); green=soluble; yellow=moderately soluble; red=insoluble; PG: protecting groups

^aSolubilisation monitored at 0.2 M concentration unless 0.1 M is specified.

Representative examples of solubility of Fmoc-amino acids in pyrrolidones in presence of selected coupling reagent combinations

Figure S16. Fmoc-Aib-OH (1 eq) after 5 minutes stirring in 1 mL NOP (left), NCP (center) or NBnP (right) mixed with a) DIC/Oxyma Pure® (1 eq); b) HOBt/DIC (1 eq); c) COMU/DIPEA (1 eq)

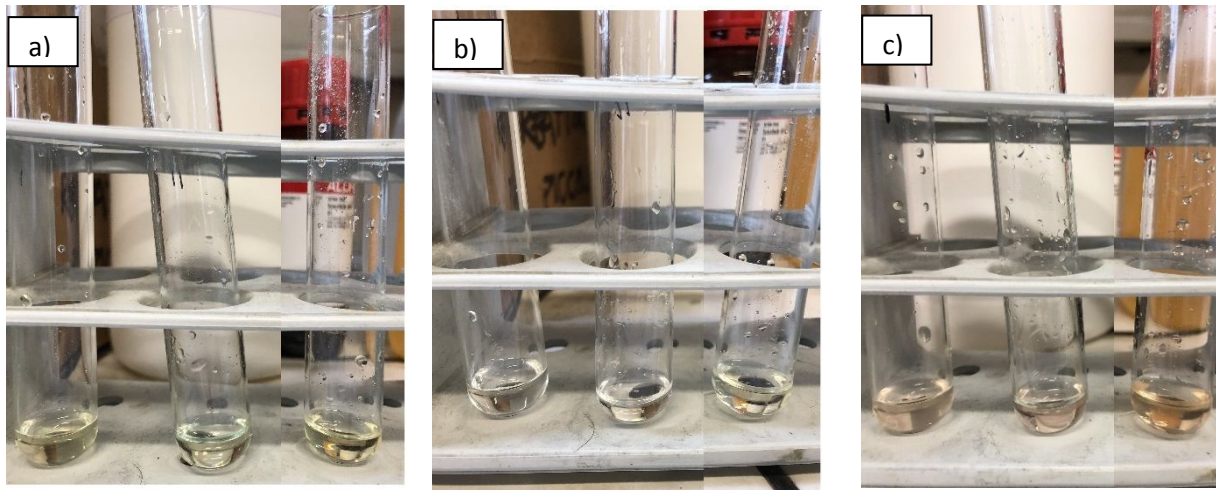


Figure S17. Fmoc-Phe-OH (1 eq) after 5 minutes stirring in 1 mL NOP (left), NCP (center) or NBnP (right) mixed with a) DIC/Oxyma Pure® (1 eq); b) HOBt/DIC (1 eq); c) COMU/DIPEA (1 eq)

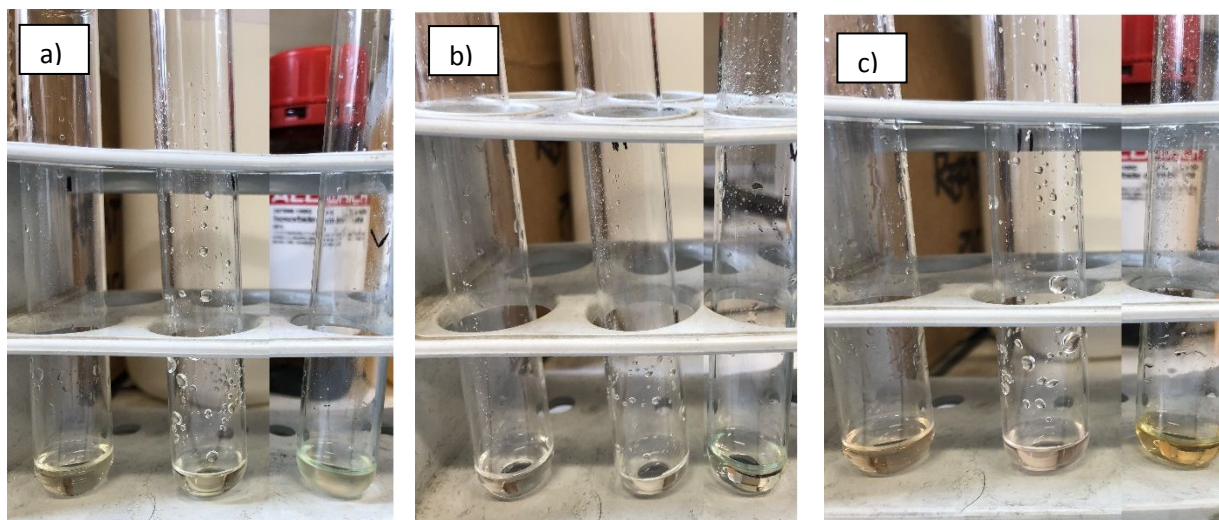
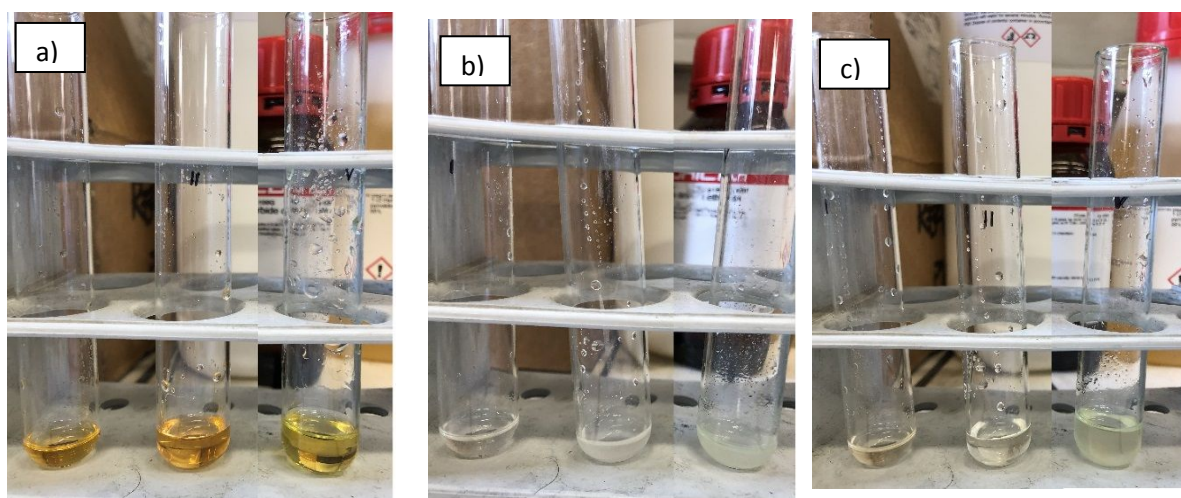


Figure S18. Fmoc-Cys(Trt)-OH (1 eq) after 5 minutes stirring in 1 mL NOP (left), NCP (center) or NBnP (right) alone (a) or mixed with b) DIC/Oxyma Pure® (1 eq); c) COMU/DIPEA (1 eq). In cases a) and c), the mixture in NBnP was further diluted to 0.1M to allow complete dissolution, as reported in the main text



Swelling tests

Table S3. Physical parameters of resins evaluated for swelling tests

Resin	Bead size (μm)	Bead size (mesh)	Loading ($\text{mmol}\cdot\text{g}^{-1}$)	Cross-linking (%)
PS-Wang	75-150	100-200	1.1	1
PS-Trt-Cl	37-75	200-400	1.85	1
PS-RinkAmide	500-560	35-37	0.4-0.7	1
TG-Wang	90	170	0.20	-
TG-RinkAmide	100-200	75-150	0.23	-
CM-Wang	150-500	35-100	0.5-1.2	-
CM-RinkAmide	150-500	35-100	0.4-0.6	-

Table S4. Calculations of standard deviations for the swelling measurements of the reported resins

<i>PS-Wang resin</i>					
	Swell 1	Swell 2	Swell 3	Swelling (mean value)	Standard deviation
DMF	5,6	5,5	5,6	5,6	0,05
NOP	5,4	5,6	5,6	5,5	0,09
NCP	5,1	5	5,2	5,1	0,08
NBnP	2,3	2,1	2,4	2,3	0,12
NBP	4,3	4,4	4,7	4,5	0,17
NOP/DMC 80:20	5,1	5,3	5,2	5,2	0,08
DMC	3,2	3,4	3,2	3,3	0,09

<i>PS-Trt-Cl resin</i>					
	Swell 1	Swell 2	Swell 3	Swelling (mean value)	Standard deviation
DMF	3,1	3,3	3,3	3,2	0,12
NOP	3,4	3,5	3,2	3,4	0,12
NCP	3,5	3,6	3,6	3,6	0,05
NBnP	1,4	1,7	1,6	1,6	0,12
NBP	5	4,9	5	5,0	0,05
NOP/DMC 80:20	3,1	3,1	2,9	3,0	0,09
DMC	3,3	3,2	3,5	3,3	0,12

<i>PS-Rink Amide resin</i>					
	Swell 1	Swell 2	Swell 3	Swelling (mean value)	Standard deviation
DMF	3,3	3	3,4	3,2	0,17
NOP	1,4	1,7	1,6	1,6	0,12
NCP	1,5	1,5	1,6	1,5	0,05
NBnP	1,5	1,7	1,6	1,6	0,08
NBP	2,1	2	2	2,0	0,05

<i>TG-Wang resin</i>					
	Swell 1	Swell 2	Swell 3	Swelling (mean value)	Standard deviation
DMF	6,2	5,8	6,1	6,0	0,17
NOP	1,7	1,6	1,8	1,7	0,08
NCP	2,3	2,6	2,5	2,5	0,12
NBnP	1,1	1,4	1,4	1,3	0,14

<i>TG-Rink Amide</i>					
	Swell 1	Swell 2	Swell 3	Swelling (mean value)	Standard deviation
DMF	6,3	6	6,4	6,2	0,17
NOP	4,2	4,5	4,1	4,3	0,17
NCP	3,3	3,4	3,4	3,4	0,05
NBnP	4,2	3,9	3,9	4,0	0,14

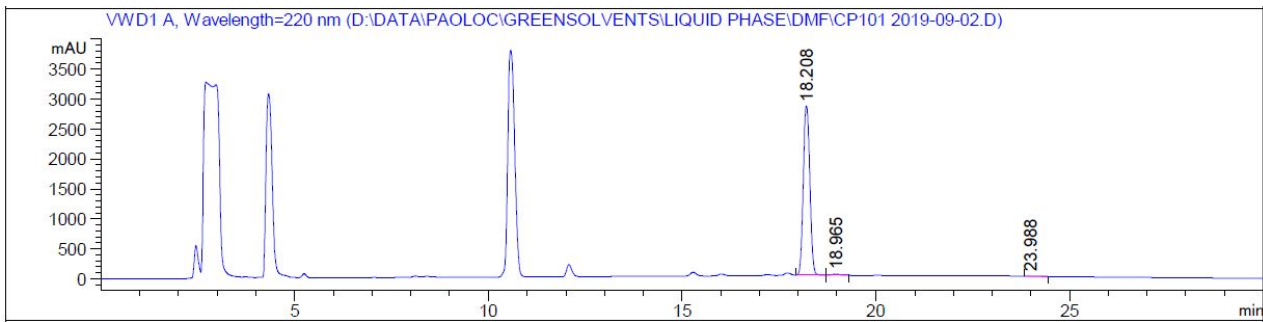
<i>CM-Wang resin</i>					
	Swell 1	Swell 2	Swell 3	Swelling (mean value)	Standard deviation
DMF	4,3	4,5	4,5	4,4	0,09
NOP	1,4	1,2	1,5	1,4	0,12
NCP	1,5	1,7	1,7	1,6	0,09
NBnP	1,6	1,4	1,5	1,5	0,08

<i>CM-Rink Amide</i>					
	Swell 1	Swell 2	Swell 3	Swelling (mean value)	Standard deviation
DMF	8,0	7,7	7,8	7,8	0,12
NOP	3,5	3,3	3,5	3,4	0,09
NCP	6,0	6,1	6,1	6,1	0,05
NBnP	6,7	6,9	6,6	6,7	0,12

Coupling reactions in solution phase

Chromatograms referred to selected entries of Table 6 (main text) are reported below. Peaks of target Z-Phg-Pro-NH₂, Z-D-Phg-Pro-NH₂ and starting Z-Phg-OH (if still present) are considered in the spectra.

Figure S19. Chromatogram of Z-Phg-Pro-NH₂, liquid phase synthesis in DMF with COMU/DIPEA

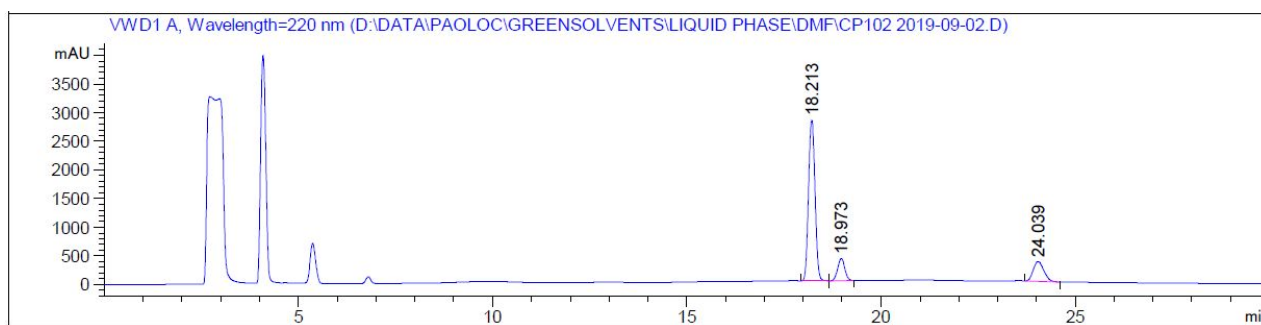


Signal 2: VWD1 A, Wavelength=220 nm

Peak #	RetTime [min]	Type	Width [min]	Area [mAU*s]	Height [mAU]	Area %
1	18.208	BB	0.1883	3.30223e4	2827.07617	98.9838
2	18.965	BB	0.1985	300.55829	23.94113	0.9009
3	23.988	BBA	0.3489	38.46123	1.77398	0.1153

Totals : 3.33614e4 2852.79128

Product	Rt (min)	Area (%)
Z-Phg-Pro-NH ₂	18.208	99.0
Z-D-Phg-Pro-NH ₂	18.965	0.9
Z-Phg-OH	23.988	0.1

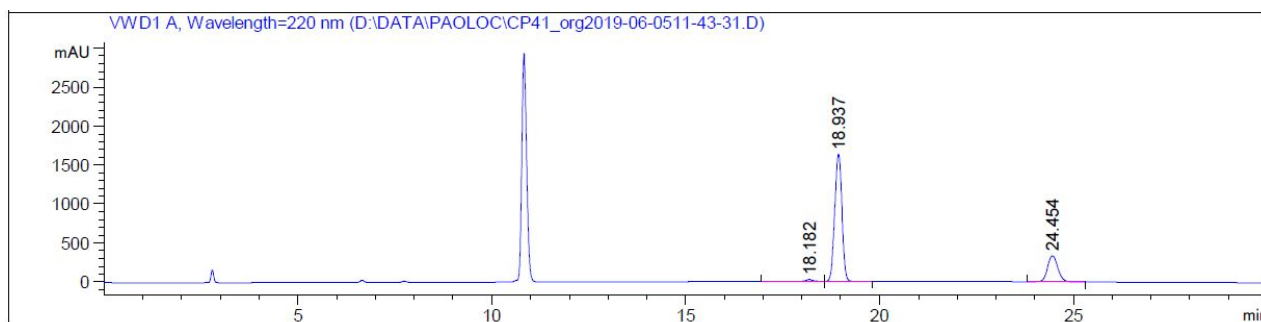
Figure S20. Chromatogram of Z-Phg-Pro-NH₂, liquid phase synthesis in DMF with HOBt/DIC

Signal 2: VWD1 A, Wavelength=220 nm

Peak #	RetTime [min]	Type	Width [min]	Area [mAU*s]	Height [mAU]	Area %
1	18.213	BB	0.1856	3.26085e4	2805.47949	73.9204
2	18.973	BB	0.1995	4973.25342	388.14386	11.2739
3	24.039	BBA	0.3013	6531.19727	344.37027	14.8056

Totals : 4.41129e4 3537.99362

Product	Rt (min)	Area (%)
Z-Phg-Pro-NH ₂	18.213	73.9
Z-D-Phg-Pro-NH ₂	18.973	11.3
Z-Phg-OH	24.039	14.8

Figure S21. Chromatogram of Z-D-Phg-Pro-NH₂, liquid phase synthesis in DMF with DIC/OxymaPure®

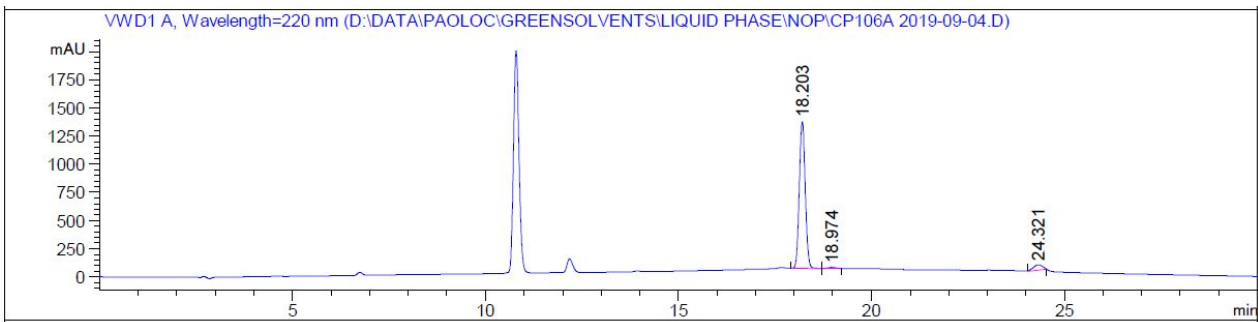
Signal 2: VWD1 A, Wavelength=220 nm

Peak #	RetTime [min]	Type	Width [min]	Area [mAU*s]	Height [mAU]	Area %
1	18.182	BB	0.1921	327.00656	24.44429	1.1886
2	18.937	BB	0.2025	2.10566e4	1632.74902	76.5341
3	24.454	BB	0.2857	6129.09180	334.60367	22.2774

Totals : 2.75127e4 1991.79698

Product	Rt (min)	Area (%)
Z-Phg-Pro-NH ₂	18.182	1.2
Z-D-Phg-Pro-NH ₂	18.937	76.5
Z-Phg-OH	24.454	22.2

Figure S22. Chromatogram of Z-Phg-Pro-NH₂, liquid phase synthesis in NOP with DIC/OxymaPure®



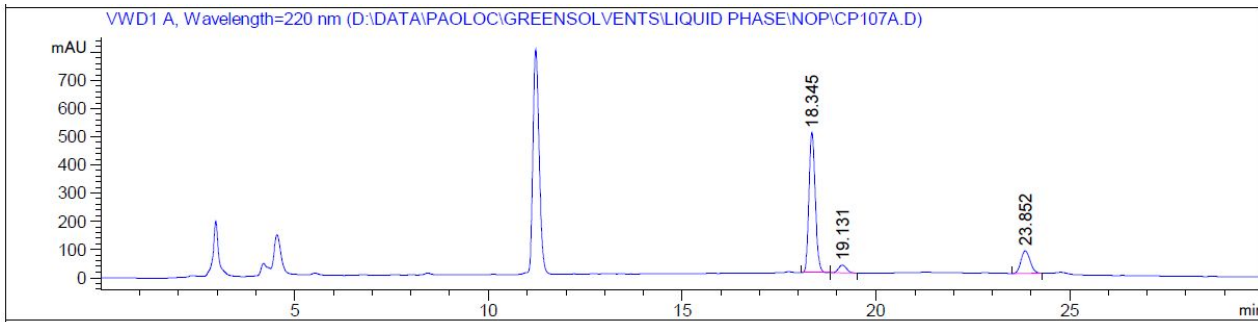
Signal 2: VWD1 A, Wavelength=220 nm

Peak #	RetTime [min]	Type	Width [min]	Area [mAU*s]	Height [mAU]	Area %
1	18.203	BB	0.1686	1.39291e4	1303.77344	93.7300
2	18.974	BB	0.1951	139.24954	11.35123	0.9370
3	24.321	MM	0.2738	792.52600	48.23468	5.3330

Totals : 1.48608e4 1363.35934

Product	Rt (min)	Area (%)
Z-Phg-Pro-NH ₂	18.203	93.7
Z-D-Phg-Pro-NH ₂	18.974	0.9
Z-Phg-OH	24.321	5.3

Figure S23. Chromatogram of Z-Phg-Pro-NH₂, liquid phase synthesis in NOP with COMU/DIPEA



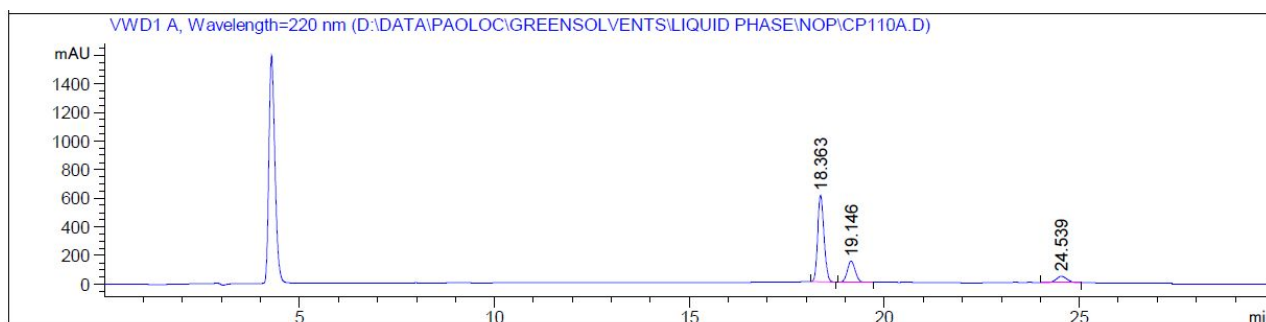
Signal 2: VWD1 A, Wavelength=220 nm

Peak #	RetTime [min]	Type	Width [min]	Area [mAU*s]	Height [mAU]	Area %
1	18.345	BB	0.1737	5635.76367	499.20959	76.7876
2	19.131	BB	0.2220	395.47168	27.45575	5.3883
3	23.852	BB	0.2567	1308.18469	80.03396	17.8241

Totals : 7339.42004 606.69930

Product	Rt (min)	Area (%)
Z-Phg-Pro-NH ₂	18.208	99.0
Z-D-Phg-Pro-NH ₂	18.965	0.9
Z-Phg-OH	23.988	0.1

Figure S24. Chromatogram of Z-Phg-Pro-NH₂, liquid phase synthesis in NOP with PyBOP/HOBt/DIPEA



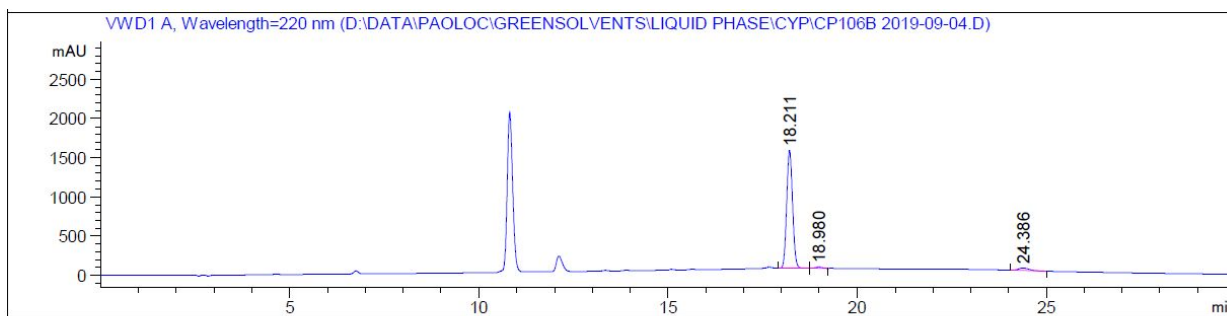
Signal 2: VWD1 A, Wavelength=220 nm

Peak #	RetTime [min]	Type	Width [min]	Area [mAU*s]	Height [mAU]	Area %
1	18.363	BB	0.1741	6843.63623	604.44281	69.6726
2	19.146	BB	0.2204	2084.97290	147.93764	21.2263
3	24.539	BB	0.3056	893.96100	45.42034	9.1011

Totals : 9822.57013 797.80079

Product	Rt (min)	Area (%)
Z-Phg-Pro-NH ₂	18.363	69.7
Z-D-Phg-Pro-NH ₂	19.146	21.2
Z-Phg-OH	24.539	9.1

Figure S25. Chromatogram of Z-Phg-Pro-NH₂, liquid phase synthesis in NCP with DIC/OxymaPure®



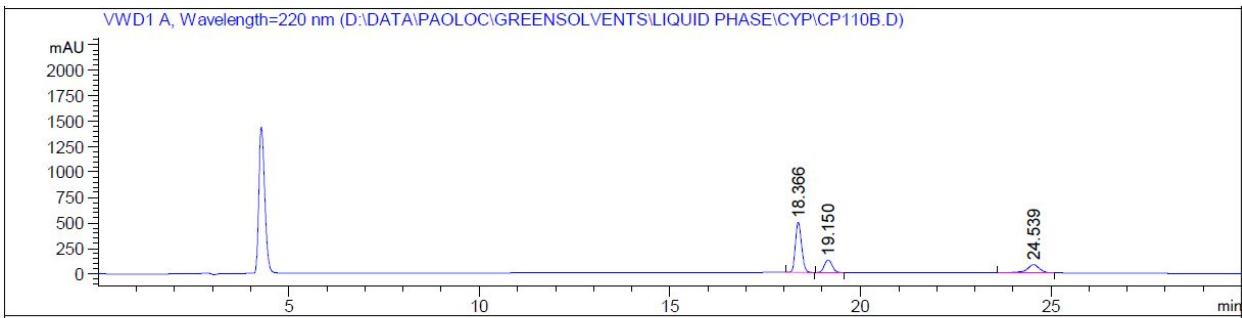
Signal 2: VWD1 A, Wavelength=220 nm

Peak #	RetTime [min]	Type	Width [min]	Area [mAU*s]	Height [mAU]	Area %
1	18.211	BB	0.1702	1.62625e4	1503.28638	95.1064
2	18.980	BB	0.1958	181.97142	14.75985	1.0642
3	24.386	BBA	0.3154	654.79907	32.72625	3.8294

Totals : 1.70993e4 1550.77247

Product	Rt (min)	Area (%)
Z-Phg-Pro-NH ₂	18.211	95.1
Z-D-Phg-Pro-NH ₂	18.980	1.1
Z-Phg-OH	24.386	3.8

Figure S26. Chromatogram of Z-Phg-Pro-NH₂, liquid phase synthesis in NCP with PyBOP/HOBt/DIPEA



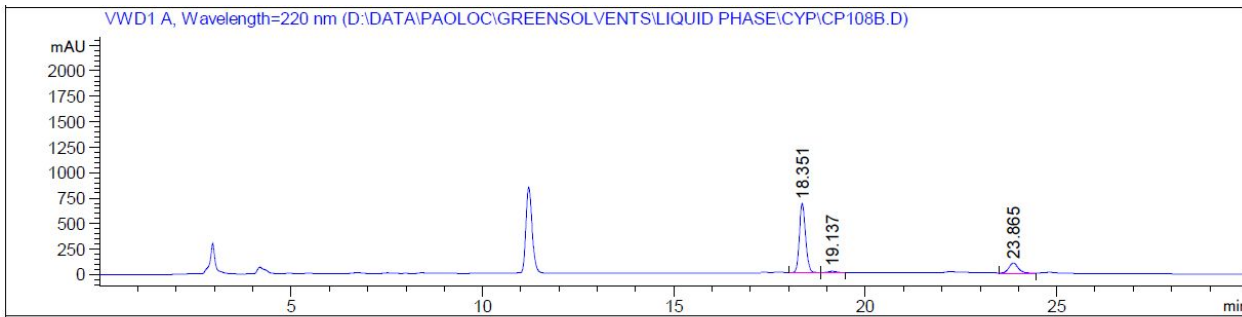
Signal 2: VWD1 A, Wavelength=220 nm

Peak #	RetTime [min]	Type	Width [min]	Area [mAU*s]	Height [mAU]	Area %
1	18.366	BB	0.1743	5578.51953	491.92984	60.8877
2	19.150	BB	0.2202	1744.89819	124.00921	19.0450
3	24.539	BB	0.3412	1838.56287	80.87137	20.0673

Totals : 9161.98059 696.81042

Product	Rt (min)	Area (%)
Z-Phg-Pro-NH ₂	18.366	60.9
Z-D-Phg-Pro-NH ₂	19.150	19.0
Z-Phg-OH	24.539	20.1

Figure S27. Chromatogram of Z-Phg-Pro-NH₂, liquid phase synthesis in NCP with PyOxyma/DIPEA



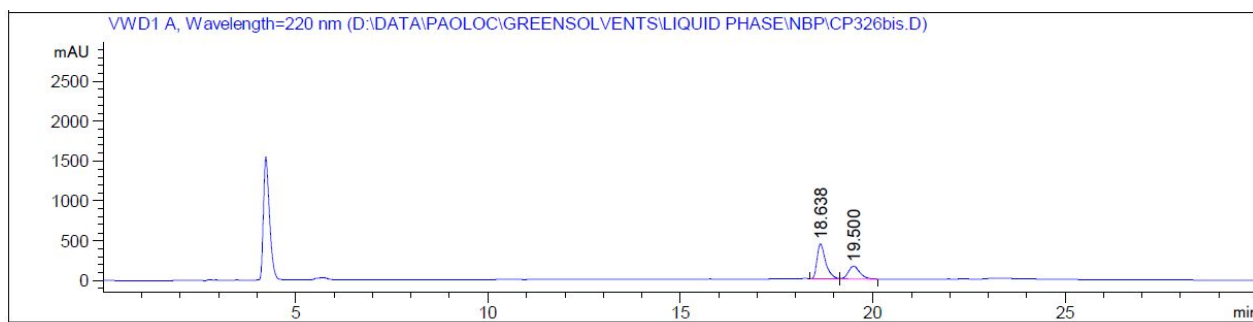
Signal 2: VWD1 A, Wavelength=220 nm

Peak #	RetTime [min]	Type	Width [min]	Area [mAU*s]	Height [mAU]	Area %
1	18.351	BB	0.1739	7652.02441	676.83398	81.1264
2	19.137	BB	0.2208	181.47392	12.85008	1.9240
3	23.865	BB	0.2590	1598.73096	96.66351	16.9497

Totals : 9432.22929 786.34758

Product	Rt (min)	Area (%)
Z-Phg-Pro-NH ₂	18.351	81.1
Z-D-Phg-Pro-NH ₂	19.137	1.9
Z-Phg-OH	23.865	16.9

Figure S28. Chromatogram of Z-Phg-Pro-NH₂, liquid phase synthesis in NBnP with PyBOP/HOBt/DIPEA



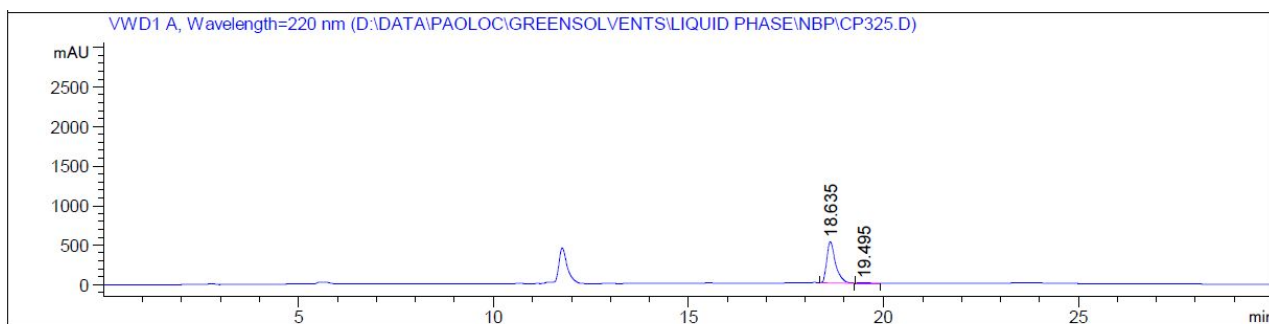
Signal 2: VWD1 A, Wavelength=220 nm

Peak #	RetTime [min]	Type	Width [min]	Area [mAU*s]	Height [mAU]	Area %
1	18.638	BB	0.2294	6626.39258	435.76483	67.8210
2	19.500	BB	0.3048	3144.01807	157.53407	32.1790

Totals : 9770.41064 593.29890

Product	Rt (min)	Area (%)
Z-Phg-Pro-NH ₂	18.638	67.8
Z-D-Phg-Pro-NH ₂	19.500	32.2

Figure S29. Chromatogram of Z-Phg-Pro-NH₂, liquid phase synthesis in NBnP with PyOxyma/DIPEA



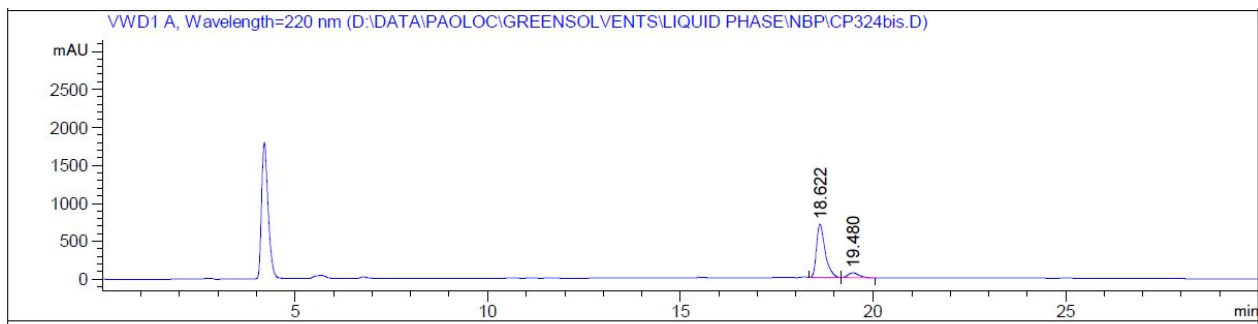
Signal 2: VWD1 A, Wavelength=220 nm

Peak #	RetTime [min]	Type	Width [min]	Area [mAU*s]	Height [mAU]	Area %
1	18.635	BB	0.2301	8040.38184	520.78162	99.2990
2	19.495	BB	0.2715	56.76353	3.35316	0.7010

Totals : 8097.14536 524.13478

Product	Rt (min)	Area (%)
Z-Phg-Pro-NH ₂	18.635	99.3
Z-D-Phg-Pro-NH ₂	19.495	0.7

Figure S30. Chromatogram of Z-Phg-Pro-NH₂, liquid phase synthesis in NBnP with HOBT/DIC



Signal 2: VWD1 A, Wavelength=220 nm

Peak #	RetTime [min]	Type	Width [min]	Area [mAU*s]	Height [mAU]	Area %
1	18.622	BB	0.2317	1.07921e4	700.55780	89.9444
2	19.480	BB	0.2963	1206.53198	62.74966	10.0556

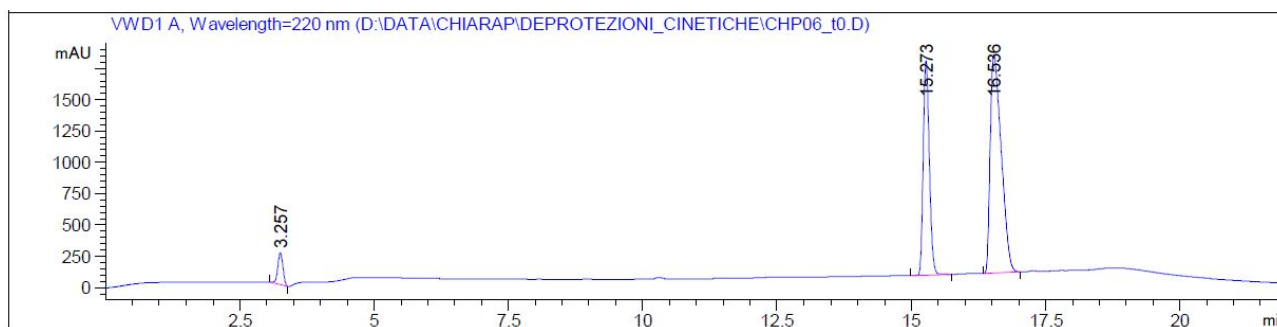
Totals : 1.19987e4 763.30746

Product	Rt (min)	Area (%)
Z-Phg-Pro-NH ₂	18.622	89.9
Z-D-Phg-Pro-NH ₂	19.480	10.1

Deprotection kinetic tests

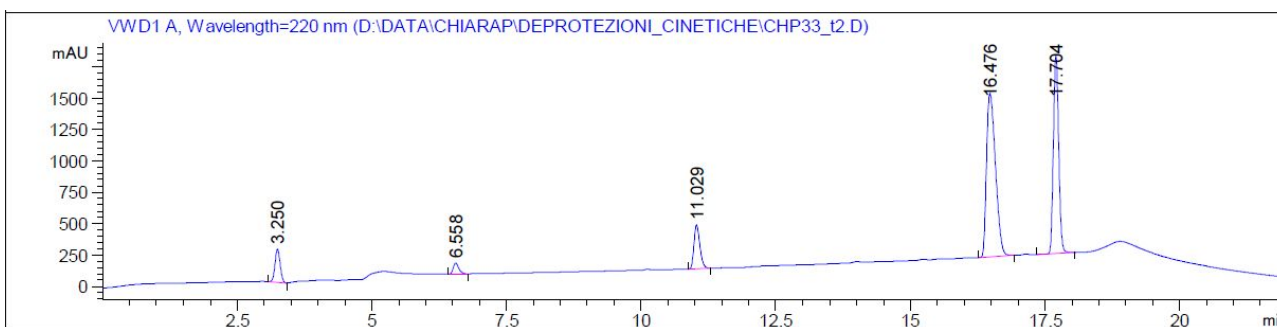
Deprotection kinetic tests in all investigated pyrrolidones revealed complete Fmoc removal in 2 minutes. A selected example in NOP is reported below.

Figure S31. Chromatogram of Fmoc-Phe-OH deprotection in NOP at t=0 (before base addition)



Legend: Piperidine = peak at 3.257 min; Fmoc-Phe-OH = peak at 15.273 min; NOP = peak at 16.536 min

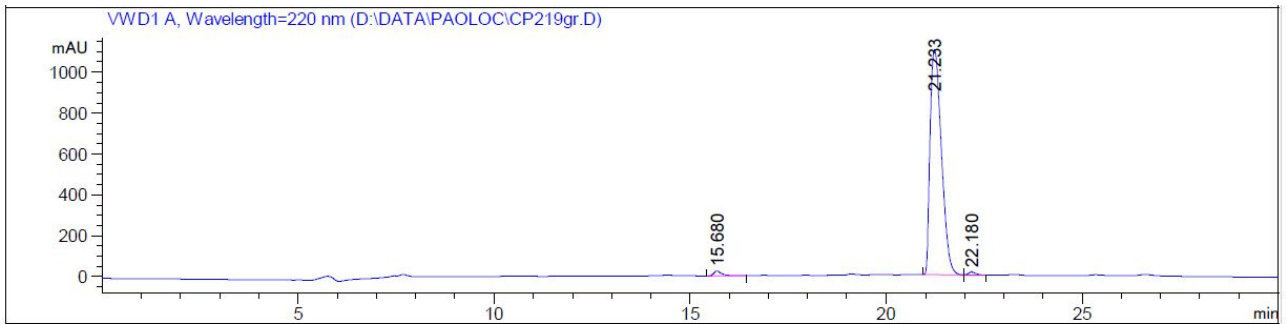
Figure S32. Chromatogram of Fmoc-Phe-OH deprotection in NOP at t=2 minutes



Legend: Piperidine = peak at 3.250 min; H-Phe-OH = peak at 6.558 min; DBF-piperidine adduct = peak at 11.029 min; NOP = peak at 16.476 min; dibenzofulvene (DBF) = peak at 17.704 min

SPPS of Aib-Enkephalin in Green Solvents

Figure S33. Chromatogram of Aib-Enkephalin pentapeptide, manual SPPS in NOP on PS-Wang resin



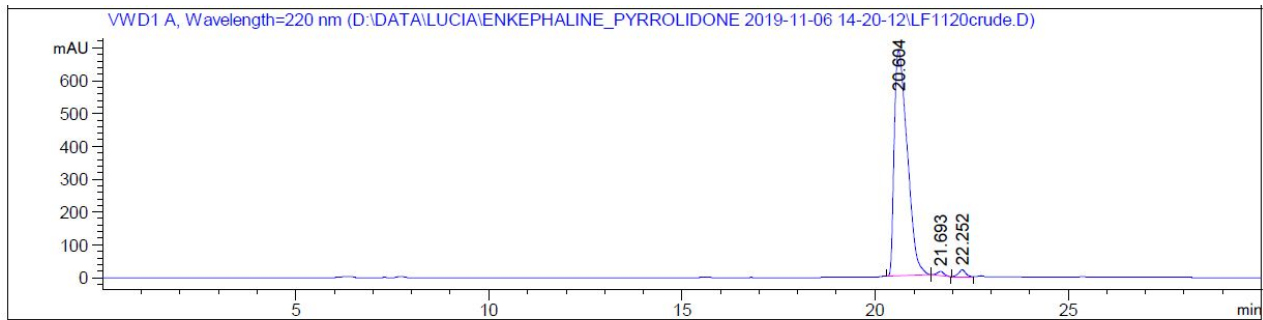
Signal 2: VWD1 A, Wavelength=220 nm

Peak #	RetTime [min]	Type	Width [min]	Area [mAU*s]	Height [mAU]	Area %
1	15.680	BB	0.2123	329.22705	22.81919	1.4622
2	21.233	BB	0.3216	2.20013e4	1098.72717	97.7158
3	22.180	BB	0.2012	185.07613	14.09826	0.8220

Totals : 2.25156e4 1135.64462

Peptide	Rt (min)	RRT	Area (%)
Des-Phe	15.680	0.74	1.5
Aib-Enkephalin	21.233	1.00	97.7
Des-Aib	22.180	1.04	0.8

Figure S34. Chromatogram of Aib-Enkephalin pentapeptide, manual SPPS in NOP on PS-Trt-Cl resin



Signal 2: VWD1 A, Wavelength=220 nm

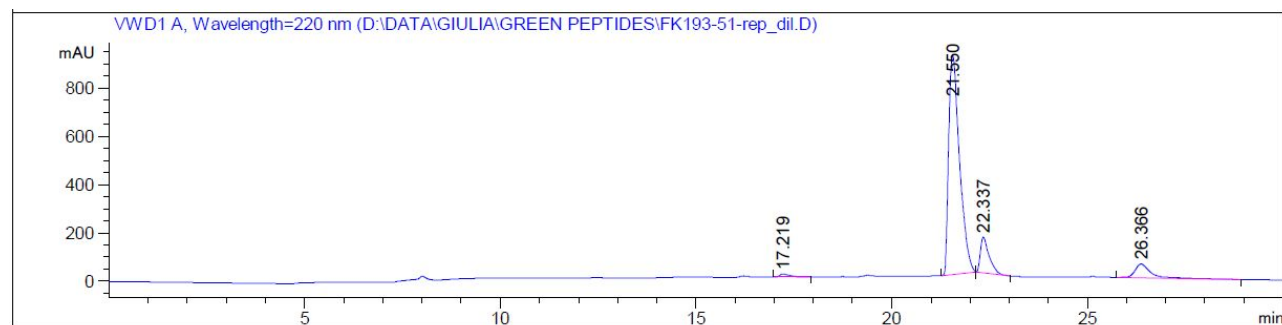
Peak #	RetTime [min]	Type	Width [min]	Area [mAU*s]	Height [mAU]	Area %
1	20.604	BB	0.3613	1.60242e4	689.11395	97.4135
2	21.693	BB	0.1815	157.17870	13.14057	0.9555
3	22.252	BB	0.1893	268.28781	21.25153	1.6310

Totals : 1.64497e4 723.50605

Peptide	Rt (min)	RRT	Area (%)
Aib-Enkephalin	20.604	1.00	97.4

Des-Aib	21.693	1.04	1.0
Des-Aib+tBu+TFA	22.252	1.08	1.6

Figure S35. Chromatogram of Aib-Enkephalin pentapeptide, manual SPPS in NCP on PS-Wang resin



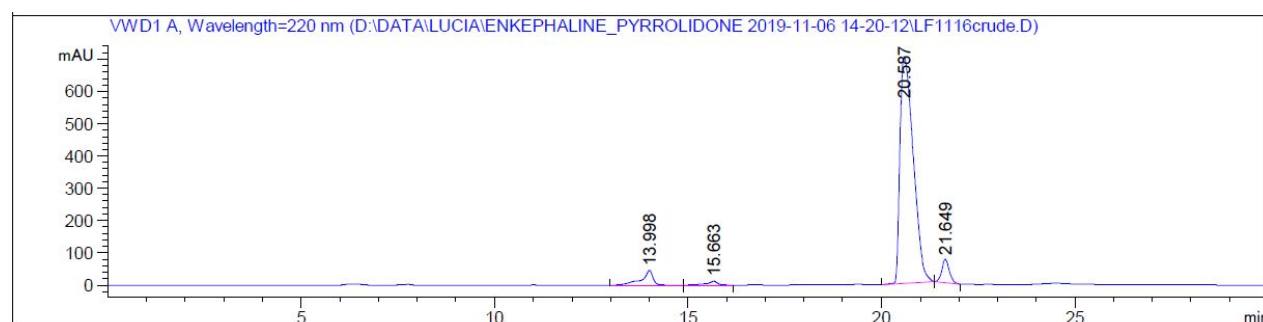
Signal 2: VWD1 A, Wavelength=220 nm

Peak #	RetTime [min]	Type	Width [min]	Area [mAU*s]	Height [mAU]	Area %
1	17.219	BB	0.2546	222.67754	12.45164	1.0294
2	21.550	BB	0.2902	1.75010e4	910.80939	80.9062
3	22.337	BB	0.2256	2278.07446	147.96461	10.5314
4	26.366	BB	0.4191	1629.48035	56.73232	7.5330

Totals : 2.16313e4 1127.95797

Peptide	Rt (min)	RRT	Area (%)
Des-Aib-Tyr	17.219	0.80	1.0
Aib-Enkephalin	21.550	1.00	80.9
Des-Aib	22.337	1.04	10.5
Aib-Enkephalin+TFA	26.366	1.23	7.6

Figure S36. Chromatogram of Aib-Enkephalin pentapeptide, manual SPPS in NCP on PS-Trt-Cl resin



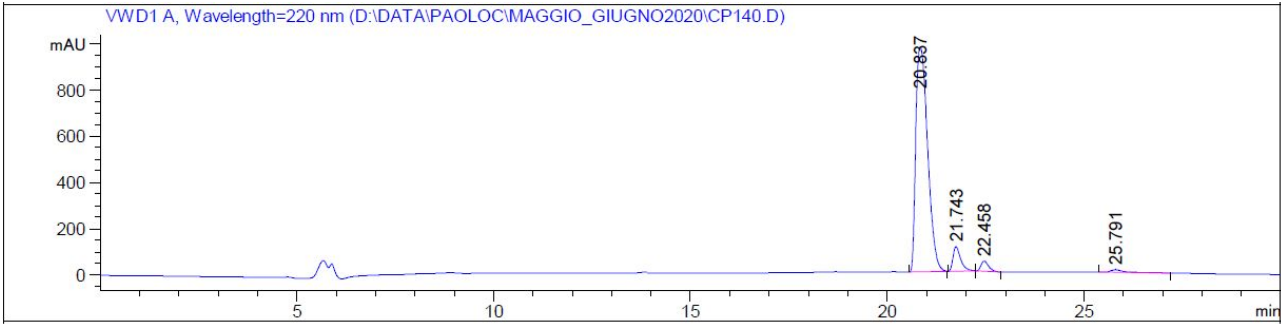
Signal 2: VWD1 A, Wavelength=220 nm

Peak #	RetTime [min]	Type	Width [min]	Area [mAU*s]	Height [mAU]	Area %
1	13.998	BB	0.2773	912.86908	45.26573	4.8253
2	15.663	BB	0.2435	206.71103	11.85194	1.0927
3	20.587	BB	0.3778	1.68199e4	701.40295	88.9086
4	21.649	BB	0.2063	978.72028	72.14259	5.1734

Totals : 1.89182e4 830.66321

Peptide	Rt (min)	RRT	Area (%)
Des-Phe-Aib	13.998	0.68	4.8
Des-Phe	15.663	0.76	1.1
Aib-Enkephalin	20.587	1.00	88.9
Des-Aib	21.649	1.04	5.2

Figure S37. Chromatogram of Aib-Enkephalin pentapeptide, manual SPPS in NBP on PS-Wang resin

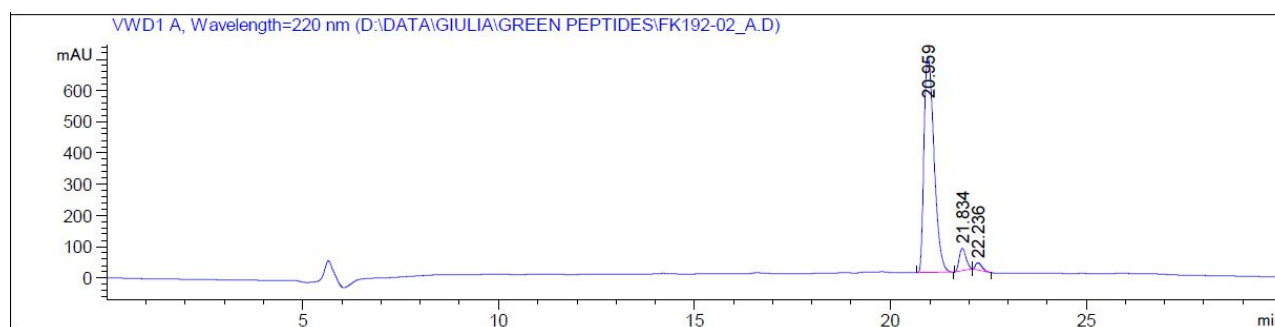


Signal 2: VWD1 A, Wavelength=220 nm

Peak #	RetTime [min]	Type	Width [min]	Area [mAU*s]	Height [mAU]	Area %
1	20.837	BB	0.3368	2.02126e4	971.16205	89.7160
2	21.743	BB	0.2046	1414.25427	105.33276	6.2773
3	22.458	BB	0.1992	575.41437	43.81619	2.5540
4	25.791	BB	0.3745	327.27429	12.29867	1.4526

Totals : 2.25295e4 1132.60966

Peptide	Rt (min)	RRT	Area (%)
Aib-Enkephalin	20.837	1.00	89.7
Des-Aib	21.743	1.04	6.3
Des-Aib+tBu+TFA	22.458	1.08	2.6
Aib-Enkephalin+TFA	25.791	1.23	1.4

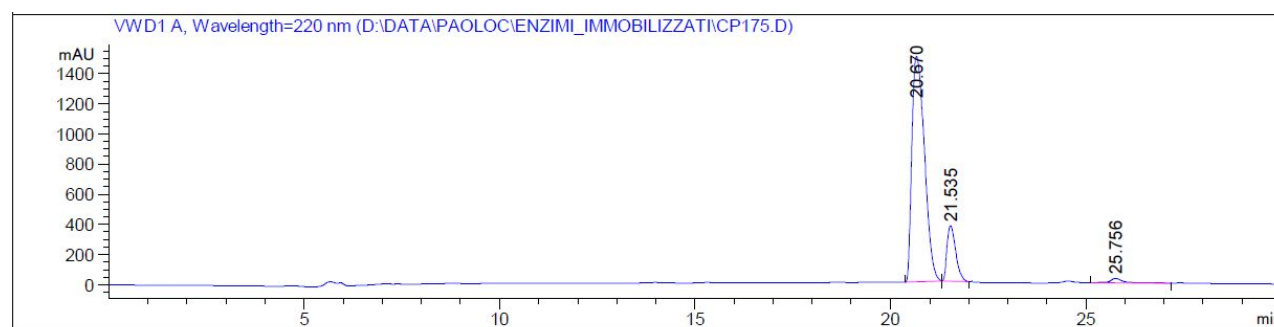
Figure S38. Chromatogram of Aib-Enkephalin pentapeptide, manual SPPS in NBP on PS-Trt-Cl resin

Signal 2: VWD1 A, Wavelength=220 nm

Peak #	RetTime [min]	Type	Width [min]	Area [mAU*s]	Height [mAU]	Area %
1	20.959	BB	0.2817	1.23417e4	693.12585	91.6110
2	21.834	BB	0.1851	862.24347	72.29428	6.4003
3	22.236	BB	0.1763	267.91568	23.62984	1.9887

Totals : 1.34719e4 789.04997

Peptide	Rt (min)	RRT	Area (%)
Aib-Enkephalin	20.959	1.00	91.6
Des-Aib	21.834	1.04	6.4
Des-Aib+tBu+TFA	22.236	1.06	2.0

Figure S39. Chromatogram of Aib-Enkephalin pentapeptide, manual SPPS in DMF on PS-Wang resin

Signal 2: VWD1 A, Wavelength=220 nm

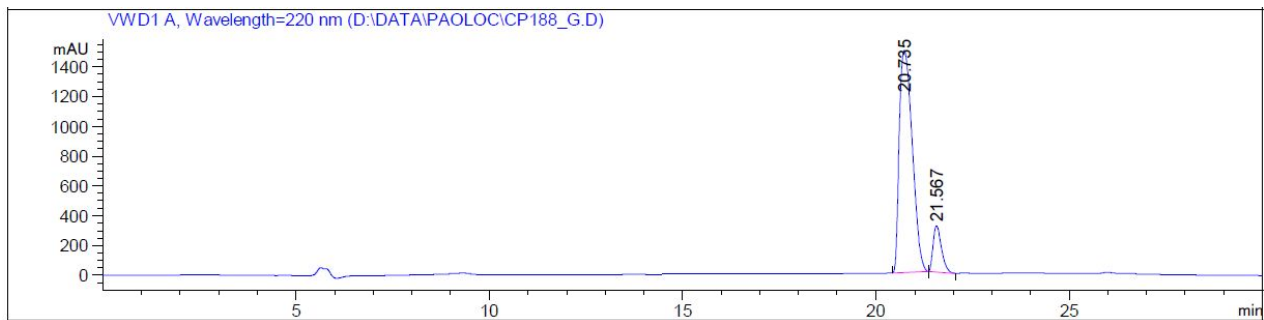
Peak #	RetTime [min]	Type	Width [min]	Area [mAU*s]	Height [mAU]	Area %
1	20.670	BB	0.3657	3.35146e4	1494.20105	84.0369
2	21.535	BB	0.2424	5678.86670	367.24759	14.2396
3	25.756	BB	0.3358	687.37134	29.29332	1.7236

Totals : 3.98808e4 1890.74195

Peptide	Rt (min)	RRT	Area (%)
Aib-Enkephalin	20.670	1.00	84.0

Des-Aib	21.535	1.04	14.2
Aib-Enkephalin+TFA	25.756	1.23	1.8

Figure S40. Chromatogram of Aib-Enkephalin pentapeptide, manual SPPS in DMF on PS-Trt-Cl resin



Signal 2: VWD1 A, Wavelength=220 nm

Peak #	RetTime [min]	Type	Width [min]	Area [mAU*s]	Height [mAU]	Area %
1	20.735	BB	0.3830	3.49027e4	1491.34082	88.1380
2	21.567	BB	0.2361	4697.35010	311.21463	11.8620

Totals : 3.96001e4 1802.55545

Peptide	Rt (min)	RRT	Area (%)
Aib-Enkephalin	20.735	1.00	88.1
Des-Aib	21.567	1.04	11.9

Figure S41. Mass spectrum of H₂N-Tyr-Aib-Aib-Phe-Leu-COOH (Aib-Enkephalin)

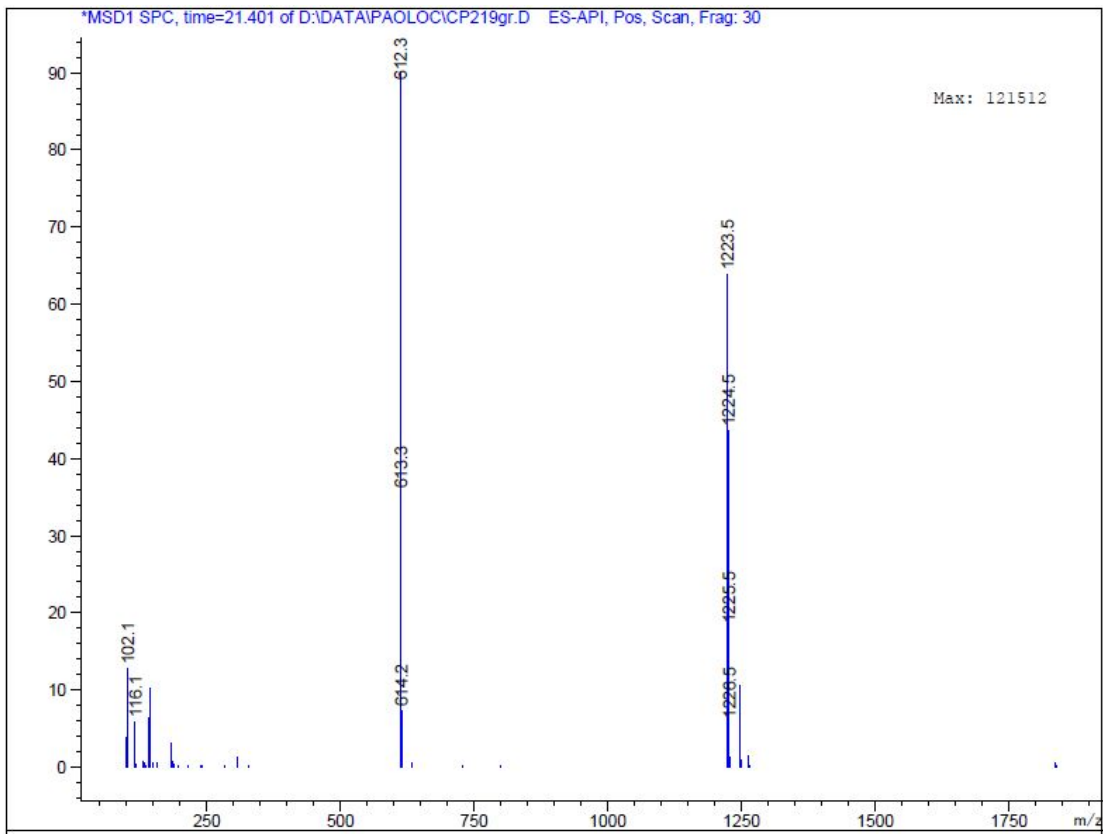
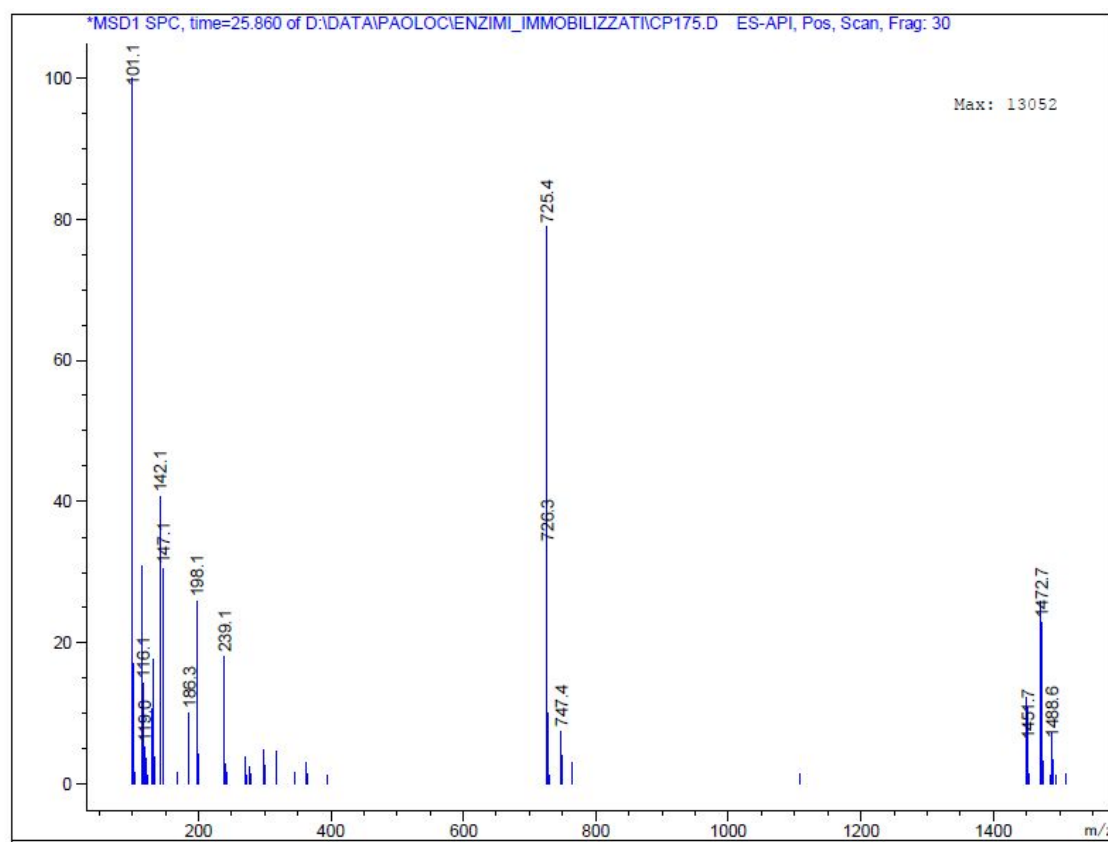


Figure S42. Mass spectrum of H₂N-Tyr-Aib-Aib-Phe-Leu-COOH + TFA (Aib-Enkephalin+TFA)**Figure S43.** Mass spectrum of H₂N-Tyr-Aib-Phe-Leu-COOH (des-Aib)

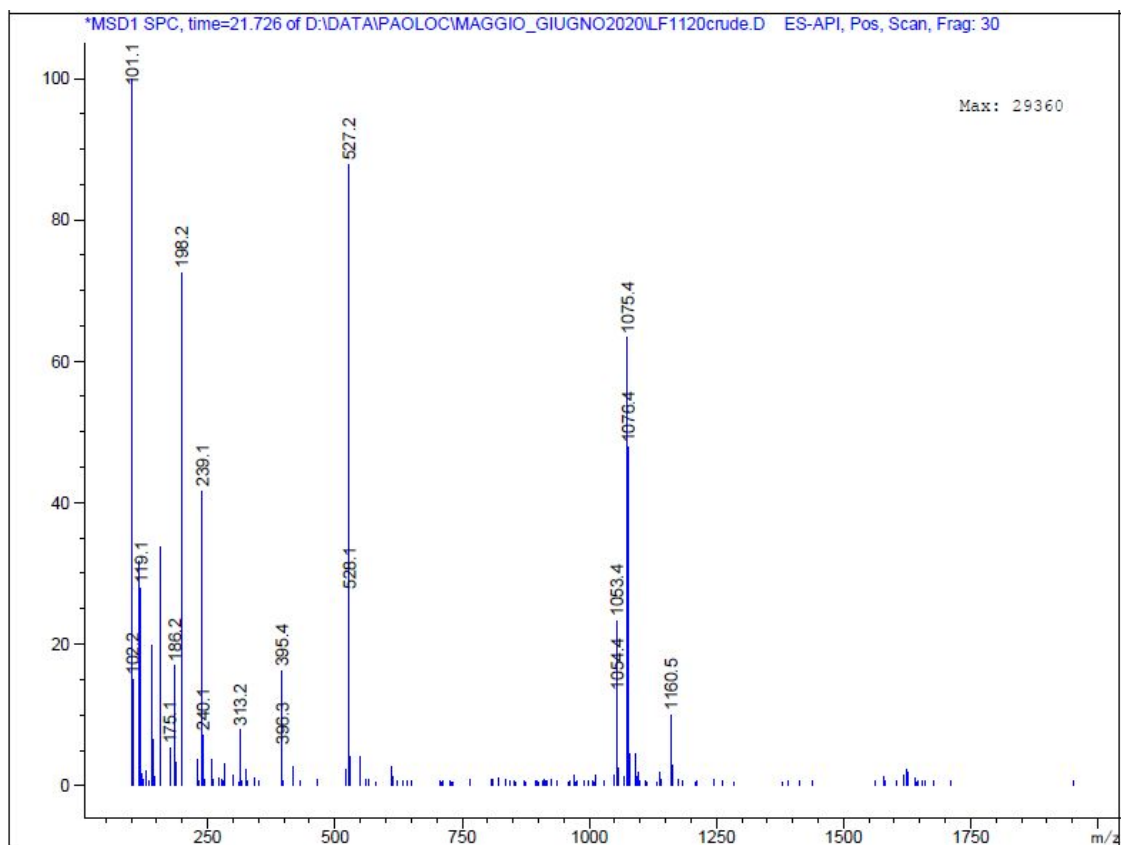


Figure S44. Mass spectrum of H₂N-Tyr-Aib-Phe-Leu-COOH+tBu+TFA (des-Aib+tBu+TFA)

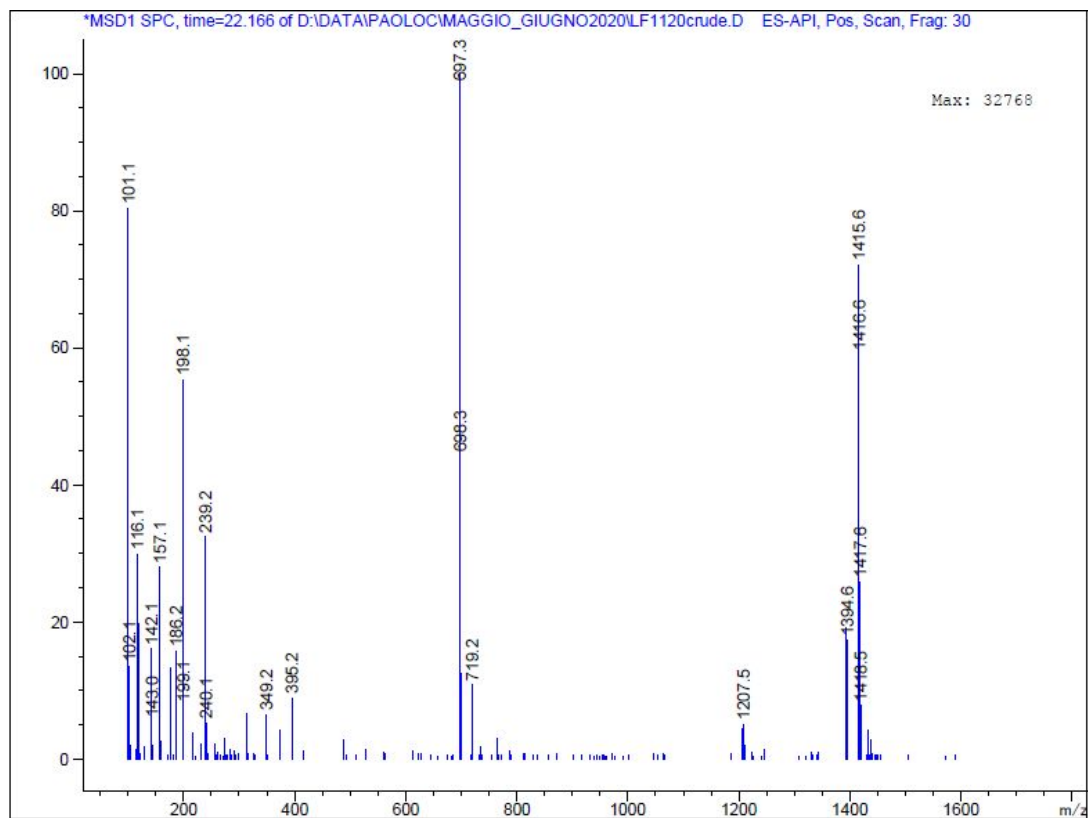


Figure S45. Mass spectrum of H₂N-Tyr-Aib-Aib-Leu-COOH (des-Phe)

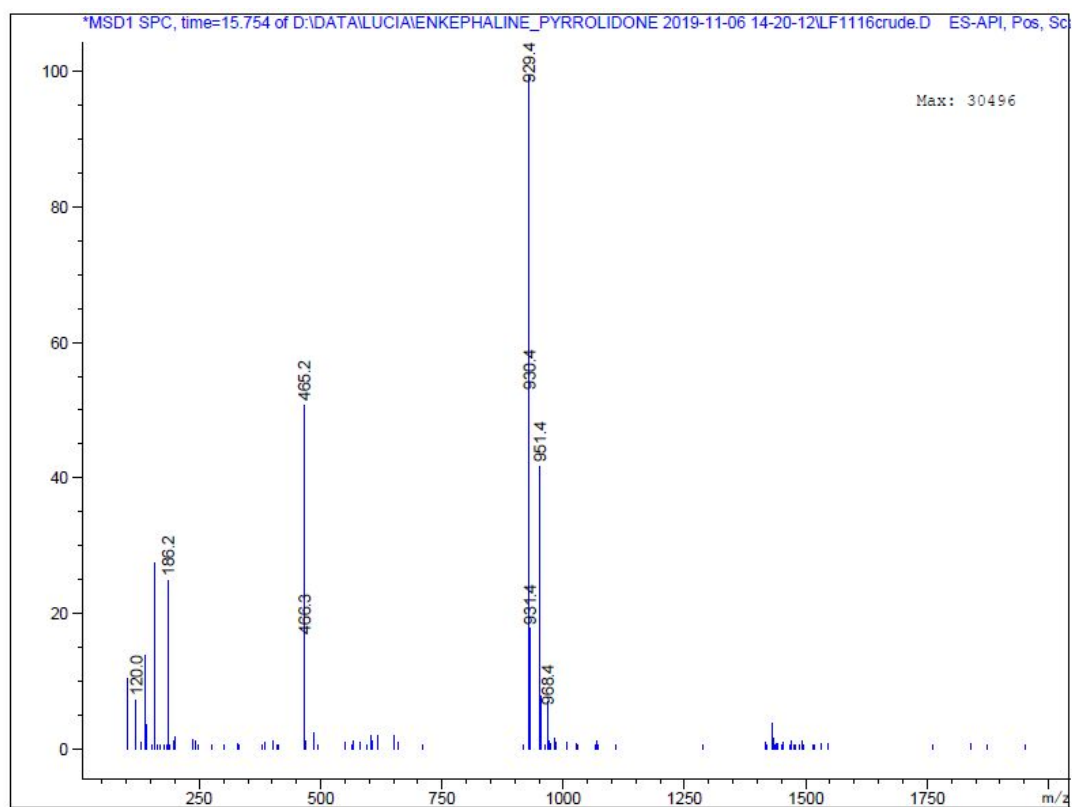


Figure S46. Mass spectrum of H₂N-Aib-Phe-Leu-COOH (des-Aib-Tyr)

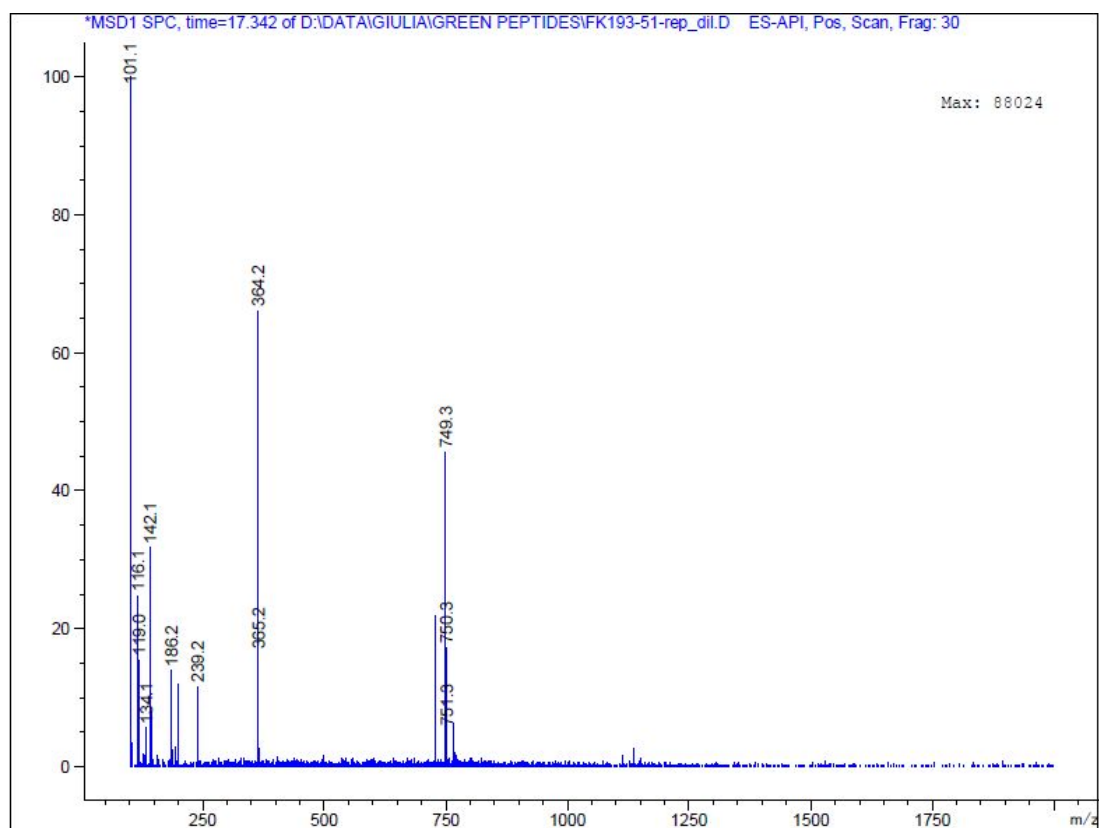
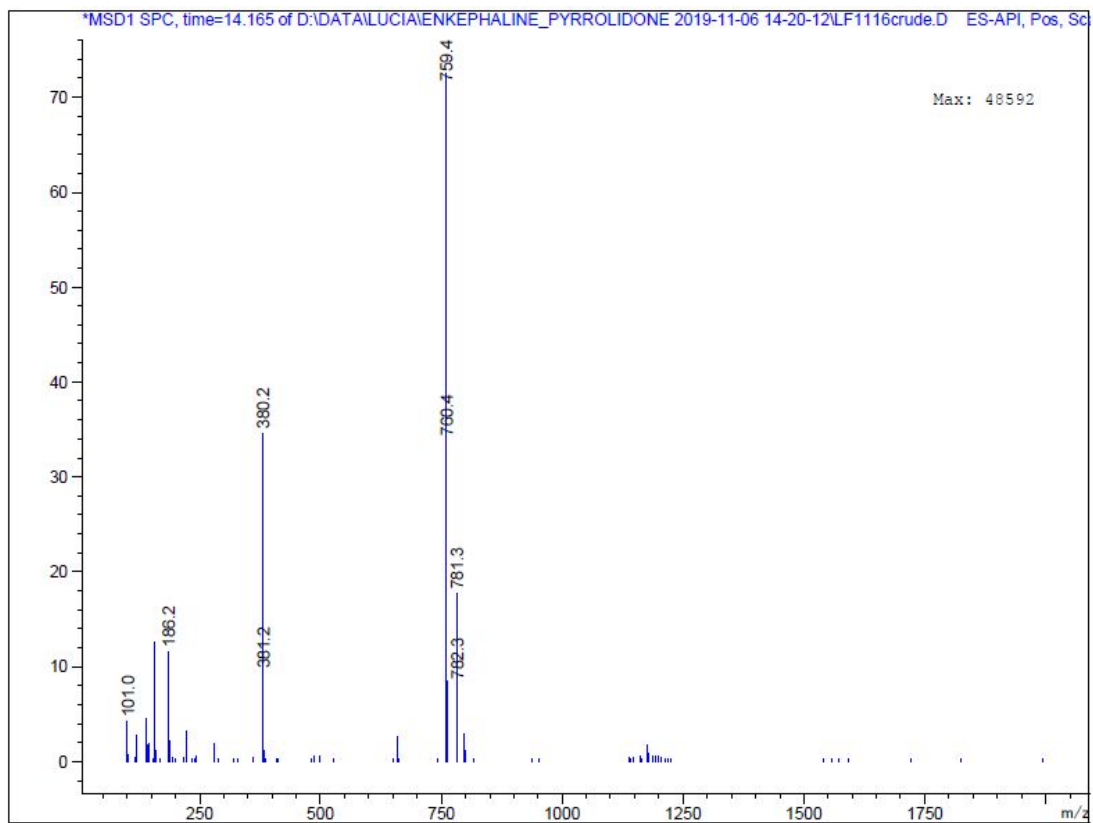
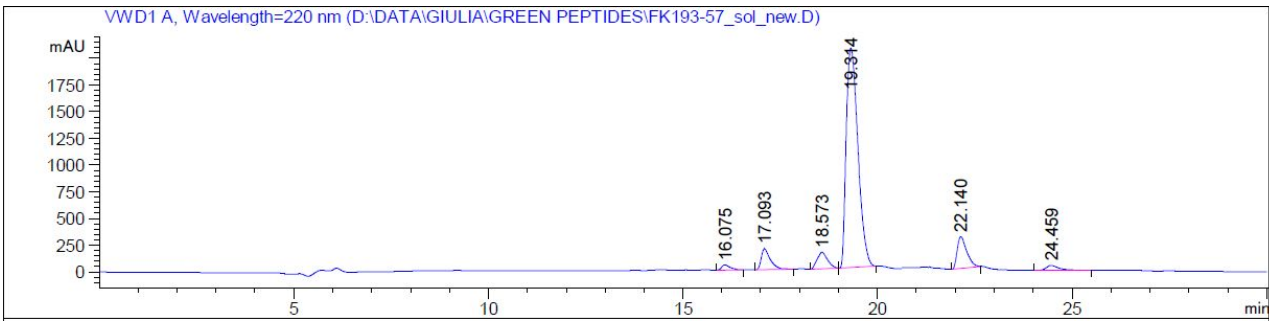


Figure S47. Mass spectrum of H₂N-Tyr-Aib-Leu-COOH (des-Phe-Aib)



SPPS of linear Octreotide in Green Solvents

Figure S48. Chromatogram of linear Octreotide, manual SPPS in DMF



Signal 3: VWD1 A, Wavelength=220 nm

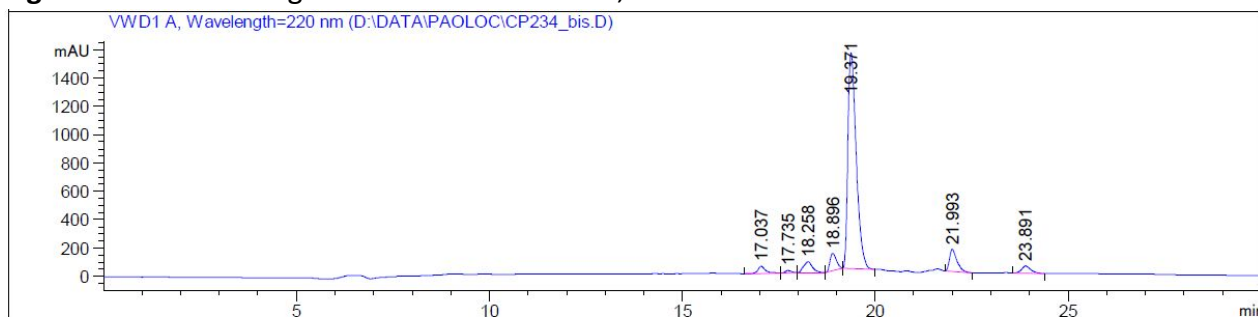
Peak #	RetTime [min]	Type	Width [min]	Area [mAU*s]	Height [mAU]	Area %
1	16.075	BB	0.2235	768.38983	50.49308	1.3774
2	17.093	BB	0.2418	3249.43457	197.66211	5.8250
3	18.573	BB	0.2689	2855.27539	154.98911	5.1184
4	19.314	BB	0.3333	4.28366e4	2054.30322	76.7901
5	22.140	BB	0.2549	5004.95947	296.59695	8.9720
6	24.459	BB	0.3338	1069.39221	47.28645	1.9170

Totals : 5.57841e4 2801.33093

Peptide	Rt (min)	RRT	Area (%)
Cyclized Octreotide N,O shift	16.075	0.83	1.4

Cyclized Octreotide	17.093	0.88	5.8
Linear Octreotide + CO ₂	18.573	0.97	5.1
Linear Octreotide	19.314	1.00	76.8
Linear Octreotide + tBu	22.140	1.14	9.0
Linear Octreotide + tBu2	24.459	1.26	1.9

Figure S49. Chromatogram of linear Octreotide, manual SPPS in NBP



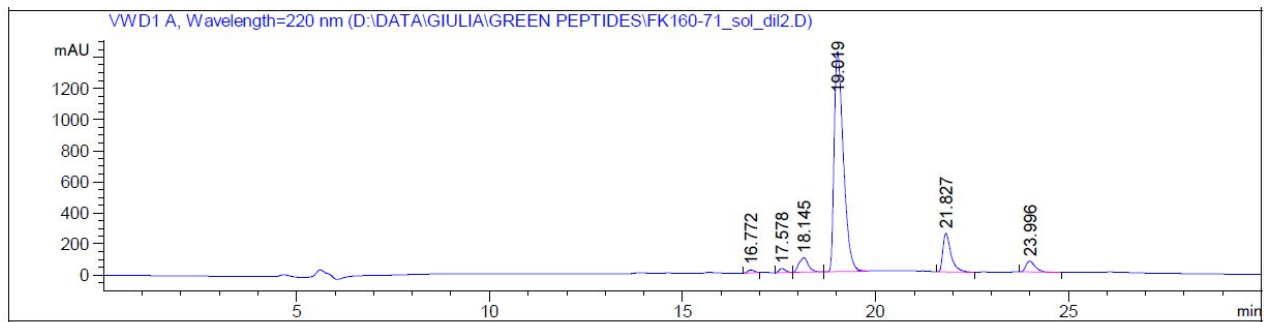
Signal 3: VWD1 A, Wavelength=220 nm

Peak #	RetTime [min]	Type	Width [min]	Area [mAU*s]	Height [mAU]	Area %
1	17.037	BB	0.2040	725.18536	51.58432	2.4587
2	17.735	BB	0.1741	197.43239	17.70697	0.6694
3	18.258	BB	0.2302	1245.63489	77.20074	4.2233
4	18.896	BB	0.1741	1401.56506	123.80760	4.7520
5	19.371	BB	0.2314	2.29071e4	1523.86560	77.6661
6	21.993	BB	0.2023	2130.73779	157.06062	7.2242
7	23.891	BB	0.2446	886.67169	53.16150	3.0062

Totals : 2.94943e4 2004.38736

Peptide	Rt (min)	RRT	Area (%)
Cyclized Octreotide	17.037	0.88	2.4
Linear Octreotide N,O-shift 1	17.735	0.92	0.7
Linear Octreotide N,O-shift 2	18.258	0.95	4.2
Linear Octreotide+CO ₂	18.896	0.97	4.8
Linear Octreotide	19.371	1.00	77.7
Linear Octreotide+tBu	21.993	1.14	7.2
Linear Octreotide+tBu2	23.891	1.26	3.0

Figure S50. Chromatogram of linear Octreotide, manual SPPS in NOP

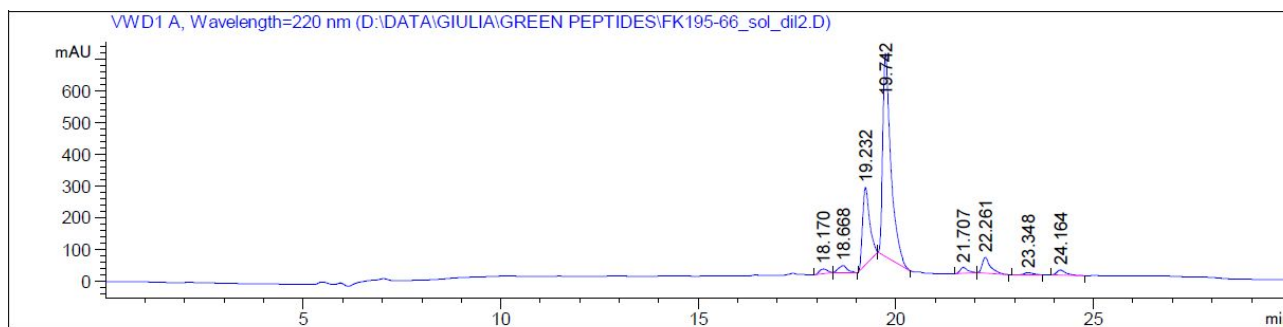


Signal 2: VWD1 A, Wavelength=220 nm

Peak #	RetTime [min]	Type	Width [min]	Area [mAU*s]	Height [mAU]	Area %
1	16.772	BB	0.1705	201.14771	18.26477	0.6597
2	17.578	BB	0.1728	302.99942	27.01583	0.9937
3	18.145	BB	0.2352	1585.15430	94.75126	5.1985
4	19.019	BB	0.2611	2.36682e4	1414.98083	77.6199
5	21.827	BB	0.2139	3569.33667	248.07680	11.7057
6	23.996	BB	0.2528	1165.58362	69.82388	3.8225

Totals : 3.04924e4 1872.91337

Peptide	Rt (min)	RRT	Area (%)
Cyclized Octreotide	16.772	0.88	0.7
Linear Octreotide N,O-shift 1	17.578	0.92	1.0
Linear Octreotide N,O-shift 2	18.145	0.95	5.2
Linear Octreotide	19.019	1.00	77.6
Linear Octreotide+tBu	21.827	1.14	11.7
Linear Octreotide+tBu2	23.996	1.26	3.8

Figure S51. Chromatogram of linear Octreotide, manual SPPS in NOP/DMC 80:20

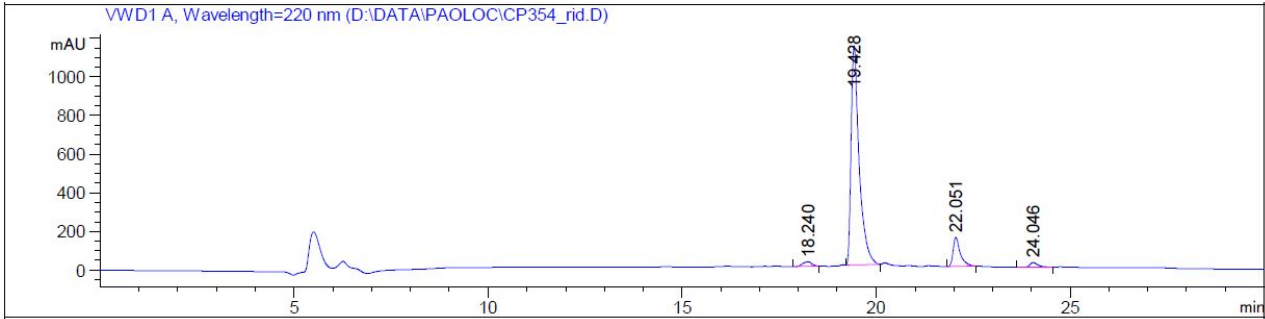
Signal 2: VWD1 A, Wavelength=220 nm

Peak #	RetTime [min]	Type	Width [min]	Area [mAU*s]	Height [mAU]	Area %
1	18.170	BB	0.2206	201.05826	14.60746	1.4404
2	18.668	BB	0.2137	340.64853	22.36730	2.4404
3	19.232	BB	0.1835	3011.40967	244.75949	21.5734
4	19.742	BB	0.2053	9083.64355	641.24805	65.0743
5	21.707	BB	0.1934	243.02454	18.72661	1.7410
6	22.261	BB	0.2100	720.24097	49.42918	5.1597
7	23.348	BB	0.2255	106.01482	7.04599	0.7595
8	24.164	BB	0.2386	252.84393	15.64409	1.8113

Totals : 1.39589e4 1013.82816

Peptide	Rt (min)	RRT	Area (%)
Linear Octreotide N,O-shift 1	18.170	0.92	1.4
Linear Octreotide N,O-shift 2	18.668	0.95	2.4
Linear Octreotide+CO ₂	19.232	0.97	21.6
Linear Octreotide	19.742	1.00	65.1
Linear Octreotide+Boc	21.707	1.10	1.7
Linear Octreotide+tBu	22.261	1.14	5.2
Linear Octreotide+Boc2	23.348	1.18	0.8
Linear Octreotide+tBu2	24.164	1.26	1.8

Figure S52. Chromatogram of linear Octreotide, automated SPPS in NOP/DMC 80:20



Signal 2: VWD1 A, Wavelength=220 nm

Peak #	RetTime [min]	Type	Width [min]	Area [mAU*s]	Height [mAU]	Area %
1	18.240	BB	0.2179	385.12341	24.43648	2.0225
2	19.428	BB	0.2146	1.63817e4	1133.47070	86.0280
3	22.051	BB	0.1853	1913.27478	151.52823	10.0475
4	24.046	BB	0.2174	362.18839	24.65477	1.9020

Totals : 1.90423e4 1334.09018

Peptide	Rt (min)	RRT	Area (%)
Linear Octreotide N,O-shift 2	18.240	0.95	2.0
Linear Octreotide	19.428	1.00	86.0
Linear Octreotide+tBu	22.051	1.14	10.0
Linear Octreotide+tBu2	24.046	1.26	2.0

Figure S53. Mass spectrum of linear Octreotide

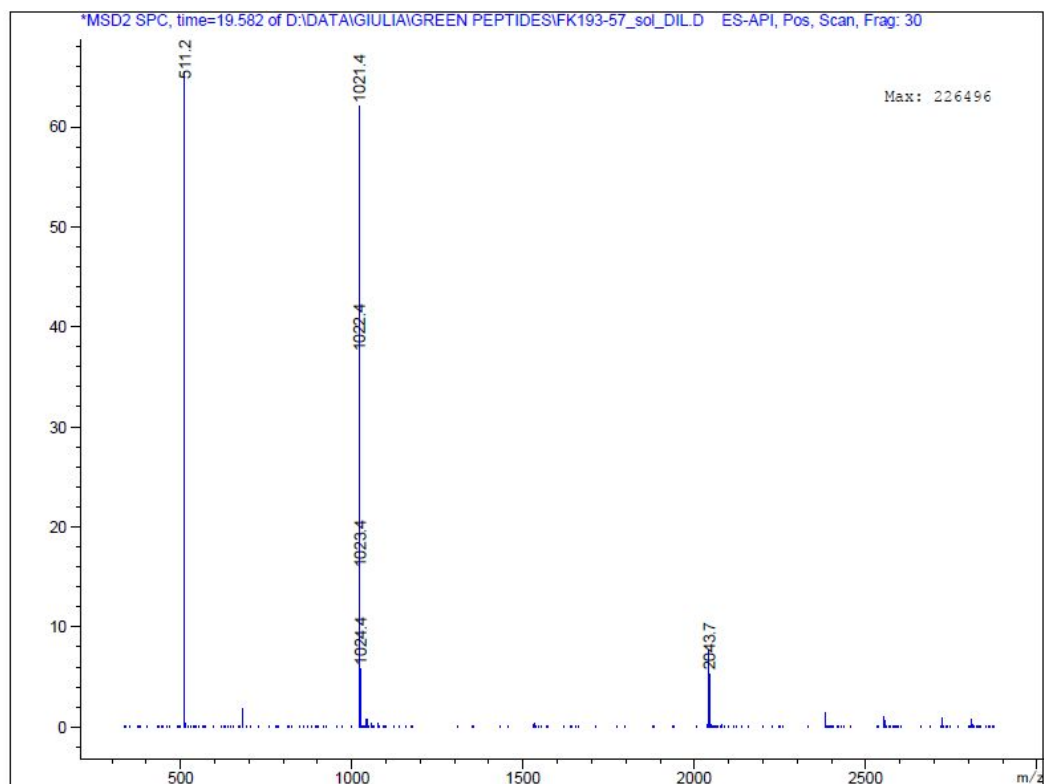


Figure S54. Mass spectrum of linear Octreotide+CO₂

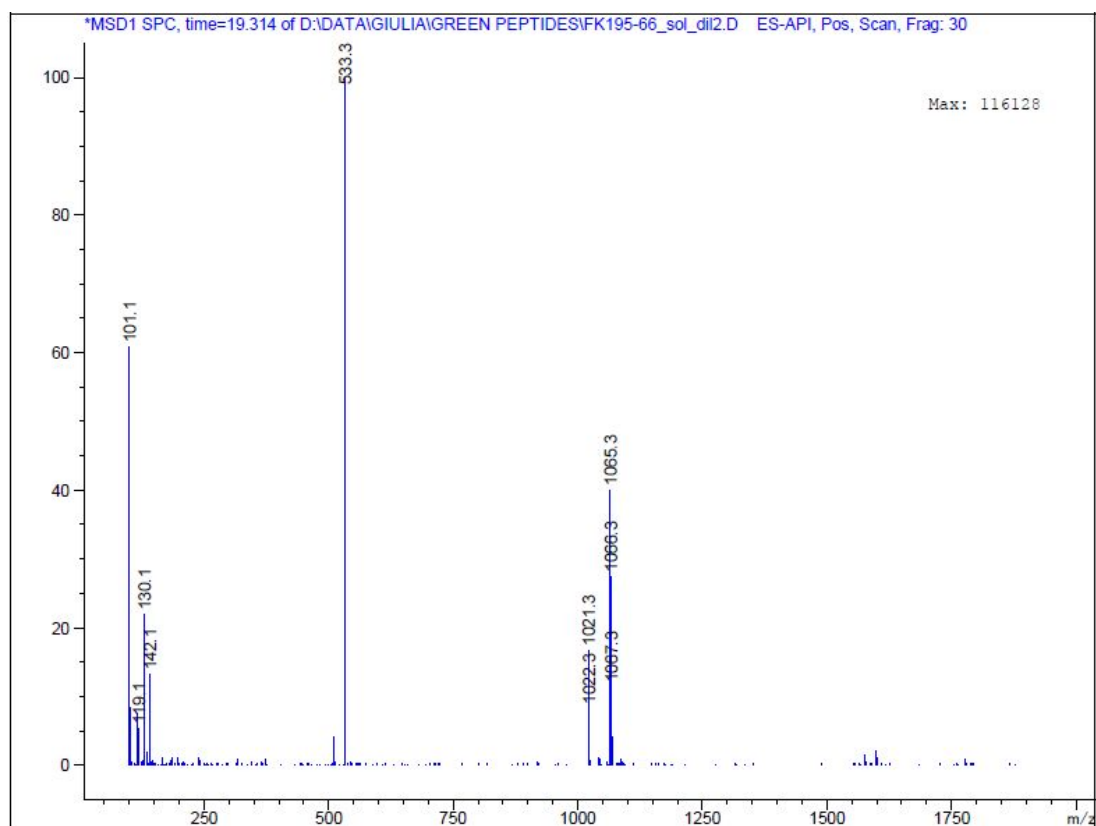


Figure S55. Mass spectrum of linear Octreotide+tBu

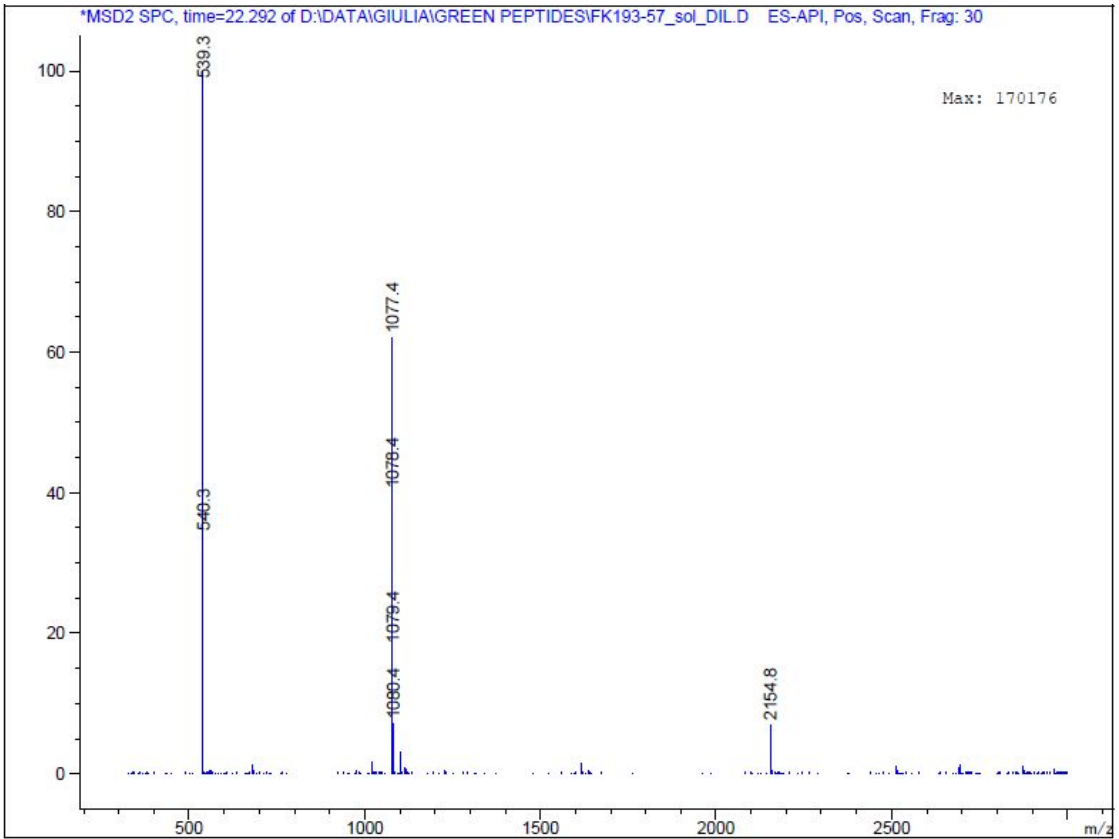


Figure S56. Mass spectrum of linear Octreotide+Boc

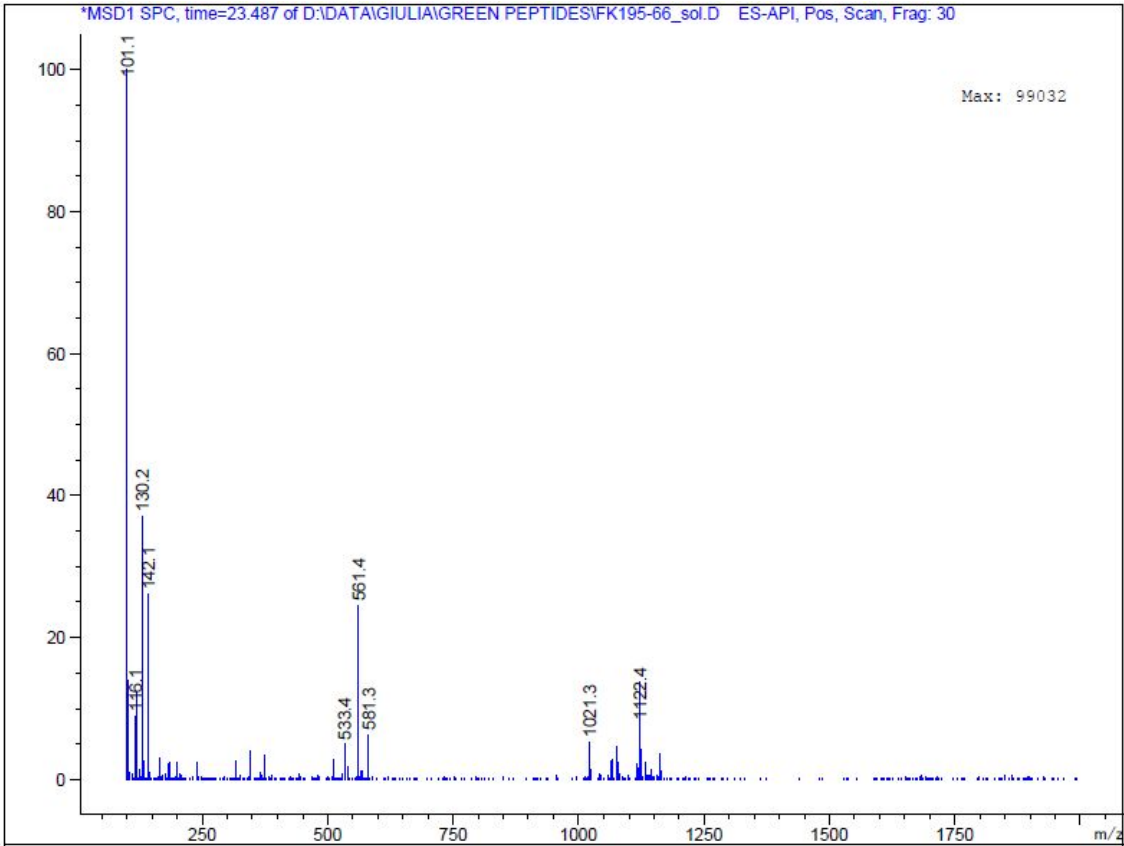
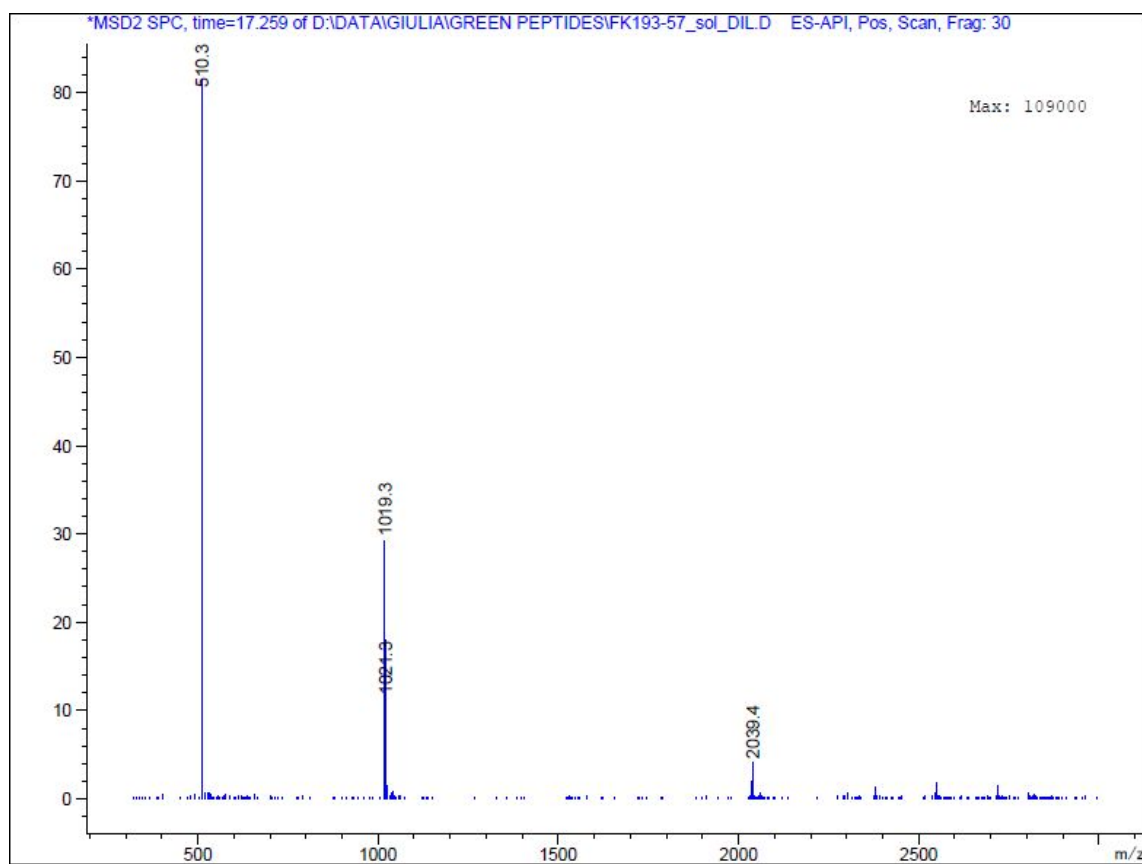


Figure S57. Mass spectrum of cyclic Octreotide



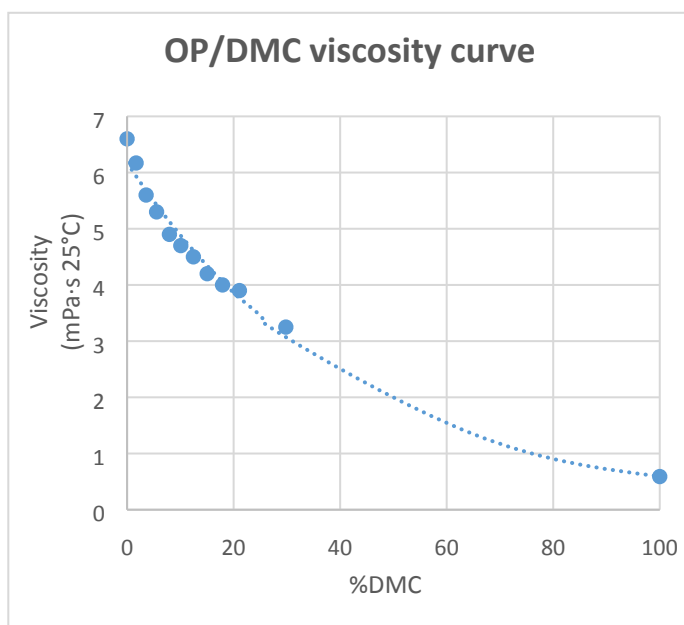
Green solvent mixtures

The viscosity was determined according to the following relation¹:

$$\text{Viscosity} = \text{shear stress}/\text{shear rate}$$

Table S5. NOP/DMC mixtures viscosity measurements at 25°C and relative plot at different ratios

V% NOP	V% DMC	Viscosity (mPa·s 25°C)
100	0	6,6
98,3	1,7	6,2
96,4	3,6	5,6
94,5	5,5	5,3
92,1	7,9	4,9
89,9	10,1	4,7
87,6	12,4	4,5
85	15,0	4,2
82,1	17,9	4



78,9	21,1	3,9
70,2	29,8	3,3
0	100	0,59

Recycling of linear Octreotide SPPS waste stream

Five cases of linear Octreotide are compared, in order to determine the PMI of each process: i) conventional synthesis in DMF; ii) green synthesis in NOP; iii) green synthesis in NOP/DMC 80:20; iv) green synthesis in NOP with recycling of NOP (85%) and piperidine (95%); v) green synthesis in NOP/DMC 80:20 with recycling of NOP (85%), DMC (95%) and piperidine (95%).

To notice, piperidine involved in the formation of DBF-piperidine adduct was subtracted from the total recoverable piperidine volume.

SPPS of linear Octreotide was conducted applying always the same protocol, as reported in the Experimental Section (main text), apart from the employed solvent. In all five cases the total SPPS solvent consumption is considered to be the same, according to the protocol reported in the Experimental Section (main text). When the mixture NOP/DMC 80:20 was used, the ratio between the two solvents was maintained along all the synthetic steps.

The scale of the linear Octreotide SPPS was 0.22 mmol in all cases. The amount of the crude obtained was considered to be the same in all five cases (0.204 g), based on the amount of crude linear Octreotide isolated using the SPPS in NOP.

Stream of deprotection waste (including washings) and stream of coupling waste (including resin swelling and washings) were collected and distilled separately (see Experimental Section).

PMI calculation for linear Octreotide SPPS

Process Mass Intensity (PMI)ⁱⁱ is defined as the ratio between the total mass of materials and the mass of the isolated product and was calculated according to the following equation:

$$PMI = \frac{\sum \text{mass of materials}}{\text{mass of isolated product}}$$

Specifically, mass of materials includes:

- Starting materials: Fmoc-AA-OH, DIC, Oxyma Pure®, resin, cleavage cocktail (TFA+scavengers)
- Solvents (DMF or NOP or NOP/DMC 80:20, DCM for pre-cleavage resin washings and Et₂O for crude peptide precipitation)
- Base (piperidine)

Mass of starting materials, base, DCM and Et₂O are unvaried for all SPPS (Table S6), independently from the used solvent, while total mass of the used solvent (DMF or NOP or NOP/DMC 80:20) slightly varies according to their different densities (Table S7).

Total mass of materials employed in cases i), ii) and iv) (without recycling) is reported in Table S8.

Table S6. Overview of starting materials, base, DCM and Et₂O that are unvaried for all SPPS (independently from the used solvent) and their total mass

	MW (g/mol)	d (g/mL)	eq	mmol	Volume (mL)	Mass (g)	repetitions	Total mass (g)
Fmoc-Thr(tBu)-ol-Trt-PS resin			1	0,22		0,2	1	0,2
Coupling								
Fmoc-Cys(Trt)-OH	585,71		3	0,66		0,39	3	1,16
Fmoc-Thr(tBu)-OH	397,43		3	0,66		0,26	1	0,26
Fmoc-Lys(Boc)-OH	468,54		3	0,66		0,31	1	0,31
Fmoc-D-Trp(Boc)-OH	526,28		3	0,66		0,35	1	0,35
Fmoc-Phe-OH	387,43		3	0,66		0,26	1	0,26
Fmoc-D-Phe-OH	387,43		3	0,66		0,26	1	0,26
OxymaPure	142,11		3	0,66		0,09	8	0,75
DIC	126,2	0,815	3	0,66		0,08	8	0,67
Deprotection								
Piperidine	85,15	0,862			0,6	0,52	16	8,28
Cleavage and precipitation								
TFA	114,02	1,489			5,75	8,56	1	8,56
TIPS	158,36	0,773			0,125	0,10	1	0,10
H ₂ O	18,02	0,997			0,125	0,12	1	0,12
DCM	84,93	1,325			2	2,65	3	7,95
Et ₂ O	102,17	0,725			25	18,13	1	18,13
							Total	47,36

Table S7. Overview of the solvents used for SPPS with DMF, NOP and NOP/DMC 80:20 and their total mass for each SPPS

	MW (g/mol)	d (g/mL)	eq	mmol	Volume (mL)	Mass (g)	repetitions	Total mass (g)
DMF								
DMF swelling	73,09	0,944			2	1,9	1	1,89
DMF couplings	73,09	0,944			2,5	2,36	8	18,88
DMF washings after couplings	73,09	0,944			4,5	4,25	7	29,74
DMF deprotection	73,09	0,944			1,2	1,13	16	18,12
DMF washings after deprotection	73,09	0,944			4,5	4,25	8	33,98
							Total	102,61
NOP								
NOP swelling	197,32	0,92			2	1,80	1	1,84
NOP couplings	197,32	0,92			2,5	2,30	8	18,40
NOP washings after couplings	197,32	0,92			4,5	4,14	7	28,98
NOP deprotection	197,32	0,92			1,2	1,10	16	17,66
NOP washings after deprotection	197,32	0,92			4,5	4,14	8	33,12
							Total	100,00
NOP/DMC 80:20								
NOP swelling	197,32	0,92			1,6	1,5	1	1,47

NOP couplings	197,32	0,92			2	1,84	8	14,72
NOP washings after couplings	197,32	0,92			3,6	3,31	7	23,18
DMC swelling	90,08	1,07			0,4	0,43	7	3,00
DMC couplings	90,08	1,07			0,5	0,54	7	3,75
DMC washings after couplings	90,08	1,07			0,9	0,96	7	6,74
NOP deprotection	197,32	0,92			0,96	0,8832	16	14,13
NOP washings after deprotection	197,32	0,92			3,6	3,312	8	26,50
DMC deprotection	90,08	1,07			0,24	0,2568	16	4,11
DMC washings after deprotection	90,08	1,07			0,9	0,963	8	7,70
							Total	105,30

Table S8. Total mass of materials employed for SPPS without recycling

	<i>SPPS solvents</i>		
	DMF	NOP	NOP/DMC 80:20
\sum starting materials ^a (g)	13,0	13,0	13,0
\sum solvents ^b (g)	128,7	126,1	131,4
\sum base (g)	8,3	8,3	8,3
Total (g)	150,0	147,4	152,7

^aStarting materials include Fmoc-AA-OH, DIC, Oxyma Pure®, resin, cleavage cocktail (TFA+scavengers)^bSolvents include DCM for pre-cleavage resin washings and Et₂O for crude peptide precipitation

When solvents (NOP or NOP/DMC 80:20) and base (piperidine) were recycled (cases iii and v), final PMI was calculated by subtracting the mass of recovery materials from the mass of used materials.

$$PMI \text{ (for SPPS with recycling)} = \frac{\sum \text{mass of materials} - \sum \text{mass of recovered materials}}{\text{mass of isolated product}}$$

Table S9 depicts the amount of total recovered mass of NOP or NOP/DMC 80:20 and piperidine when the recycling approach was employed. PMI calculations for all SPPS (cases i-v) are reported in Table 9 in the main body text and in Table S10.

Table S9. Total mass of solvents (NOP or NOP/DMC 80:20) and piperidine employed for SPPS and their recovered mass

	<i>SPPS solvent</i>	
	NOP	NOP/DMC 80:20
\sum NOP (g)	100,0	80,0
\sum NOP recycled (g)	85,0	68,0
\sum DMC (g)	-	25,3
\sum DMC recycled (g)	-	24,0
\sum base (g)	8,28	8,3
\sum base recycled (g)	7,72	7,72
Total solvents + base recycled (g)	92,7	99,7

Table S10. PMI for linear Octreotide SPPS processes

	<i>SPPS solvents</i>				
	DMF	NOP	NOP+recycling	NOP/DMC 80:20	NOP/DMC 80:20 + recycling
Σ starting materials ^a (g)	13.0	13.0	13.0	13.0	13.0
Σ solvents ^b (g)	128.7	126.1	41.1	131.4	39.3
Σ base (g)	8.3	8.3	0.6	8.3	0.6
PMI^c	735	722	268	748	256

^aStarting materials include Fmoc-AA-OH, DIC, Oxyma Pure®, resin, cleavage cocktail (TFA + scavengers)

^bSolvents include DCM for pre-cleavage resin washing and Et₂O for crude peptide precipitation

^cPMI = Σm (starting materials) + Σm (solvents) + Σm (base) / m (crude linear Octreotide product)

Purities of distilled NOP, DMC (from coupling stream waste), piperidine or DMC/piperidine mixture was assessed > 95% from ¹H NMR (Figures S58-59). Recovered NOP, DMC and piperidine was reused as such.

Figure S58. ¹H NMR spectrum (400 MHz, CDCl₃) of NOP recovered from distillation processes

¹H NMR (400 MHz, CDCl₃) δ (ppm) 3.35 (t, J = 7.0 Hz, 2H), 3.24 (t, J = 7.4 Hz, 2H), 2.36 (t, J = 8.1 Hz, 2H), 2.04 – 1.93 (m, 2H), 1.54 – 1.43 (m, 2H), 1.18 – 1.30 (m, 10H), 0.86 (t, J = 6.8 Hz, 3H).

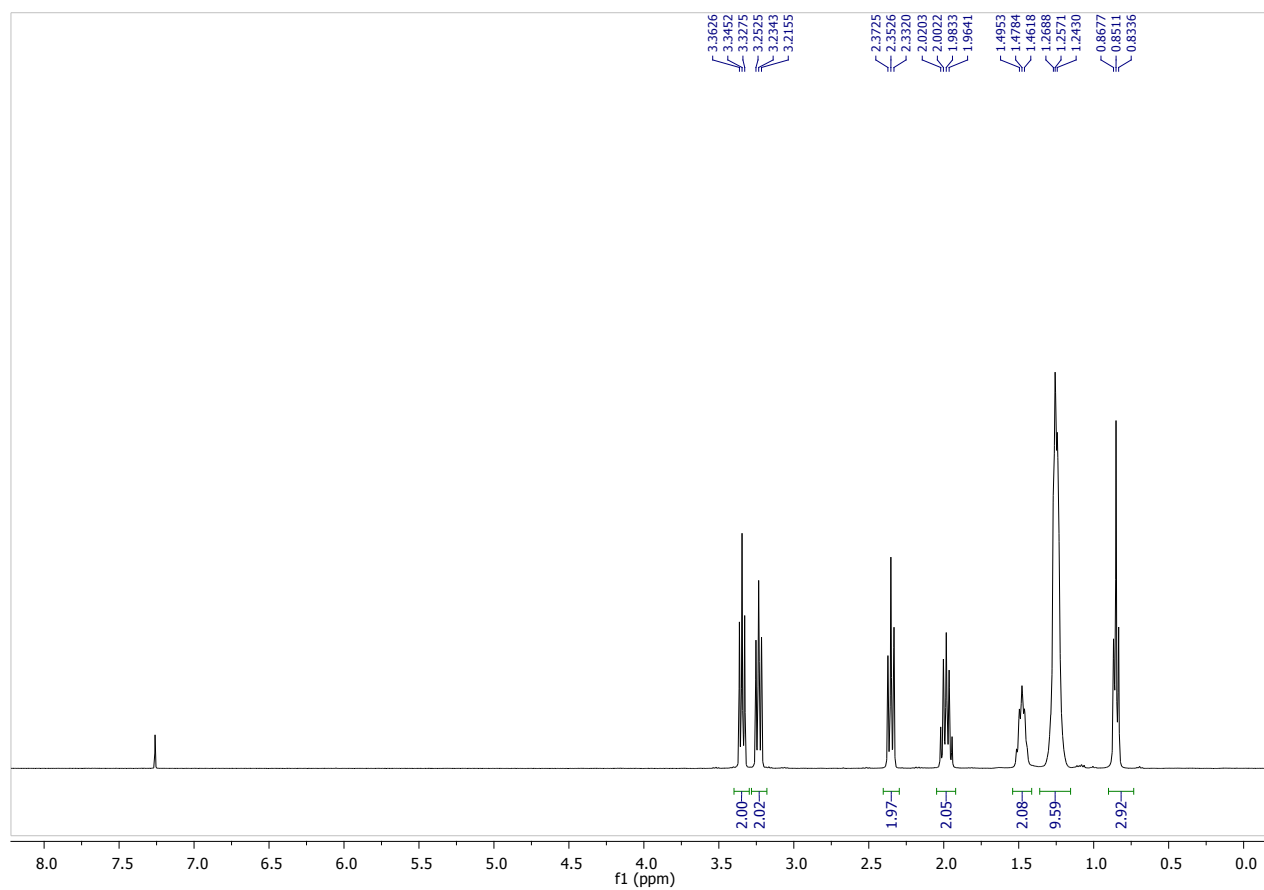
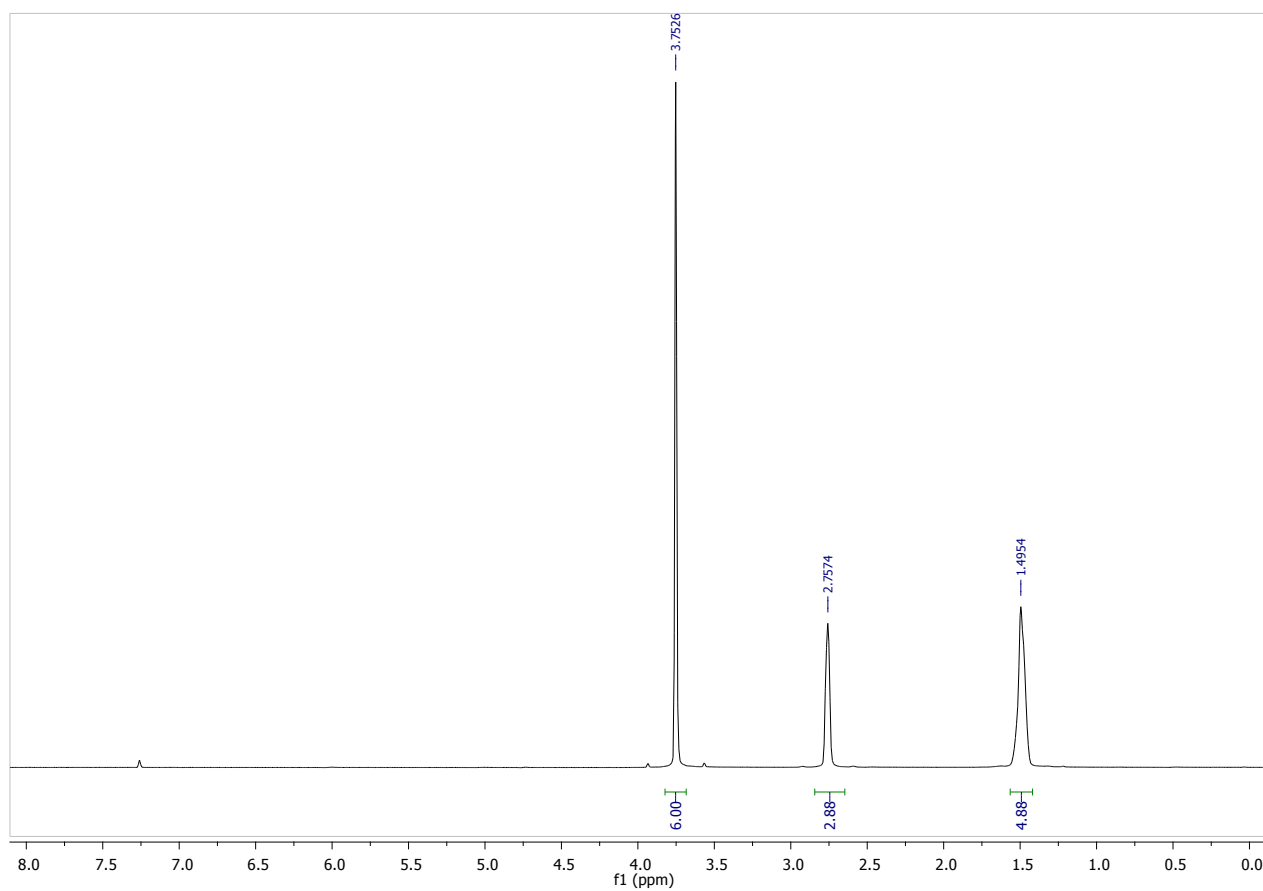


Figure S59. ¹H NMR spectrum (400 MHz, CDCl₃) of piperidine/DMC mixture recovered from distillation process of deprotection waste stream of linear Octreotide SPPS in NOP/DMC

^1H NMR (400 MHz, CDCl_3) δ (ppm) DMC: 3.75 (s, 6H); piperidine: 2.76 (s, 4H), 1.50 (s, 6H). DMC and piperidine are in a 1:0.86 V/V ratio corresponding to 1:0.75 mol/mol ratio.



ⁱ G. Schramm, A practical approach to Rheology and Rheometry 2nd Edition by Gebruder HAAKE GmbH, 2000, p.15

ⁱⁱ E. R. Monteith, P. Mampuys, L. Summerton, J. H. Clark, B. U. W. Maes, C. R. McElroy, *Green Chem.*, 2020, **22**, 123.